Epaxial muscles and ossified tendons in dinosaurs : anatomy, development, histology, and biomechanics

by Christopher Lee Organ

A dissertation submitted in partial fulfillment of the requirements for the degree of Doctor of Philosophy in Biological Sciences
Montana State University

Abstract:
Intratendinous ossification in dinosaurs (including birds) is a wide spread phenomenon that has implications for physiology, posture, biomechanics, behavior, and systematics. Four separate studies were undertaken to elucidate ossified tendon biology in extinct dinosaurs and birds. The first investigation reconstructs dorsal epaxial musculature in extinct dinosaurs. Crocodilian and avian dorsal epaxial muscles are homologized. Using the extant phylogenetic bracketing approach, the three-layered trellis of Hadrosauriformes is homologized to the M. transversospinalis slips in crocodilians and the M. longus colli dorsalis thoracica in birds. These tendons are ossified in Hadrosauriformes and some birds. The parallel ossified tendons in other ornithischians are homologized to the M. longissimus dorsi in Alligator. The second investigation determines how ossified tendons in non-avian dinosaurs developed. Atrophied muscle was previously thought to be the origin of ossified tendons in non-avian dinosaurs. Using different age classes of hadrosaurs (Brachylophosaurus and Maiasaura) and turkeys (Meleagris), the developmental process of ossified tendons in hadrosaurs is shown to be homologous with intratendinous ossification in birds. But, the degree of ossification is greater in hadrosaurs, whose tendons also possess primary osteons, an external fundamental system and lines of arrested growth. The third investigation determines the histological diversity of ossified tendons in Dinosauria. Despite various anatomical locations and large differences in size, ossified tendons have uniform microstructure even in specimens that do not normally experience intratendinous ossification (such as Ceratosaurus and Camarosaurus). The greater degree of ossification noted above occurs in all non-avian dinosaurs. Also, variation in periosteal bone development occurs along the length of individual tendons. Ossified tendons from marginocephalians are unique in that they have larger portions of fibrolamellar bone and radial vascularity. In the fourth investigation, computer finite element models are constructed for two ornithopods to assess ossified tendon biomechanics. An Alligator is used to empirically determine joint properties. Ossified tendons probably reduced tail deflection and played a role in locomotion in all ornithopods. The ossified tendon trellis of Hadrosauriformes may have increased the skeleton's ability to bear large body mass. Neural spine height and bone material properties have the greatest impact on spinal rigidity.

EPAXIAL MUSCLES AND OSSIFIED TENDONS IN DINOSAURS:

ANATOMY, DEVELOPMENT, HISTOLOGY, AND BIOMECHANICS

by

Christopher Lee Organ

A dissertation submitted in partial fulfillment
of the requirements for the degree

of

Doctor of Philosophy

in

Biological Sciences

MONTANA STATE UNIVERSITY
Bozeman, Montana

December 2003

APPROVAL

of a dissertation submitted by

Christopher Lee Organ

This dissertation has been read by each member of the dissertation committee and has been found to be satisfactory regarding content, English usage, format, citations, bibliographic style, and consistency, and is ready for submission to the College of Graduate Studies.

John R. Horner _____ 12/2/03
(Signature) Date

Kevin M. O'Neill _____ 12/10/03
(Signature) Date

Approved for the Department of Cell Biology and Neuroscience

Gwen A. Jacobs _____ 12/03/03
(Signature) Date

Approved for the College of Graduate Studies

Bruce R. McLeod _____ 12-23-03
(Signature) Date

STATEMENT OF PERMISSION TO USE

In presenting this dissertation in partial fulfillment of the requirements for a doctoral degree at Montana State University, I agree that the Library shall make it available to borrowers under rules of the Library. I further agree that copying of this dissertation is allowable only for scholarly purposes, consistent with "fair use" as prescribed in the U.S. Copyright Law. Requests for extensive copying or reproduction of this dissertation should be referred to Bell & Howell Information and Learning, 300 North Zeeb Road, Ann Arbor, Michigan 48106, to whom I have granted "the exclusive right to reproduce and distribute my dissertation in and from microform along with the non-exclusive right to reproduce and distribute my abstract in any format in whole or in part."

Signature 

Date 12-02-03

ACKNOWLEDGEMENTS

I would like to thank Paul Sereno, William Simpson, Janet Hinshaw, and Jim Gardner for access and discussion over specimens. I would also like to thank Robert Storer for insightful discussions on intratendinous ossification in birds. Seder Ridge Turkey Farm, Ruth Elsey at the Rockefeller Wildlife Refuge (Louisiana Department of Wildlife and Fisheries), and the Bozeman Raptor Center kindly donated extant specimens.

Jack Horner, Cynthia Marshall, Armand de Ricqlès Tobin Hieronymus, Jason Adams, Nicole Hobbs, Sean Faul, Ellen Lamm, Jim Dent, Rick Blob, Joe Cooley, Joe Beaman, Jeff LaRock, Martha Middlebrooks, Katie Organ, R. McNeil Alexander, Steve Gatesy, Matt Carrano, John Hutchinson, Walter Coombs, and others whom I may have forgotten deserve thanks for discussions or reviews of my project, though all errors are certainly mine to bear.

Matt Carrano gave me advice on translating Old German and French papers, for which I am grateful. Also, I must thank Erich Staudacher for helping me figure out some inscrutable Old German. Neither are responsible for possible errors in translation.

Funding was provided in part by a 2001 doctoral grant from the International Society of Biomechanics, the Museum of the Rockies (Department of Paleontology), and the Department of Cell Biology and Neuroscience at Montana State University. I would particularly like to thank Gwen Jacobs for the support and opportunities she has graciously given me.

I am grateful to my committee members Jack Horner, Kevin O'Neill, Matt Lavin, Gwen Jacobs, and Deb King for their guidance and friendship.

Finally, I am indebted to my parents William Organ and Susan Hadley for inspiring my passion for science and creativity and to my love, Nicole Hobbs, who has stood with me in good times and bad.

TABLE OF CONTENTS

TABLE OF CONTENTS - CONTINUED

LIST OF FIGURES

LIST OF FIGURES - CONTINUED

LIST OF TABLES

ABSTRACT

Intratendinous ossification in dinosaurs (including birds) is a wide spread phenomenon that has implications for physiology, posture, biomechanics, behavior, and systematics. Four separate studies were undertaken to elucidate ossified tendon biology in extinct dinosaurs and birds. The first investigation reconstructs dorsal epaxial musculature in extinct dinosaurs. Crocodilian and avian dorsal epaxial muscles are homologized. Using the extant phylogenetic bracketing approach, the three-layered trellis of Hadrosauriformes is homologized to the M. transversospinalis slips in crocodilians and the M. longus colli dorsalis thoracica in birds. These tendons are ossified in Hadrosauriformes and some birds. The parallel ossified tendons in other ornithischians are homologized to the M. longissimus dorsi in *Alligator*. The second investigation determines how ossified tendons in non-avian dinosaurs developed. Atrophied muscle was previously thought to be the origin of ossified tendons in non-avian dinosaurs. Using different age classes of hadrosaurs (*Brachylophosaurus* and *Maiasaura*) and turkeys (*Meleagris*), the developmental process of ossified tendons in hadrosaurs is shown to be homologous with intratendinous ossification in birds. But, the degree of ossification is greater in hadrosaurs, whose tendons also possess primary osteons, an external fundamental system and lines of arrested growth. The third investigation determines the histological diversity of ossified tendons in Dinosauria. Despite various anatomical locations and large differences in size, ossified tendons have uniform microstructure even in specimens that do not normally experience intratendinous ossification (such as *Ceratosaurus* and *Camarosaurus*). The greater degree of ossification noted above occurs in all non-avian dinosaurs. Also, variation in periosteal bone development occurs along the length of individual tendons. Ossified tendons from marginocephalians are unique in that they have larger portions of fibrolamellar bone and radial vascularity. In the fourth investigation, computer finite element models are constructed for two ornithopods to assess ossified tendon biomechanics. An *Alligator* is used to empirically determine joint properties. Ossified tendons probably reduced tail deflection and played a role in locomotion in all ornithopods. The ossified tendon trellis of Hadrosauriformes may have increased the skeleton's ability to bear large body mass. Neural spine height and bone material properties have the greatest impact on spinal rigidity.

CHAPTER 1

DORSAL EPAXIAL MUSCULATURE IN DINOSAURS

Introduction

Archosaur epaxial musculature is generally considered conserved compared with the diversity of muscles in the appendicular skeleton. Consequently, interest in muscular reconstruction in extinct archosaurs has focused on the shoulder girdle, pelvis, or limbs (Romer 1923a; Romer 1923b; Romer 1927; Galton 1969; Walker 1977; Gatesy 1994; Dilkes 2000; Hutchinson 2001a; Hutchinson 2001b; Carrano and Hutchinson 2002). Some of these studies deal with epaxial muscles in a peripheral manner by grouping them into the "dorsalis trunci". But, the dorsal vertebral column has diverged significantly in living archosaurs. For example, birds possess a synsacrum and many develop a notarium and "vertebral struts" (Storer 1982). The dorsal epaxial musculature associated with avian vertebral fusion is reduced in size and divisions compared with crocodilians. In many birds the epaxial muscles are pinched off by the anteromedial union of the iliac blades. In contrast, crocodilians retain plesiomorphic epaxial muscles, except for the synapomorphic M. tendino-articularis that contains anteriorly directed cones of myosepta (Gasc 1981).

The only attempts at detailed reconstruction of dorsal epaxial musculature in extinct dinosaurs are concerned with ossified epaxial tendons in Minmi (Molnar and Frey 1987) and Iguanodon (Dollo 1886). Molnar and Frey (*idem*) used crocodilian while Dollo (*idem*) used avian anatomy comparisons for muscle reconstruction. But recent studies (Hutchinson 2001a; Hutchinson 2001b) have

shown the resolution power and robustness that an explicit phylogenetic context using many specimens can provide for muscle reconstruction and the evolution of soft tissues. Muscle reconstruction that uses a phylogenetic context relies on osteological correlates (hard tissue indicators of soft tissue, such as bumps or scars) for inferring the condition of soft tissues (Witmer 1995). But ossified tendons are more than just an osteological correlate consisting of bone surface rugosity or projections caused by muscle or tendon attachment. They are literally part of a soft tissue that became ossified and then fossilized. Therefore, ossified tendons are ideal for inferring soft tissues. Unfortunately, they only regularly occur in ornithischian dinosaurs, where they are used as a diagnostic character (synapomorphy).

Dorsal epaxial muscles are associated with breathing in birds (Baumel et al. 1990) and terrestrial locomotion in crocodilians (Frey 1985). The epaxial tendon trellis thought to be unique to hadrosaurs, lambeosaurs, and iguanodons (Hadrosauriformes) are always interpreted as rigidifying structures that affect bipedal posture (Ostrom 1964) and locomotion (Dollo 1886). Also, the existence of the trellis is used to argue for claims of semi-aquatic (Brown 1916; Colbert 1951) or terrestrial (Ostrom 1964) behavior. These arguments assume that the ossified trellis is an anatomical structure unique to Hadrosauriformes. In addition, because ossified tendons are also used in systematics, a better understanding of their muscular reconstruction is important for assessing characters commonly used to support multiple dinosaurian clades (e.g. Ornithischia and Hadrosauriformes). This study's purpose is to reconstruct the dorsal epaxial musculature in extinct dinosaurs using a phylogenetic approach. The morphology and function of dorsal epaxial muscles are discussed in this context. This reconstruction will provide a basis for interpreting the biology of

epaxial muscles and ossified tendons in all dinosaurs. Furthermore, because the epaxial musculature in birds is poorly resolved (Baumel et al. 1993), this study will help elucidate the structure and function of the dorsal region in birds.

Materials and Methods

Osteological data were collected from extinct dinosaurs at the Museum of the Rockies (MOR), Royal Tyrrell Museum of Paleontology (RTMP), Field Museum of Natural History (FMNH), and University of Chicago Department of Organismal Biology and Anatomy. Most of the structural data from ossified tendons was based on an articulated *Brachylophosaurus canadensis* (MOR-794) that possesses a three-layered trellis of ossified tendons *in situ*.

Osteological data from birds were collected at the MOR and Montana State University (MSU), but mostly at the University of Michigan Museum of Zoology (UMMZ). Specimens were chosen based on availability and spanned seven orders: Anseriformes (*Chuana torquata*), Charadriiformes (*Limnodromus scolopaceus*, and *Ptychoramphus aleuticus*), Falconiformes (*Accipiter cooperi*), Gruiformes (*Porphyrio mantelli*), Podicipediformes (5 specimens of *Podilymbus gigas*, 8 specimens of *Podilymbus podiceps, and Aechmorphus occidentalis*; and 4 specimens of *Podilymbus major*), Psittaciformes (*Amazona amazonica*), and Struthioniformes (*Apteryx australis*).

Myological data were collected from donated specimens dissected on the campus of Montana State University, Bozeman. Avian specimens spanned five orders: Ciconiiformes (*Ardea herodias*), Columbiformes (*Columba livia*), Falconiformes (*Buteo jamaicensis*), Galliformes (7 specimens of *Meleagris gallopavo* and *Gallus domesticus*), and Podicipediformes (*Podilymbus podiceps*). Three

crocodilians (*Alligator mississippiensis*) and two lizards (*Tupinambis* and *Anolis carolinensis*) were also dissected.

The nomenclature used for crocodilian anatomy follows Gasc (1981) and Frey et al. (1989), though some homologies and synonyms from Gasc (*idem*) are preferred. Avian anatomy nomenclature follows Baumel et al. (1993).

Homology

The term "Homology", as used in this study, refers specifically to supraspecific homology (Roth 1994), which is a correspondence among characters in different taxa that share a recent common ancestor. That is, homologies are synapomorphies (Patterson 1982; de Pinna 1991; Roth 1994; Hawkins et al. 1997), which define monophyletic groups (clades). Homologies identified in this study are also taxic (characters). Transformational (change in character state) homology is considered by the inclusion of extinct forms.

Using these definitions, there are three ways to test hypotheses of homology: similarity, conjunction, and congruence. The first test is similarity, which is the simplest but weakest tool (de Pinna 1991). It consists of identifying homologies based on appearance. As Patterson (1982) notes, similarity is not a test, but provides supporting data for proposing a hypothesis of homology. Despite these caveats, it is powerful because any kind of similarity may be used, such as composition, ontogeny, position, and so on.

The second test for homology hypotheses is conjunction, whereby the proposed homologous structures are searched for in the same organism. If such structures are discovered, hypothesis falsification follows (Patterson 1982). For example, wings in a bird cannot be homologous with the hind limbs of mammals, because birds possess hind limbs as well. Despite the conclusiveness

of this test, it is of limited utility for transformation (character state) hypotheses of homology.

The third test, which is considered the strongest, is congruence. A homologous character should only arise once for a group (it should be a synapomorphy). This uses comparisons of other homologies in a phylogenetic framework to strengthen the proposed hypothesis of homology. The greater the number of structures found to be homologous between two taxa, the more support the proposed hypothesis has. Like many other historical sciences, this test uses a "convergence of independent evidence" approach where the hypothesis becomes more robust according to the degree of support (number of characters found to be congruent).

Phylogenetic Framework for Soft Tissue Inferences

Reconstruction of unpreserved soft tissues in extinct taxa is problematic because of variables such as muscle attachment type, ontogeny, shifts in function, and so forth (Bryant and Seymour 1990; Bryant and Russell 1992). The best way to address these problems is by using an explicit phylogenetic framework (Witmer 1995) to infer unpreserved soft tissues. This method uses living sister (bracket) taxa to provide phylogenetic support for hypothesizing unpreserved features in extinct organisms. Inferences are ranked according to the degree of phylogenetic support they provide. A level I inference is made when both extant bracketing taxa possess a soft tissue and associated osteological correlates. This is unequivocal support for inferring an unpreserved soft tissue. A level I' inference is made when both bracketing taxa possess a soft tissue that lacks osteological correlates. Level I' inferences are less robust than a level I inference, but more supportive than a level II inference. A level II inference is made when one of

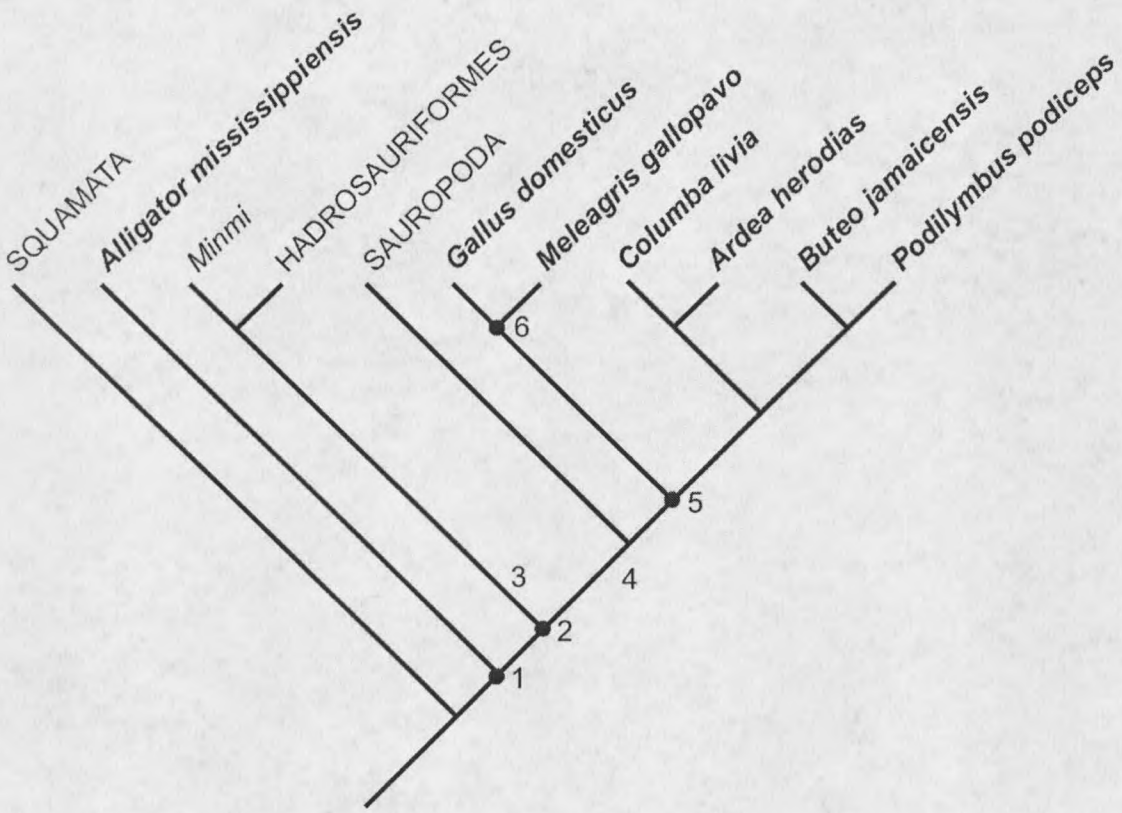

Figure 1. Phylogenetic framework used in this study. Stem-based groups are labeled at the branches and node-based groups are labeled at nodes. 1, Archosauria; 2, Dinosauria; 3, Ornithischia; 4, Saurischia; 5, Neornithes; 6, Galliformes. Bold taxa are extant. Modified from Gauthier (1986), Cracraft (1988), and Sereno (1999).

the bracketing taxa possesses a soft tissue and associated osteological correlates of the soft tissue in question. This provides limited support for inferring an unpreserved soft tissue. A level II′ inference is made when one of the bracketing taxa possess a soft tissue that lacks osteological correlates. Level II′ inferences are less robust than a level II inference, but more supportive than a level III inference. A level III inference is made when neither of the bracketing taxa possesses a soft tissue. This provides no phylogenetic support for inferring an unpreserved soft tissue. Only level I , I′, II, and II′ inferences are used in this study. Limitations on level I′ and II′ are discussed on an individual basis.

The phylogenetic framework used in this study (Fig. 1) is constructed from several sources. Gauthier (1986) is used for the base of the tree, Sereno (1999) is used to expand Dinosauria, and Cracraft (1988) is used to expand Neornithes.

Results

Crocodilia

Epaxial musculature in crocodilians is straightforward and does not differ dramatically from the condition encountered in squamates. However, epaxial muscles are less diverse in crocodilians than those in squamates because of osteoderms and the propulsive function of the tail (Gasc 1981). The following anatomy is based on the dissections of *Alligator* and the literature (Vallois 1922; Gasc 1981; Frey 1982; Molnar and Frey 1987; Frey et al. 1989).

Intrinsic Vertebral Muscles Mm. interneuralis (also called M. interspinales) and Mm. interarcuales connect neural spines together at their anterior and posterior edges. Their fibers run anteroposterior and are indistinguishable from one another. Therefore, they will together be referred to together as the Mm. interneuralis. Medial to this muscle lies the interspinal ligament. Mm. interarticularis superiores connects successive pre and postzygapophyses. The anterior border of the Mm. interarticularis superiores inserts on the posterior aspect of the zygapophyseal joint by a short fan shaped tendon. Because the epaxial muscles are fibrous, the preceding muscle divisions were not easily distinguishable. Lateral to this muscle is the Mm. intertransversarii, which connects successive transverse processes.

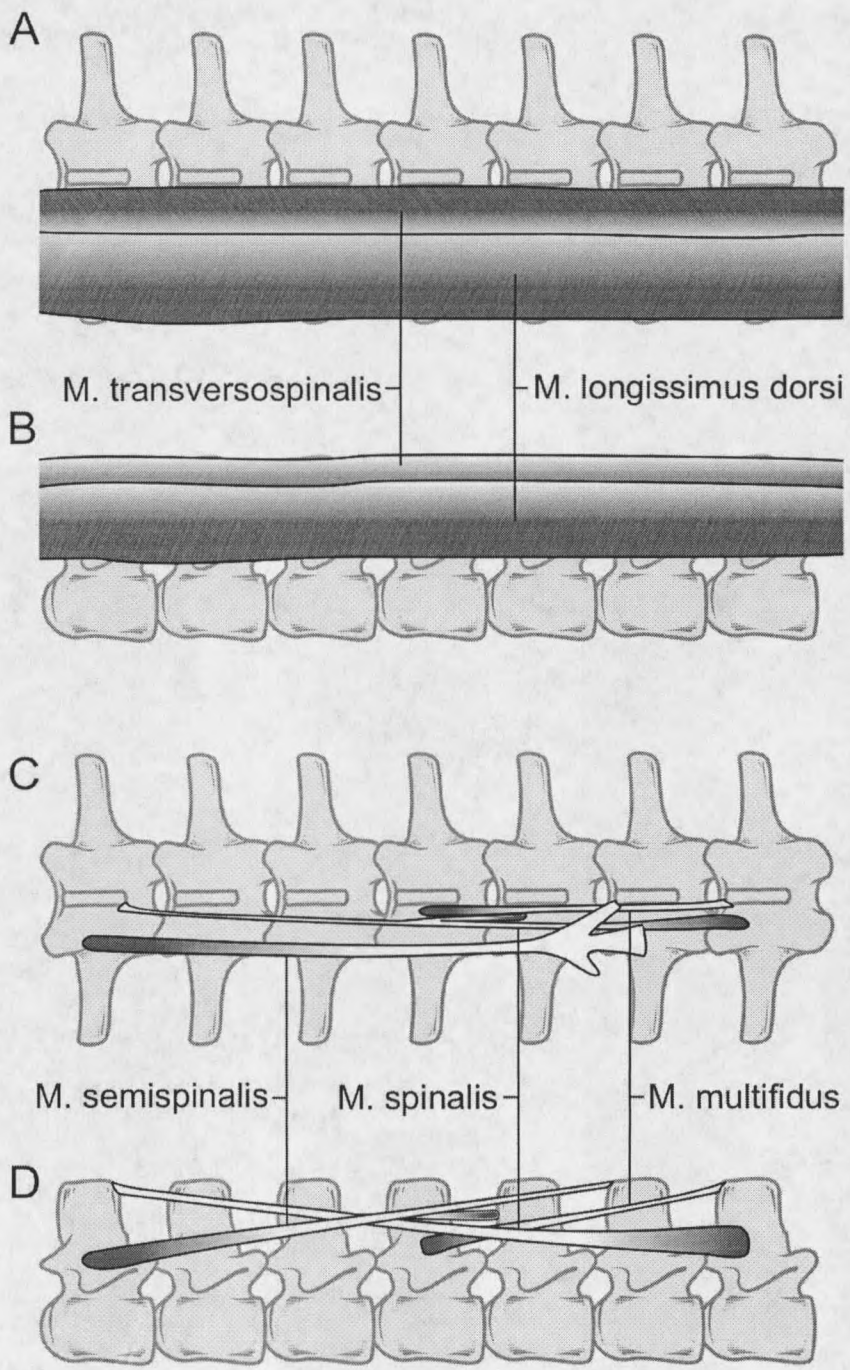

Figure 2. Diagram of dorsal epaxial muscles in *Alligator*. A and B, dorsal and lateral views of major muscles. C and D, slips of the M. transversospinalis excluding the tendino-articularis. Anterior is to the right.

M. Transversospinalis Lateral to the intrinsic vertebral muscles are a series of slips that form the bulk of the M. transversospinalis (Fig. 2). The M. multifidus, M. neurospinalis of Frey (1982) and Vallios (1922), is the most medial slip and lies next to the lateral surface of the neural spines. The tendon from the M. multifidus originates as a small mediolaterally fattened sheet in front of the neural spine. This passes anterodorsal over two vertebrae and inserts on the posterior summit of the third neural spine just under the attachment of the medial tendinous head of the M. semispinalis (M. articulo-spinalis).

Immediately lateral to this tendon, separated by only a thin layer of muscle fibers, is the M. spinalis, M. spino-articularis of Frey (1982) and Vallios (1922). This muscle slip originates near the prezygapophysis as a mediolaterally flattened sheet and runs posterodorsally to insert on the anterior summit of the neural spine five to seven vertebrae posterior (Fig. 2C and D). In the lumbar region, this tendon bifurcates twice, anteriorly receiving another tendon from the muscle belly and posteriorly a tendon from the anterior aspect of the neural spine.

The M. semispinalis lies lateral to the M. spinalis and is separated from it by muscle tissue (Fig. 2C and D). It is divisible into different sections, the M. articulo-spinalis and M. tendino-articularis. The M. articulo-spinalis is the medial division, which originates at the base of the neural spine and passes anterodorsally past four vertebrae. Here it flattens out and splits into three tendinous heads. The medial head inserts on the posterior aspect of the summit of the next neural spine. The lateral head connects to the fascia of the M. tendino-articularis.

The lateral division of the semispinalis is the M. tendino-articularis. Anteriorly pointed cones of myosepta form successive slips in this muscle. It is

interconnected to the M. articulo-spinalis by a lateral tendon branch.

M. Longissimus Dorsi Lateral to the M. transversospinalis and separated from it by myosepta lies the larger M. longissimus dorsi (Fig. 2A and B). Posteriorly pointed cones of myosepta form the slips of this muscle. The internal margin connects to the lateral aspect of the M. tendino-articularis while the external margin connects with the M. iliocostalis. Each conical slip extends over three vertebrae and inserts on the distal part of the transverse processes. Fibers from the M. intertransversarii interweave with the fibers of the M. longissimus dorsi. The muscle originates on the anteromedial aspect of the ilium and inserts on the dorsal aspect of the transverse processes.

Neornithes

The dorsal epaxial musculature in birds is poorly understood with the M. longissimus dorsi compared with mammalian spinal muscles by Baumel, et al. (1993). Therefore, aside from several references that describe the dorsal epaxial muscles as a whole (Harvey et al. 1968; Zusi and Bentz 1984; Baumel et al. 1993), epaxial muscle divisions are based on the dissections of this study.

Intrinsic Vertebral Muscles The intrinsic vertebral muscles of the dorsal region are reduced because of dorsal vertebral fusion into the notarium. The Mm. interneuralis (also called Mm. interspinales) are absent. Even at the notarial-synsacral articulation and free dorsal vertebrae, the interspinus ligament is more developed than the Mm. interneuralis. The Mm. intercristales in birds might be homologous to Mm. interarcuales based on its lateral position to the Mm. interneuralis.

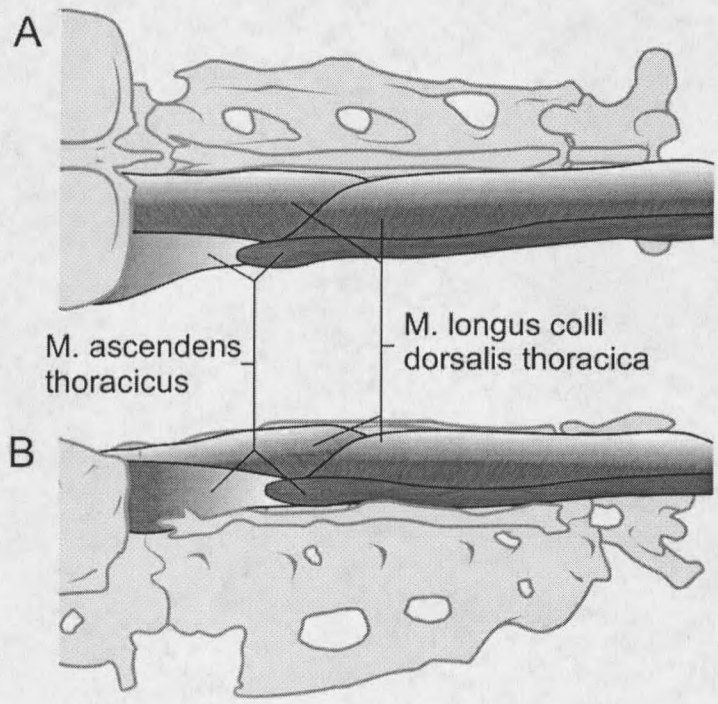

Figure 3. Diagram of major dorsal epxial muscles in *Meleagris*. A, dorsal view. B, lateral view. Anterior is to the right.

Mm. interarticularis superiores is also disrupted by the notarium, which generally lacks laterally projecting zygapophyses associated with this muscle. However, on the posterior free vertebra of the notarium and free dorsal vertebra, a fan shaped tendon attaches to the posterior aspect of the zygapophyseal joint. This tendon passes posteriorly to blend in with the fibers of the M. longissimus dorsi. This is the only candidate for the homologue to the crocodilian Mm. interarticularis superiores based on tendon insertion.

Mm. intertransversarii are present in the cervical region, but are absent over the notarium due to the osseous development between transverse processes, though the M. longissimus dorsi sends fibers ventrad through the transverse foramina. The anterior free dorsal vertebrae contains Mm. intertransversarii

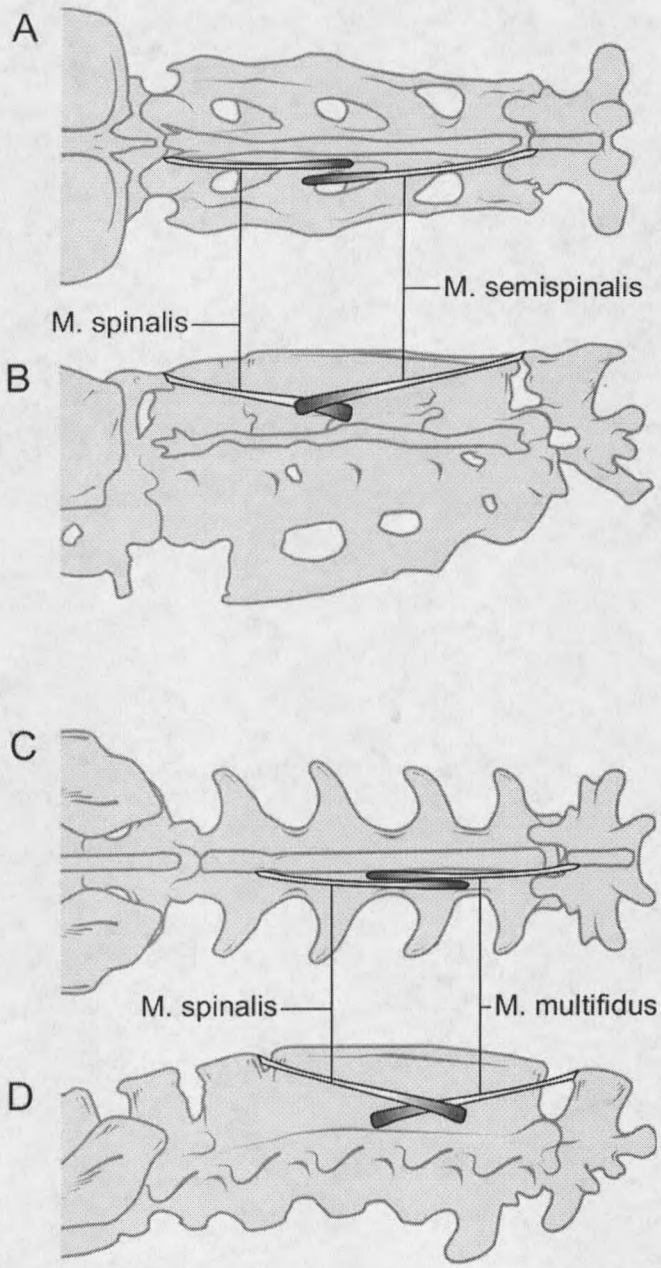

Figure 4. Diagram of the M. longus colli dorsalis thoracica slips in birds. A and B, dorsal and lateral view of the slips in *Meleagris*. C and D, dorsal and lateral view of the slips in *Podilymbus*. A and B demonstrate one condition in birds with an external layer homologous with the M. semispinalis of crocodilians. C and D demonstrate another condition in birds with an interal layer homologous with the M. multifidus of crocodilians. Anterior is to the right.

connecting it to the transverse processes of the neck and the notarium. A thick tendon of the lateral epaxial musculature laterally bounds this muscle.

M. Longus Colli Dorsalis Thoracica This muscle continues uninterrupted into the M. longus colli dorsalis of the neck and lies immediately lateral to the neural spines. And, it has obliquely running tendons located on its medial surface. These insert on the posterior or anterior summits of the neural spines, a complex morphology also seen in M. transversospinals of crocodilians. Given its location adjacent to the neural spines and obliquely angled tendons, this muscle is hypothesized to be the homologue of the M. transversospinals of crocodilians. Confusingly, this muscle is also called the M. longissimus dorsi in birds (Harvey et al. 1968), but M. longus colli dorsalis thoracica is preferred to avoid confusion with the M. longissimus in crocodilians, which it is not homologous with.

Like the homologous M. transversospinalis of other reptiles, this muscle complex is composed of various slips defined by their long tendons (Fig. 4). Unlike those in crocodilians, the fibers of this muscle are blended together and not easily divisible. Consequently, this complex muscle is better understood in a phylogenetic context. Birds possess two morphologies of the slips. In each morphology, the M. spinalis is present. This muscle slip is identified and homologized based on its origin at the base of the neural spine and tendons that run posterodorsally attaching to the anterior aspect of the neural spines or corresponding locations on the crest of the notarium or synsacrum. The number of tendons is variable and appears to be dependent on synsacral and notarial development. For example, in Galliformes only three tendons are present. The first tendon attaches onto the neural spine summit of the free vertebra at the notarial-synsacral articulation. The other two tendons attach to the roof of the

canal formed by the medial connection of the anterior iliac blades. In other birds, such as *Buteo, Podilymbus,* and *Ardea,* these tendons run along the entire dorsal region.

The two morphologies mentioned above are distinguishable based on whether the second oblique tendon layer is medial or lateral to the M. spinalis. If a medial layer is present, the lateral layer is absent and vice versa. The layer medial to the M. spinalis is hypothesized to be homologous to the M. multifidus based its medial anatomical location in relation to the M. spinalis. And, its origin at the base of the neural spine and tendons that run anterodorsally attaching on the posterior aspect of the neural spines also suggest that it is homologous to the M. multifidus. It is not interrupted by the notarium or synsacrum. The M. multifidus is present in Charadriiformes, Podicipediformes, and Struthioniformes.

The other morphology is characterized by a slip lateral to the M. spinalis, which it is separated from by a thin sheet of muscle tissue. This is hypothesized to be homologous to the crocodilian the M. semispinalis based on its lateral anatomical location in relation to the M. spinalis. Unlike the condition seen in crocodilians, it does not appear to be divisible into separate muscle slips anteriorly. This muscle originates at the base of the neural spine and passes anterodorsally to insert on the posterior summits of the neural spines or corresponding locations on the notarial or synsacral crests. Although it often passes along the dorsal region uninterrupted, in Galliformes the M. semispinalis inserts on the neural spine summit of the first free dorsal vertebra by one long tendon and on the posterior region of the notarium by two long tendons. Thus, like the M. spinalis, tendonous insertions over the notarium may be absent. The M. semispinalis occurs in Ciconiiformes, Galliformes, and Falconiformes.

Table 1. Muscle homologies between crocodilians and birds. Asterisks indicate mutually exclsuive presence of muscles.

Squamata	Crocodilia	Neornithes
	Intrinsic Vertebral Muscles	
M. interneuralis	M. interneuralis	M. interneuralis
M. interarticularis superiores	M. interarticularis superiores	M. interarticularis superiores
M. intertransversarius	M. intertransversarius	M. intertransversarius
	Dorsal Epaxial Muscles	
M. Transversospinalis	M. Transversospinalis	M. longus colli dorsalis thoracica
M. multifidus	M. multifidus	M. multifidus*
M. spinalis	M. spinalis	M. spinalis
M. semispinalis	M. articulo-spinalis	M. semispinalis*
	M. tendino-articularis	
M. longissimus dorsi	M. longissimus dorsi	M. ascendens thoracicus

In birds, the M. multifidus and M. semispinalis do not occur together. In either morphology, the posterior tendons run with muscle tissue through the canal formed the medial fusion of the preacetabular iliac blades. The M. longus colli dorsalis thoracica ends posteriorly at the posterior margin of the canal or outside it on the dorsal surface of the synsacrum medial to the anterior part of the M. levator caudae.

M. Ascendens Thoracicus This is lateral to the M. longus colli dorsalis thoracica (Fig. 3). It originates on the anterior margin of the iliac blades and the dorsal surface of the transverse processes. After inserting on the dorsal vertebrae (notarium) it passes forward to insert on cervical vertebrae. It may have two slips separated by an aponeurosis, as is the situation for *Meleagris*. In either case, longitudinally oriented tendons are often present deep within this muscle and insert on the transverse processes of first free dorsal vertebra. The position of this

muscle lateral to the M. longus colli dorsalis thoracica (homologized with the crocodilian M. transversospinalis), its attachment onto the ilium and transverse processes suggest that this muscle is homologous with the M. longissimus dorsi in crocodilians. Nishi (1938) suggests that this muscle is homologous with the crocodilian M. tendino-articularis. However, given its unique myosepta in crocodilians and the presence of the M. semispinalis in some birds, it seems more parsimonious to hypothesize homology between the M. ascendens thoracicus with the crocodilian M. longissimus dorsi. However, the evidence supporting either viewpoint is rather weak.

Muscle Reconstruction in Extinct Dinosaurs

Aside from the proposed muscle homologies (Table 1), the muscle-tendon systems described for crocodilians and birds share another feature, an architectural one, that might not be obvious from the preceding descriptions. The tendons of the M. multifidus and M. spinalis in crocodilians form a two layered rhomboidal trellis that lies vertically along the lateral aspects of the neural spines. More laterally, a third layer (M. semi-spinalis) is obvious upon dissection in *Alligator*. This three layered rhomboidal trellis is formed entirely by the M. transversospinalis tendon slips. The medial most layer runs anterodorsal, the intermediate layer posterodorsal, and the lateral layer anterodorsal. In birds, a two layered trellis is formed in the M. longus colli dorsalis thoracica by either the M. multifidus and M. spinalis or by the M. spinalis and M. semispinalis. Given the current phylogeny of Aves (Cracraft 1988; Sibley 1994) there does not appear to be a phylogenetic pattern for these morphologies. Another feature of the dorsal epaxial musculature that appears to have evolved independently is

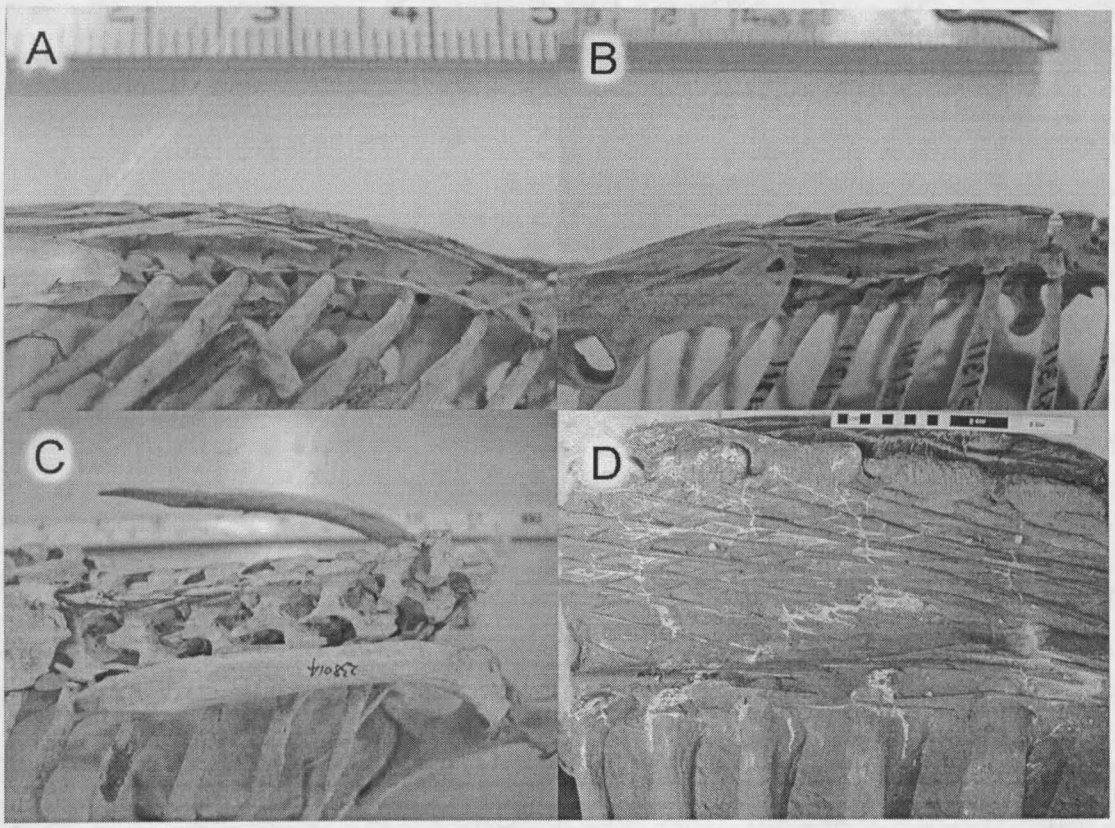

Figure 5. Ossified epaxial tendons in dinosaurs. The two layered trellis of the M. longus colli dorsalis thoracica in A, *Ptychoramphus aleuticus* (Cassin's auklet, Charadriiformes); B, *Podilymbus podiceps* (pied-billed grebe, Podicipediformes); and C, *Chuana torquata* (screamer, Anseriformes). A three layered trellis in a hadrosaur (*Brachylophosaurus*, MOR-794). Anterior is to the right in all panels.

an ossifying trellis. It is ossified in Charadriiformes, Podicipediformes and in *Meleagris*. In all birds that possess them, the ossified tendons of the trellis are fused to the neural spines. These are the "vertebral struts" of Storer (1982) and their length varies from short vertebral projections (e.g. *Chuana*) to long rods from the entire tendon (e.g. *Ptychoramphus*).

Unfortunately, the vertebral strut morphology only occurs in some birds. Since epaxial muscles do not appear to leave traces on the surfaces of vertebral bone, the struts (ossified tendons) provide the only osteological correlate from

vertebrae. However, ossified tendons are not only osteological correlates, but are fossilized parts of the muscle-tendon systems. Ossified tendons in Hadrosauriformes form a regular rhomboidal trellis structure along the neural spines of the dorsal, sacral, and caudal vertebrae. They begin in the latter cervicals, as is the case of *Iguanodon* (Norman 1980), or the anterior dorsals, in *Brachylophosaurus* (Prieto-Márquez 2001) and extend into the distal third of the tail. The lattice consists of three layers with a weakly developed medial layer, though all three might not be preserved (Dollo 1886; Norman 1986; Prieto-Márquez 2001).

In crocodilians and birds, the M. spinalis is easily identifiable because it is the only slip with a ventral anterior end that runs posterodorsally. In Hadrosauriformes, the lateral most layer also runs this direction. Therefore, it is a level I inference to reconstruct the lateral layer as the M. spinalis. The M. multifidus and M. semispinalis run anterodorsally, but only the M. multifidus is medial to the M. spinalis. Because the M. multifidus is present in crocodilians and in some birds, it is a level I inference to reconstruct the intermediate layer as the multifidus. The medial most layer of the Hadrosauriformes trellis runs parallel to the outer layer (M. spinalis) but has no apparent homologue in living archosaurs. Undoubtedly, this layer is the remains of another set of slips in the M. transversospinalis, and is probably unique (apomorphic). Although tendons of the M. semispinalis are not ossified, it is a level I′ inference to reconstruct this muscle slip in all non-avian dinosaurs.

There are rare fossil specimens that possess abnormal ossified epaxial tendons. For example, Molnar and Frey (1987) reconstruct the M. transversospinalis in *Minmi* from abnormal ossified tendons that form a lattice typical of the M. transversospinalis. Also, the ossified tendons in *Dryosaurus*

(Galton 1981) were possibly part of the M. transversospinalis based on their distribution along the neural spines.

Given these level I and I′ inferences, the trellis is probably the fossilized remains of the M. transversospinalis, not the M. longissimus dorsi. This reconstruction places the trellis close to the vertebral column, separated by only thin layers of muscle. Therefore, the Hadrosauriformes trellis was likely oriented in the parasagittal plane like those in birds and crocodilians. They undoubtedly attached to neural spines by unmineralized tendon entheses and to muscle by myotendinous junctions. This morphology of a bony core and flexible termini is common in ossified tendons in birds (Vanden Berge and Storer 1995; Landis and Silver 2002). Most ossified tendons have a tapered and flared terminus. Based comparisons with birds, the tapered end likely continued on as unmineralized tendon. The flared end either mineralized into the myotendinous junction or onto the fascia, giving it a fimbricated appearance. Ossified tendons are not usually attached to the vertebral column in non-avian dinosaurs. But some exceptions do exist. For example, it has been noted that some sacral tendons in *Iguanodon* are attached to the neural spines of that region (Norman 1986).

Reconstruction of the M. transversospinalis is harder to support in other groups of non-avian dinosaurs that lack a trellis of ossified tendons. Still, it is a level I′ inference to reconstruct the rest of the non-avian dinosaurs with the M. transversospinalis (including M. multifidus, M. spinalis, and M. semispinalis). Reconstruction of the outer M. tendino-articularis is a level II′ inference. This muscle slip, which has uniquely developed myosepta in crocodilians and apparently absence in birds, will not be considered further due to the lack of support inherent in a level II′ inference.

Other dinosaurs, such as some Hadrosauriformes (Dollo 1886; Prieto-

Márquez 2001), *Heterdontosaurus* (Santa Luca 1980), *Tenontosaurus* (Forster 1990; Winkler et al. 1997), and *Pachycephalosaurus* (Sues and Galton 1987) display parallel bundles of ossified tendons. Norman (1980) suggests that the ligamentum apicum dorsalis and the ligamentum transversarii in *Iguanodon* were displayed tendons from the lattice. But, the presence of these tendons in other ornithopods and *Pachycephalosaurus* suggest that they were not displaced. The parallel bundles of ossified tendons could be correlates to the Mm. interarticularis superiores or the M. longissimus dorsi. They could also be ossified tendons from both muscles, though the Mm. interarticularis superiores usually gives rise to short fan-like tendons in living archosaurs. In birds the M. ascendens thoracicus usually gives rise to longitudinally arrayed tendons, which may ossify (as in grebes). Therefore, it is a level II inference to reconstruct the parallel bundles of tendons at the base of the neural spines as the M. longissimus dorsi.

In Aves, the dorsal epaxial musculature is reduced and simplified compared with crocodilians. It also disrupted along the notarium and the synsacrum. The evolution of the dorsal epaxial musculature (such as the disappearance of the M. multifidus) is hypothesized to coincide with changes in the notarium and the synsacrum. Evolution of the dorsal epaxial musculature probably followed changes in progressive inclusion of sacral vertebrae in Neotheropoda, Maniraptora, Confuciusornithidae, Ornithothoraces, Ornithurae, and Neornithes (Hutchinson 2001b). Anterior expansion and medial migration of the preacetabular ilium correlates with vertebral fusion (Hutchinson 2001b) and notarial development, which began in *Archaeopteryx* (Baumel et al. 1993).

Discussion

Dollo (1886) supposed that the Hadrosauriformes ossified tendon trellis consisted of the M. spinalis dorsi, M. multifidus, and M. obliquu-spinales. However, he homologized the muscle tissue of living birds with the ossified tendons in *Iguanodon*. Thus, he proposed that the Hadrosauriforme trellis formed by atrophy of muscle tissue into ligament, which then ossified. Like Dollo, Norman (1980; 1986) suggests that epaxial muscles are reduced to ossified rods (tendons) for reasons of metabolic efficiency. Ostrom (1964) also agreed with Dollo's assessment, while Alexander (1985) suggests that the trellis represented the M. multifidus and M. spinalis based on Gasc's work on crocodilians (1981). Despite this recognition, epaxial musculature has consistently been reconstructed simply as the M. longissimus dorsi (Romer 1923b; Romer 1927; Lull and Wright 1942; Norman 1986; Hutchinson 2001b). Parks (1924) reconstructs the epaxial musculature based on slips defined by the ossified tendons, but then makes no reference to the musculature of living archosaurs.

This lack of epaxial muscle and tendon resolution has meaningful consequences for hypotheses about the paleobiology of extinct dinosaurs. Indeed, the trellis in Hadrosauriformes has long been considered a unique biological structure and is often used as a synapomorphy (Sereno 1986; Sereno 1999). In these analyses, Sereno coded the "two-layered lattice" as a character state of "ossified tendons". Given the presence of the trellis in living archosaurs and an ossifying trellis in Charadriiformes, Podicipediformes, and some Galliformes (*Meleagris*), it is plesiomorphic for archosaurs and convergently ossifies at least four times within Dinosauria.

Ossified tendons in ornithischian dinosaurs have historically been

interpreted in functional terms of rigidity (Dollo 1886; Brown 1916; Broili 1922; Colbert 1951; Ostrom 1964; Norman 1980; Norman 1986; Rothschild 1987; Bultynck 1992; Coombs 1995). These arguments are used to justify current paleobiological interpretations of Hadrosauriformes. For example, various authors (Brown 1916; Colbert 1951) use the trellis in arguments for the semi-aquatic habits of hadrosaurs. The trellis of ossified tendons is interpreted as an adaptation that provided additional support and power to lateral movements of the tail while swimming. Terrestrial interpretations of the trellis include Dollo's (1886) suggestion that it stiffened the body about the sacrum and tail. The resulting rigidity supposedly countered dorsoventral loading imparted by the M. caudofemoralis longus during locomotion. A second terrestrial interpretation suggests that the trellis of ossified tendons in Hadrosauriformes resisted sagging of the body about the hips (Ostrom 1964). The ossified tendon trellis is also suggested to have stiffened the tail mediolaterally, thus providing an additional argument against semi-aquatic hadrosaurs and iguanodons (Norman 1986). Since the trellis occurs throughout Dinosauria, these functional and behavioral claims must be reevaluated.

Conclusions

The M. multifidus and M. semispinalis are found to occur exclusively to one another in Neornithes as part of the M. longus colli dorsalis thoracica (homologous to M. transversospinalis in Crocodilia). The M. transversospinalis is reconstructed in Hadrosauriformes supported by a level I inference and in the rest of non-avian dinosaurs by a level I' inference. Reconstruction of the M. longissimus dorsi is less clear (level II phylogenetic support), but the parallel

bundles of tendons in some ornithischians are hypothesized to be the M. longissimus dorsi.

The slips of the M. transversospinalis form a two-layered rhomboidal trellis in Neornithes and a three layered rhomboidal trellis in Crocodilia. Moreover, these tendons are ossified in some birds: Charadriiformes (*Limnodromus scolopaceus* and *Ptychoramphus aleuticus*), Podicipediformes (*Podilymbus gigas, Podilymbus podiceps, Podilymbus major,* and *Aechmorphus occidentalis*), *Chuana torquata,* and *Meleagris*. Thus, various birds possess an ossified tendon trellis. This structure was thought to be unique to Hadrosauriformes. And, it has always been considered a key innovation for hadrosaurs and iguanodons. The trellis is plesiomorphic for archosaurs and ossification of the trellis occurs convergently within dinosauria. Given the widespread phylogenetic occurrence of the epaxial tendon trellis in dinosaurs, functional and behavioral interpretations as well as systematic utility, must be reevaluated.

CHAPTER 2

DEVELOPMENTAL PALEOBIOLOGY OF OSSIFIED TENDONS IN HADROSAURS

Introduction

Birds are the only living group of dinosaurs (Gauthier 1986), many of which possess tendons that mineralize and ossify during development. These avian groups include tinamous (Tinamiformes), penguins (Sphenisciformes), chickens and turkeys (Galliformes), cranes, herons, storks, ibises, and flamingos (Ciconiiformes), gulls and shorebirds (Charadriiformes), rails (Rallidae), owls (Strigiformes), hummingbirds (Trochilidae), woodcreepers (Dendrocolaptinae), and grebes (Podicipediformes) (Vanden Berge and Storer 1995). Ossification occurs in various tendons throughout the body, but most often in the shank, vertebral column, and wing. The process of avian ossified tendon development is well understood (Johnson 1960; Likins et al. 1960; Nylen et al. 1960; Abdalla 1979; Landis et al. 1995; Landis and Silver 2002).

Ossified tendons associated with the axial skeleton also occur in all Ornithischian dinosaurs, except for some thyreophorans. The most well known arrangement of these structures is found in hadrosaurs and iguanodons as a rhomboidal trellis several layers thick (Fig. 1). Dollo (1886) suggested that ossified tendons were ossified ligaments from atrophied epaxial muscle. Moodie's (1928) histological work agreed with Dollo's, though he termed the structures ossified tendons as they were thought to be derived from the tendons of the M. sacrolumbalis (Dollo 1886). In another histological analysis, Broili

(1922) suggested that the high vascular content indicates development directly from muscle tissue, skipping a ligamentous stage. Moodie (*idem*) and Broili (*idem*) mention histological work done on ossified tendons in birds (Lieberkuhn 1860). But, they did not use the developmental process of intratendinous ossification in birds to infer the development in the non-avian dinosaurs. This lack of comparison has led some authors, like Reid (1996), to conclude: "But, however their growth was initiated, the 'ossified tendon' described from *Iguanodon* is clearly not an ossified tendon in the literal sense of the term." Reid's "literal sense" may be interpreted as a tendon from a muscle-tendon unit that became ossified leaving no trace of the original tissue.

The question then arises: what are these bony structures in ornithischians? This question is important not only for physiological reasons, but because ossified tendons in ornithischian dinosaurs have historically been interpreted in functional terms of spinal rigidity (Dollo 1886; Brown 1916; Broili 1922; Colbert 1951; Ostrom 1964; Norman 1980; Norman 1986; Rothschild 1987; Bultynck 1992; Coombs 1995). These adaptationist interpretations have implications for posture, locomotion, and general biological understanding of extinct ornithischians. Since such interpretations date to Dollo (1886), who argued that these bony rods were developed from atrophied muscle, a developmental understanding of ossified tendons is essential to evaluate adaptational claims.

The aim of this study is to discover the developmental process of intratendinous ossification in ornithischian dinosaurs. This is accomplished by characterizing the histology of fossil tendons across three age classes (nestling, juvenile, and adult) of closely related hadrosaurs. These data are compared with an ontogenetic sequence of histological data from ossified tendons in birds. This comparison forms the basis for inferring intratendinous ossification

developmental patterns in hadrosaurs and other ornithischians.

Materials and Methods

Eighteen fossilized epaxial ossified tendons were sampled for histological sectioning from a nestling *Maiasaura peeblesorum* (Horner et al. 2000), two from a juvenile *Brachylophosaurus canadensis* and fifteen from an adult *Brachylophosaurus* (Prieto-Márquez 2001). Relative body size, suture fusion, and histology (e.g. lines of arrested growth or LAGs) of long bones were used to infer growth stages (Horner et al. 2000). The use of *Maiasaura* and *Brachylophosaurus* to infer developmental mechanisms in intratendinous ossification in hadrosaurs is justified by their status as sister groups (Fig. 6) and postcranial conservation in hadrosaurs (Weishampel and Horner 1990; Prieto-Márquez 2001).

Fossil specimens used in this study were collected from the Late Cretaceous Two Medicine (mid-late Campanian) and Judith River (late Campanian) Formations of Montana by Montana State University and Princeton University field crews. Taphonomically, all fossil tendons were articulated along the axial skeleton except the juvenile tendons, which came out of a monospecific bone bed for juvenile hadrosaurs. The fifteen tendons from the adult hadrosaur, a complete and articulated *Brachylophosaurus* (MOR-794, HIP 1999-20), were sampled from the dorsal, sacral, and caudal regions along the axial skeleton. Where possible, sections from MOR-794 tendons were taken from the termini and shafts of each tendon across the three laterally stacked layers. Juvenile *Brachylophosaurus* (MOR 1071, HIP 2002-14) tendon samples were taken from the shaft. Nestling *Maiasaura* (YPM-PU 22400, HIP 1990-18) samples were taken across the whole vertebral column, capturing vertebrae as well as tendons.

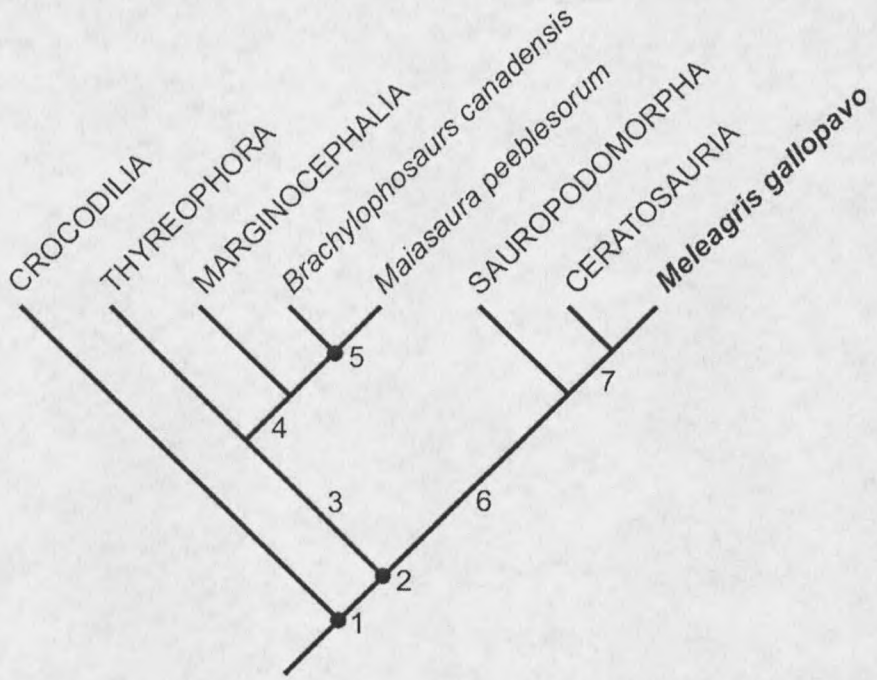

Figure 6. Phylogenetic framework used in this study. Stem-based groups are labeled at the branches and node-based groups are labeled at nodes. 1, Archosauria; 2, Dinosauria; 3, Ornithischia; 4, Neornithischia; 5, Hadrosaurinae; 6, Saurischia; 7, Theropoda. Modified from Sereno (1999).

Histological procedure followed standard paleohistological techniques (Wilson 1994).

Turkey (*Meleagris*) tendons were donated by the Seder Ridge Turkey Farm. Tendons from the M. gastrocnemius, M. fibularis longus, and M. longus colli dorsalis thoracica were sampled from two groups of turkeys: 16 week-old hens and 23 week-old toms. Using both sexes is justified because intratendinous ossification does not vary betweens sexes (Vanden Berge and Storer 1995). The tendons were fixed in 10% neutral buffered formalin for storage. Mineralized tendons from *Meleagris* were not decalcified before sectioning. *Meleagris* tendons were sectioned in different areas along their length to increase the apparent ontogenetic sampling range - avian tendons have a central ossification

center (Johnson 1960; Landis and Silver 2002). Hematoxylin and eosin (H&E) stains were used on the *Meleagris* samples. Terminology follows established nomenclature for bone (de Ricqlès 1980; Fancillon-Vieillot et al. 1990; Reid 1996; Currey 2002) and tendon microanatomy (Kannus 2000).

Histological Description

Turkey Tendon Histology

Figure 7A shows unmineralized tendon. It is ordinary vertebrate tendon, which is highly conserved across the group (Summers and Koob 2002). Mineralized tendons from the 16 week-old hen show a variety of histologic changes that are well documented in the literature (Lieberkuhn 1860; Johnson 1960; Abdalla 1979). These changes include enlarging fibroblasts within developing lacunae (Fig. 7B) that appear similar to hypertrophied chondrocytes or fibroblasts in tendon fibrocartilage (Rooney 1994; Benjamin and Ralphs 1998; Felisbino and Carvalho 1999). Associated with this change, crimp (waviness) is lost and collagen fibers become straight (Fig. 7B). Crimp loss is associated with a new matrix consisting of apatite that pervades the tendon, expanding as a mineralization front. Following these changes, resorption cavities appear, some of which possess scalloped edges indicating osteoclastic activity (Fig. 7C). Subsequently, in the 23 week-old turkeys, Haversian canals are present in the center of the tendon (Fig. 7C and D). These canals appear identical with those found in bone tissue. Primary osteons are absent, because the tissue is ossifying from the center. Vascularity is uniformly longitudinal.

The zone of transformation (mineralization) progresses from the middle of the tendon outward, centrifugally and longitudinally (Johnson 1960). This

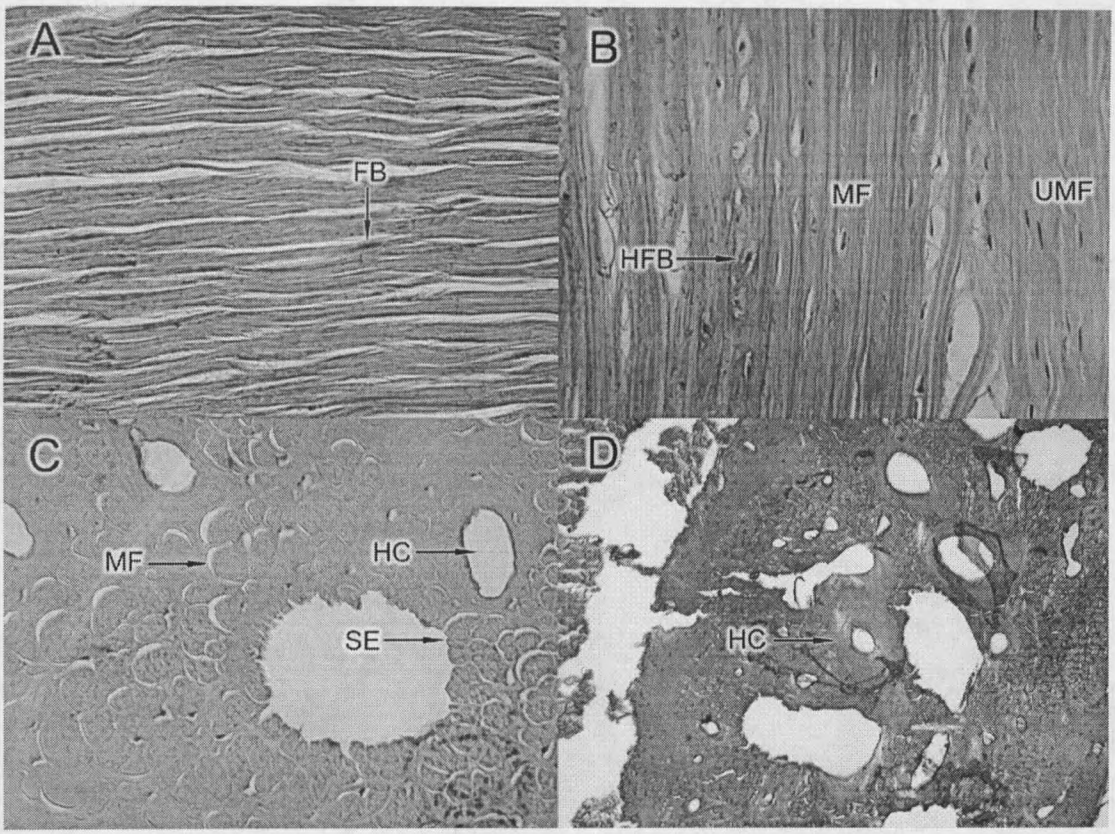

Figure 7. Histological photographs of *Meleagris* tendons. A, unmineralized tendon from a 16 week old hen with longitudinal fibroblasts (FB) lying along wavy collagen fibers (longitudinal section, 400x). B, hypertrophied fibroblasts (HFB) associated with the onset of ossification (longitudinal section, 400x). Also note the mineralized collagen fibers (MF) that have lost their characteristic waviness (UMF). C, tendon from a 23 week old tom that contains young Haversian canals (HC) and scalloped edged (SE) resorption cavities (cross section, 400x). D, a Haversian canal (HC) in an ossified tendon a 23 week old tom (cross nicols, cross section, 400x).

produces an osseous core present in most *Meleagris* tendons. Even in the 23 week-old toms, the original tendon paratenon surrounds an osseous core.

Hadrosaur Tendon Histology

Nestling *Maiasaura* tendons are characterized by a high degree of

vascularity, as is vertebral bone (Fig. 8A). Most of the cavities in the tendon are scallop-edged resorption cavities (erosion rooms). The vascular structure is uniformly longitudinal in orientation. Mineralized fibrils bound together in bundles constitute the base material. These are longitudinal like the orientation of the vascular canals. Nascent Haversian canals are present. Fibroblasts are large, round and reside between fiber bundles (Fig. 8B). Thick canaliculi project from fibroblasts.

The larger of the two juvenile samples (*Brachylophosaurus*) is identical with samples found in the adult tendons and contains three rest lines. These could be biomineralization tide marks or lines of arrested growth (LAGs). The rest lines are probably LAGs based on appearance, which implies periosteal accretion past the original boundary of the tendon. The smaller sample contains a core of dense Haversian bone in the center of the tendon (Fig. 8C). Many have cement lines around them indicating the previous existence of resorption rooms. Osteocyte lacunae and canaliculi are visible, though the latter are not always easily identified. The center of the tendon also contains longitudinal fiber bundles visible between osteons (Fig. 8D). In the periphery, the tendon possesses a different appearance, where collagen fibers are more abundant, as are primary osteons.

Ossified tendons from the adult hadrosaur (*Brachylophosaurus*) have more Haversian tissue and primary osteons than the nestling or juvenile. Figure 8E is representative of the general structure observed in mid-section. The perimeter consists of a thin layer of lightly vascularized tissue with longitudinally arrayed fibers. Vascularity in this region is almost solely comprised of primary osteons oriented longitudinally. The occurrence of multiple LAGs in every section is notable (Fig. 10A and B) compared with their absence in the turkey, nestling,

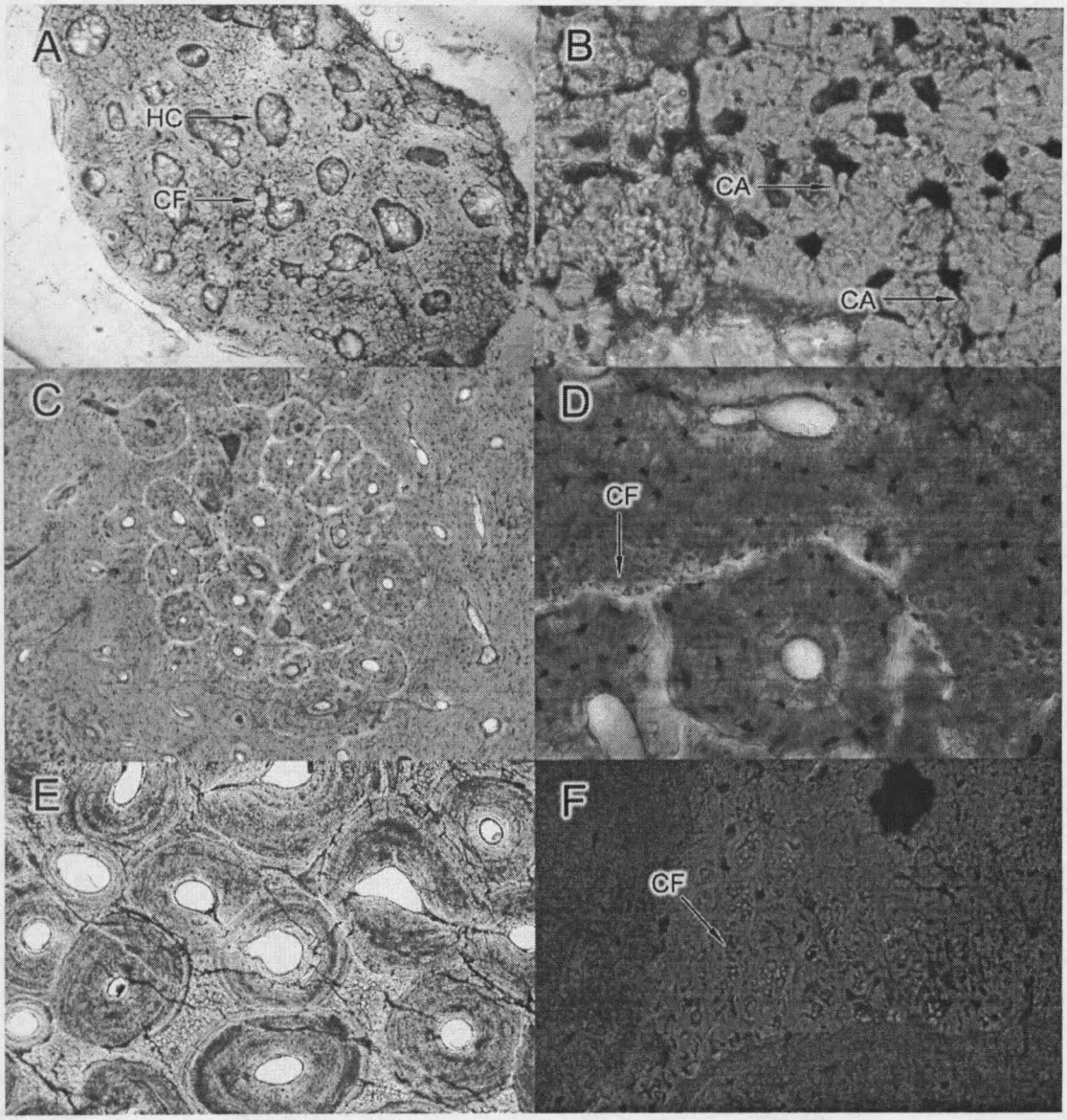

Figure 8. Histological photographs of hadrosaur tendons. A, tendon from a *Maiasaura* nestling (cross section, 40x). Note the abundance of collagen fibers (CF) and young Haversian canals (HC). B, detail image of fibroblasts and thick and stunted canaliculi (CA) (cross section, 400x). C, the juvenile *Brachylophosaurus* tendon contains a core of Haversian canals surrounded primary osteons (cross section, 40x). D, detail image of collagen fibers (CF) between Haversian canals (cross section, 400x). E, tendon from an adult *Brachylophosaurus* (cross section 100x). Note the dense Haversian bone. F, collagen fibers (CF) present between Haversian canals in another adult *Brachylophosaurus* tendon (cross nicols, cross section, 400x).

and one of the juvenile tendons. Lines of arrested growth are compressed at the surface forming an external fundamental system (EFS) in most samples. Primary osteons are present in the periphery with a high concentration of Haversian canals at the center of the tendon. While Haversian replacement is extensive in the shafts of the tendons, longitudinal collagen fibers are still present between some Haversian canals (Fig. 8F).

Sections of the proximal and distal ends of the adult tendons show dramatically less Haversian replacement and lack the LAGs seen in the shafts. Also, the ratio of fibrous tissue with respect to osteons is greater in the termini of the tendons compared with the shafts. Haversian canals are confined to the core of the tendon termini while the periphery contains mostly longitudinally arrayed fibers (Fig. 9B). Resorption cavities are concentrated centrally in the termini. Some samples also contain fields of thin dark filaments that run at oblique angles to the transverse sections of the termini. These are most likely Sharpey's fibers, suggesting that the termini interfaced with muscle or unmineralized tendon.

Discussion

Comparative Histology

Turkey tendon mineralization begins around 12 weeks with noticeable histological changes around 16 weeks of age, though the degree of mineralization varies among tendons within a particular animal (Johnson 1960; Abdalla 1979). This transformation can be thought of as a series of six stages. The first stage involves proliferation and hypertrophy of fibroblasts (tenocytes) (Johnson 1960; Abdalla 1979). Secondly, mineralization begins in extracellular vesicles, then separately in the small (40 nm) hole zone channels among sequentially

arrayed collagen molecules. These apatite crystals act as nuclei for crystal plaques that grow in the direction of the long axis of the tendon (Landis and Silver 2002). Collagen mineralization begins around the exterior of the bundles and proceeds into the fibrils (Johnson 1960). Increased vascularity also occurs at this time with the development of resorption cavities (Abdalla 1979). These features are interesting because tendon is normally not vascularized. Third, the collagen bundles enlarge to diameters of 15 μm, become dense, and lose crimp (waviness), which characterizes the so called transformation zone (Johnson 1960). This zone grows as apatite crystals form along the length of collagen fibrils (Traub et al. 1989; Landis and Silver 2002). During the fourth stage, fibroblasts develop canaliculi and become encased in lacunae through a new matrix (osteoid containing mostly collagen with lesser polysaccharide amounts and traces of lipid) that is secreted into the interstitial space among collagen bundles (Johnson 1960; Abdalla 1979). The fifth stage is marked by the onset of ossification. Osteoclasts further increase the size of the resorption cavities. Progressive Haversian system development is the final stage of intratendinous ossification (Johnson 1960). Vascularity is oriented longitudinally, an architecture parallel to the collagen fibers of the tendon.

As noted above, in avian species, mineralization begins in the central part of the tendon and proceeds axially and centrifugally (Johnson 1960; Landis and Silver 2002). The turkey tendons used in this study confirm these general findings, with the ratio of primary tendon tissue to osteonal bone higher in the 16 week-old turkeys than in the 23 week-old turkeys (Fig. 2). The histology of the hadrosaurian ossified tendons strongly suggests that this same developmental pattern was occurring. For example, the degree of osteonal development is lowest in the *Maiasaura* nestling, which contains young Haversian canals

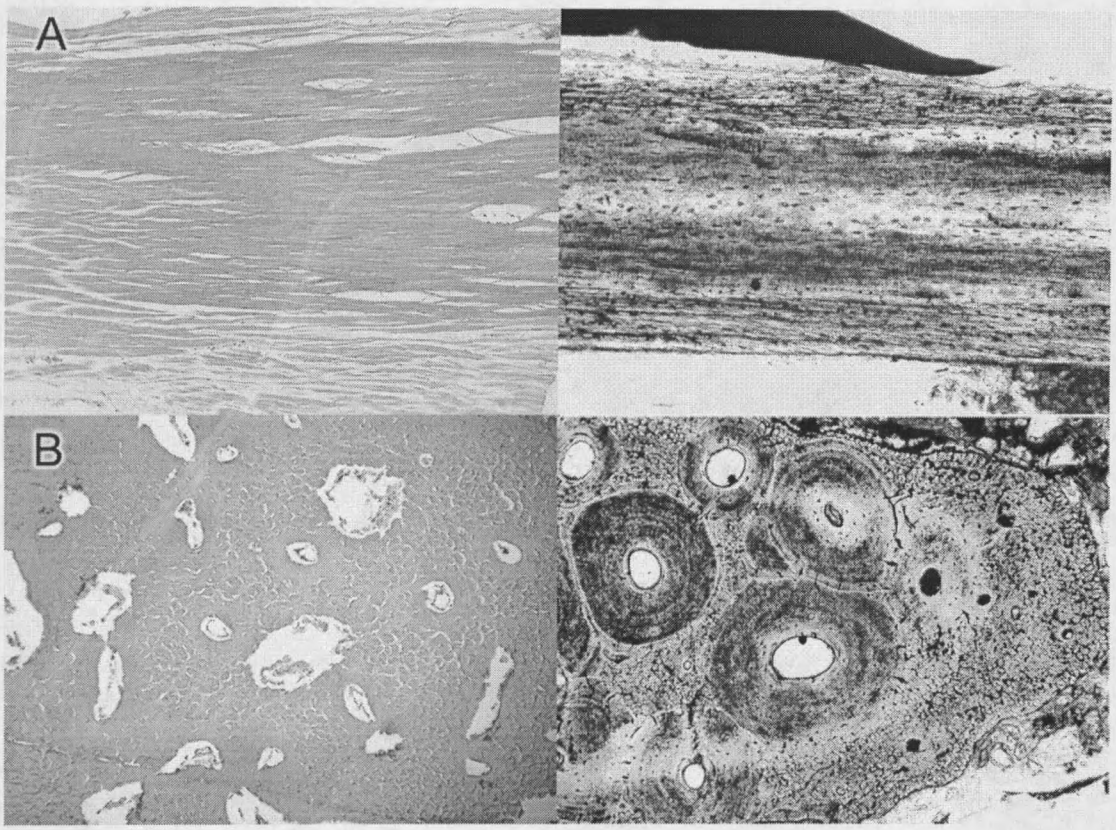

Figure 9. Juxtaposed histological images of *Meleagris* tendons on the left with *Brachylophosaurus* tendons on the right. A, core tissue surrounded by peripheral tissue (both longitudinal section, 100x). In the case of *Meleagris*, the core is composed of mineralized collagen fibers and the peripheral tissue unmineralized collagen fibers. The core of the fossilized *Brachylophosaurus* bone tissue is surrounded by straightened collagen fibers in a mineral matrix. B, cross sections arranged as above (both 100x). Mineralized core of a *Meleagris* tendon shows resorption cavities intersperced among collagen fibers. The tip of a *Brachylophosaurus* tendon shows a lesser degree of bone development than in the mid-shaft and contains scallop shaped collagen fibers similar to those seen in the *Meleagris* mineralized core.

and no primary osteons. This condition is characteristic of all 18 samples. Osteonal development is greater in the juvenile samples. The center is filled with Haversian bone demarcated by cement lines indicative of remodeling. The highest degree of Haversian development occurs in the shafts of the adult hadrosaur tendons. However, the termini of the adult hadrosaur tendons are filled with collagen fibers and few Haversian canals and primary osteons. Progressive bone development towards the center of the tendon is identical to the condition in intratendinous ossification in birds. Also, a core of dense tissue is surrounded by parallel arrayed fibers in the periphery. This suggests centrifugal ossification and is comparable to the morphology seen in lateral sections of from *Meleagris* tendons (Fig. 9A).

The base tissue in the nestling Hadrosaur tendons is composed of bundles of fibrils approximately 6 μm diameter. Fiber bundles are approximately 13 μm in diameter in the adult Hadrosaur. At higher magnification, these bundles consist of fibrils approximately 2 μm in diameter. In turkey tendons, 1 μm fibrils are packed together into bundles 15 μm in diameter (Johnson 1960). These fibril sizes are large compared with those found in non-mineralizing tendons, which range in diameter from 150-200 nm in the patellar tendon and 20-50 nm in the Achilles tendon in humans (Rooney 1994). Thus, similar size increases in fibril and bundle diameter due to intratendinous ossification in turkeys and hadrosaurs suggest a similar mode of development.

LAGs and the EFS

Lines of arrested growth are absent in the hadrosaur nestling (Fig. 8A and B). The larger sample of the juvenile tendon contains three LAGs while the smaller juvenile tendon lacks them. Along with fibrolamellar bone, multiple

LAGs characterize adult hadrosaur tendons (Fig. 10). These features are absent in the turkey tendons. Lines of arrested growth in ossified tendons of the juvenile and adult hadrosaurs is unusual in regards to their absence in the turkey specimen given their similarity on nearly all other histological features (save the degree of Haversian development). The lines could be interpreted as biomineralization tide marks, but these are not apparent in cross section of *Meleagris* tendons. Lines of arrested growth are produced by periodic cessation of periosteal growth, a plesiomorphic feature in tetrapods (Horner et al. 1999). They have been observed in dinosaur bone in most taxa and have been used in discussions of developmental paleobiology in dinosaurs and other archosaurs (de Ricqlès et al. 2000; Horner et al. 2000; de Ricqlès et al. 2001; Erickson et al. 2001; Horner et al. 2001; Stark and Chinsamy 2002). The lines in Hadrosaur ossified tendons were interpreted as LAGs by Horner and de Ricqlès *et al* (1999), where their number was found to correspond to LAG numbers in other skeletal elements across age classes. In this study, LAG numbers vary within and among tendons, a phenomenon discovered for LAGs in long bones in Hadrosaurs (Horner et al. 2000). The number of LAGs in ossified tendons at each growth stage (0 for nestling, 0-3 in the juvenile, and 2-5 in the adult) also corresponds to LAG development in hadrosaur long bones at the same growth stages (Horner et al. 2000). Moreover, the adult hadrosaur's tendon shafts appear to have an external fundamental system (EFS) formed by the compression of LAGs at the external surface. This indicates that new bone was being laid down in a manner similar to long bone appositional growth. Indeed, a nutrient vessel was discovered entering a tendon shaft in the adult hadrosaur. This feature is common in bone but absent in tendons, which are fed through the enthesis, myotendinous junction (Rooney 1994) or a vascular paratenon sheath (Kirkendall

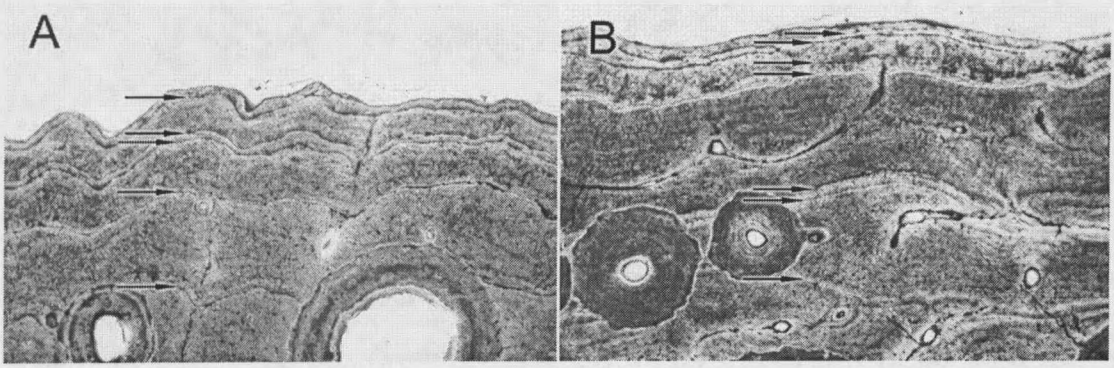

Figure 10. Adult hadrosaur tendons sectioned through the shaft. Note the arrows, which point to lines of arrested growth (LAGs). These features are normal seen in bone but are absent in the turkey tendons used in this study.

and Garrett 1997). Thus, this feature demonstrates the fully transformed condition present in the hadrosaur tendons.

What makes this interpretation novel is that intratendinous ossification is seen as a unique process of tissue transformation, so called metaplasia (Haines and Mohuiddin 1968). By definition, metaplasia is terminal tissue transformation into another type, namely bone. Thickened, stunted, or reversing canaliculi and hypertrophied fibroblasts are notable features for metaplastic bone at cartilage, ligament, and tendon entheses (Haines and Mohuiddin 1968; Reid 1996; Benjamin et al. 2002). Abnormal canaliculi are also known in new bone during repair (Kusuzaki et al. 2000). However, it has been noted (Reid 1997) that the lacunae of ossified tendons in extinct non-avian dinosaurs emit normal canaliculi. He also describes highly vascular osteoblastic tissue that could have only formed from an endosteum and a periosteum. These facts are then used to argue that dinosaurian ossified tendons were not of metaplastic origin. But, abnormal canaliculi are only found in the mineralized primary tissue not in subsequent bone deposition. And, ossified tendons in birds develop Haversian

systems with normal canaliculi (Lieberkuhn 1860; Abdalla 1979), so abnormal canaliculi should not be expected in the osteonal bone of ossified tendons in ornithischians.

Endochondral bone develops from a cartilage precursor. Chondrocytes hypertrophy, the precursor tissue mineralizes, and the bone grows centrally by marrow tube formation and peripherally by periosteal apposition (Castanet et al. 1993). Intratendinous ossification in birds occurs by the same general pattern, except the precursor tissue is tendon and it occurs late in development compared with endochondral bone ossification. But, the hypertrophied lacunae of ossifying tendon fibroblasts are not chondrocytes (Retterer and Lelievre 1911). Some authors (Suzuki et al. 2002) still refer to the hypertrophied tenocytes as chondrocytes at the fibrocartilage border of tendon entheses. However, given the association of hypertrophied fibroblasts with biomineralization in bone development, intratendinous ossification, and entheses, these cells are more appropriately identified as tenocytes not chondrocytes.

Ossified tendon development in hadrosaurs appear to have been timed with the development of their long bones, which indicates an earlier onset of ossification compared with birds. Also because hadrosaurs did not reach full size within a year, unlike living birds who reach adulthood within a year (Horner et al. 1999; Horner et al. 2000), the development of intratendinous ossification was prolonged compared with birds. This late developmental offset in tendon ossification was likely responsible for producing tendons composed of remodeled bone with a periosteum. Subsequent periosteal bone growth outside the perimeter of the original tendon best explains the occurrence of LAGS and an EFS.

Collagen fibers are present in adult hadrosaurs, but distinguishing among

fibers laid down by a periosteum and those of the original tendon is impossible based on appearance. Given the way tendons ossify in birds, the collagen fibers between Haversian systems at the tendon center may be from the original tendon tissue while those outside of the interior most LAG were probably deposited by a periosteum or a paratenon taking on a periosteal function.

Adaptation

Developmental evidence presented here suggests that caution should be exercised when forming adaptational or functional claims for ossified tendons in mechanical terms (e.g. increasing stiffness). There is no histological evidence suggesting that hadrosaur ossified tendons were derived from muscle tissue. In fact, the turkeys sampled for this study possessed ossified tendons in the M. longus colli dorsalis thoracica that did not appear atrophied at all, suggesting that Dollo's (1886) and Broili's (1922) developmental hypotheses are incorrect. Dollo's original claim that ossified tendons stiffened the vertebral column was based on the loss of epaxial muscles. Since ossified tendons did not develop from atrophied muscle, the basis for functional claims lacks support.

It has been claimed that ossification in tendons occurs mechanically through support of heavy loads and that ossified tendons in ornithischians resemble long rods of bone that develop in long tendons subjected to large continuous loads (Moodie 1927). And, pathological ossification (diffuse idiopathic skeletal hyperostosis or DISH) can occur at stress points in tendon and ligament (Rothschild and Martin 1993). Although ossified tendons are not pathologic, stress related DISH has been suggested as the mode of ossification in ornithischians (Rothschild 1987). Stress induced ossification has also been suggested for *Meleagris* (Landis and Silver 2002). However, it is unlikely that

forces generated in the hatchling physiologically caused these tendons to ossify given their small size and early onset of metaplasia before hatching. Embryonic *Hypacrosaurus* ossified tendons support this conclusion (Rothschild and Tanke 1992).

Conclusions

Ossified tendons develop by transformation of tendon into bone. Several characteristics distinguish intratendinous ossification from skeletal bone development. Skeletal bone and ossified tendons originate from precursor avascular connective tissue. The ability of fibroblasts to mineralize and vascularize this precursor tissue is shared by skeletal bone and ossified tendons. The shape of tendons constrains collagen fiber orientation into longitudinal orientation. Therefore, original tendon fibers and bone fibers laid down by a periosteum cannot be distinguished in heavily ossified hadrosaurian tendons. And, since they lack a periosteum, ossified tendons in birds cannot develop primary osteons, which are entrapped by periosteal growth. All osteons in avian ossified tendons are secondary.

Hadrosaur ossified tendons appear nearly identical with turkey ossified tendons at more advanced growth stages. Both change histologically along the length of the tendon becoming more ossified toward the center. Also, the increase in collagen fiber size through ossification is similar in both birds and hadrosaurs. These data suggest that the developmental process of intratendinous ossification is identical in both taxa, differing only in the onset, and offset of the process. While noticeable histological changes in turkey tendon appear around 16 weeks of age (Johnson 1960; Abdalla 1979), the hatchling *Maiasaura* already

has young Haversian canals developed. Since intratendinous ossification has also been reported in embryonic hadrosaurs (Rothschild and Tanke 1992), biomineralization must have begun embryonically. Thus, intratendinous ossification was initiated during a much earlier developmental stage in hadrosaurs than in birds. The degree of ossification in the adult turkey tendon slightly more developed than the hadrosaur nestling, but much less so than the juvenile hadrosaur tendon.

Hadrosaurian ossified tendons regularly develop fibrolamellar bone and secondary osteons, as well as LAGs and a periosteum. Early onset of metaplasia allows hadrosaurian ossified tendons to match the developmental patterns and timing of their long bones (Horner et al. 2000). Late offset of metaplasia produces ossified tendons that developmentally correspond with the rest of the skeleton - in terms of LAG numbers and presence of Haversian bone.

In his work on the histology of dinosaur bones, Reid (1996) states "But, however their growth was initiated, the 'ossified tendon' described from *Iguanodon* is clearly not an ossified tendon in the literal sense of the term." The histological data in this report argue against Reid's interpretation and suggest that the long bony rods found in hadrosaur dinosaurs are indeed tendons nearly identical with those found in their close living relatives, birds. Therefore, ornithischian ossified tendons should be interpreted as metaplastic tendons, not atrophied ligamentous muscle tissue or as a biologic structure of unknown origin.

This study revealed several areas concerning ossified tendon development in dinosaurs (including birds) that remain unanswered. For example, does this developmental process occur in all ornithischians? If so, is early onset and late offset of intratendinous ossification characteristic for this group? Did they evolve

by peramorphosis? Do birds of advanced age develop rest lines or LAGs? Will birds developmentally ossify their tendons even when normally metaplastic tendons are relieved of all stress? The answers to these developmental questions remain to be investigated.

CHAPTER 3

HISTOLOGY OF OSSIFIED TENDONS IN DINOSAURS

Introduction

Tendon microstructure is conserved in vertebrates (Summers and Koob 2002). But a strange phenomenon regularly occurs in many dinosaurian clades; tendons metaplastically transform into bone. This occurs in various avian species (Vanden Berge and Storer 1995) and in nearly all ornithischian dinosaurs, where they are synapomorphic (Sereno 1999). Ossified tendons are found in many body parts in birds such as the leg (Landis and Silver 2002), back (Rydzewski 1935), neck (Boas 1929), and wing (Vanden Berge and Storer 1995). Ornithischian tendons are morphologically similar to (though much larger than) ossified tendons found throughout Neornithes. They also develop by similar processes (see chapter 2). However, where in Neornithes they occur throughout the body, ossified tendons are found only along the vertebral column in ornithischian dinosaurs. Small ornithopod dinosaurs have tendon bundles that run along the dorsal aspect of the spinal column (e.g. Forster 1990). Hypaxial tendons are also present in the tail of these animals. Iguanodons, hadrosaurs, and lambeosaurs have an ossified tendon rhomboidal trellis along the dorsal aspect of their spinal column (Brown 1933; Lull and Wright 1942; Norman 1980; Norman 1986). Ankylosaurs have nested V-shaped tendons in their tails that extend anteriorly from the club (Coombs 1995). And enlarged bundles of tendons are often found at the base of pachycephalosaur spines (Sues and Galton 1987). There are also fossilized ossified tendons from taxa not known to experience intratendinous

ossification, such as *Minmi* (Molnar and Frey 1987). These isolated cases are more common than might be expected in non-avian theropods (MOR 693 and MNN TIG6) and a sauropods (DNM28).

Thus, ossified tendons occur in a wide phylogenetic range within Dinosauria. Since they are also located in many different areas in the body, they might be expected to develop by a variety of physiologic mechanisms and have disparate functions. Historically, histological descriptions have only been performed on isolated tendons and there are no data on whether ossified tendon histology varies according to anatomical region within an individual or across taxa. It is also unknown whether ossified tendon microstructure changes in different parts of the body in birds, the only living taxon that regularly experiences intratendinous ossification. Therefore, the primary aim of this study is to characterize ossified tendon histology across Dinosauria and determine their histological diversity within different body parts and across taxa. This is accomplished by histological sampling of tendons from animals that normally experience intratendinous ossification and from animals that possess abnormal ossified tendons. Tendons from living archosaurs (crocodilians and birds) are sampled to provide a phylogenetic basis for histological interpretations.

Materials and Methods

Fossil tendons were sampled from groups (Table 2) as broadly as possible within Dinosauria (Fig. 11). Fossilized ossified tendon samples consist largely of associated material from the vertebral column of adult specimens, but several (i.e. MNN TIG6 and MOR-794) were articulated with the skeleton. All fossilized tendons were sectioned across their mid-shaft with the exception of those

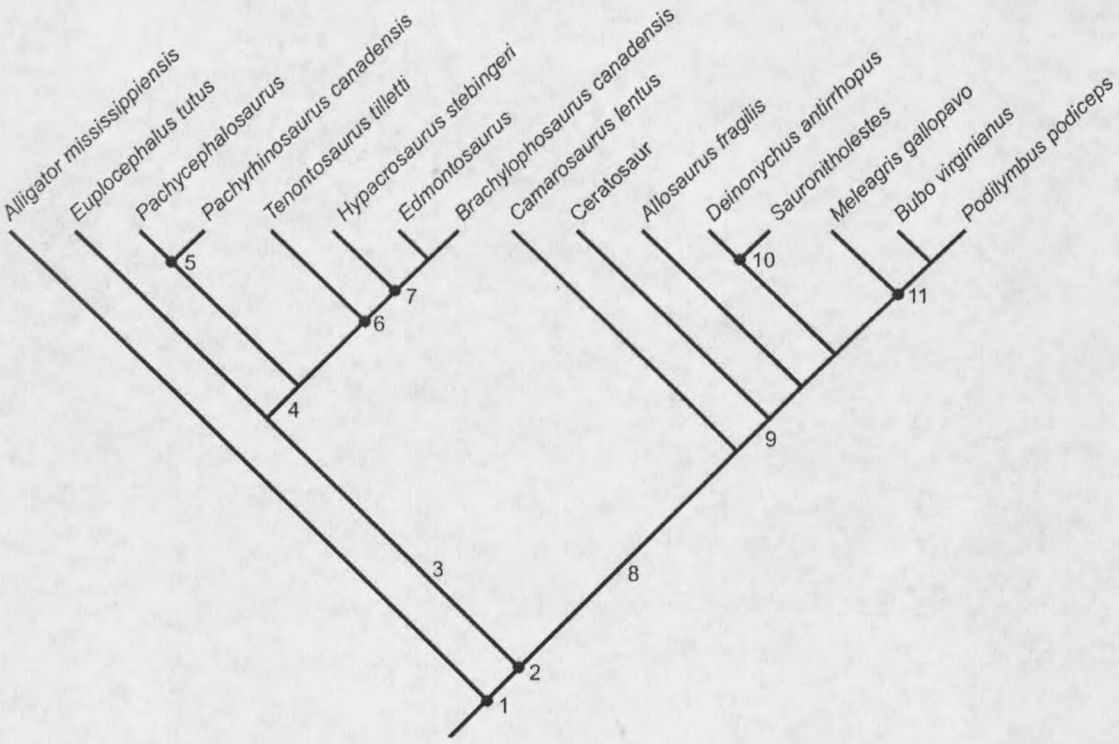

Figure 11. Phylogenetic framework used in this study. Stem-based groups are labeled at the branches and node-based groups are labeled at nodes. 1, Archosauria; 2, Dinosauria; 3, Ornithischia; 4, Neornithischia; 5, Marginocephalia; 6, Ornithopoda; 7, Hadrosauridae; 8, Saurischia; 9, Theropoda; 10, Deinonychosauria; 11, Neornithes. Modified from Gauthier (1986), Cracraft (1988), and Sereno (1999).

taken from MOR-794, which was sampled from the dorsal, sacral, and caudal regions along the axial skeleton. Where possible, sections from MOR-794 were taken from tendon termini and shafts across the three laterally stacked layers. Histological procedure followed standard paleohistology techniques (Wilson 1994).

Tendons from extant taxa were taken directly from dissected specimens (Table 2). These animals were donated to the MOR postmortem. *Meleagris gallopavo* tendons were sampled from the M. gastrocnemius, M. fibularis longus, and M. longus colli dorsalis thoracica from 16 week old hens and 23 week old

Table 2. Specimens used in this study. Asterisks denote living taxa. Institutional abbreviations are as follows: Denver Natural History Museum (DNM), Museum of the Rockies (MOR), Royal Tyrrell Museum of Paleontology (TMP), University of California Berkeley Museum of Paleontology (UCMP), National Museum of Niger (MNN TIG).

Specimen	Specimen ID	Histo ID
Outgroup (Crocodylia)		
*Alligator missippiensis**	-	2003-19r
Saurischia (Sauropoda)		
Camarosaurus lentus	DNM28	1997-9c
Saurischia (Theropoda)		
Allosaurus fragilis	MOR 693	1995-1
Ceratosaur	MNN TIG6	2003-09c
Deinonychus antirrhopus	MOR 747	2002-06
Sauronitholestes	MOR 660	1993-2
Saurischia (Theropoda: Aves)		
*Podilymbus podiceps**	-	2003-21r
*Meleagris gallopovo**	-	2003-20r
*Bubo virginianus**	-	2001-10r
Ornithischia (Ornithopoda)		
Brachylophosaurus canadensis	MOR 794	1999-20
Edmontosaurus	MOR 1142	2001-09
Hypacrosaurus stebingeri	MOR 549	1996-10
Tenontosaurus tilletti	MOR 680	2002-04
Ornithischia (Marginocephalia)		
Stygimoloch spinifer	UCMP 128383	1993-1
Pachyrhinosaurus canadensis	TMP 89.55.647	2003-14c
Ornithischia (Thyreophora)		
Euplocephalus tutus	TMP-83.36.120	2003-15c

toms. *Bubo virginianus* tendon was sampled from the M. extensor carpi radialus. The talor retinaculum and the M. gastrocnemius tendons were sampled from an *Alligator mississippiensis*. A tendon from the M. longus colli dorsalis thoracica was sampled from a *Podilymbus podiceps*.

Extant samples were fixed in 10% neutral buffered formalin for storage. Mineralized tendons were not decalcified before sectioning. The samples were

stained with hematoxylin and eosin (H&E), except for the *Bubo*, which was stained with toluidine blue. Images were taken from slides using an electronic camera. Microanatomy terminology follows established nomenclature for bone (de Ricqlès 1980; Fancillon-Vieillot et al. 1990; Reid 1996; Currey 2002) and tendon microanatomy (Kannus 2000).

Comparative Histological Description

Crocodilian Tendon Histology

Collagen fibers consisting of fibrils (Figure 12B, fibrils not apparent), arrayed longitudinally characterizes this tissue. Fibroblasts (tenocytes) run along these fibers (Figure 12B), which are sparsely arranged and cylindrical in shape in longitudinal sections. Collagen fibers demonstrate crimp common to tendon tissue. Fibers are bound together by endotenon sheathes to form fascicles (Figure 12A). Surrounding the endotenons is the peritenon (Figure 12A), which is demarcated by the transverse orientation of the tenocytes in this region.

Tendons in crocodilians are not known to mineralize in normal developmental processes. The samples from *Alligator* support the claim that crocodilian tendons are a conserved vertebrate tissue (Summers and Koob 2002).

Ornithischian Tendon Histology

Ornithopoda Within Hadrosauriformes, three taxa were sampled, a lambeosaur (*Hypacrosaurus*) and two hadrosaurs (*Brachylophosaurus* and *Edmontosaurus*). Aside from being epaxial, the exact anatomical locations of the tendons are unknown for *Hypacrosaurus* and *Edmontosaurus*. Tendons from the *Brachylophosaurus* were systematically sampled along individual tendons from

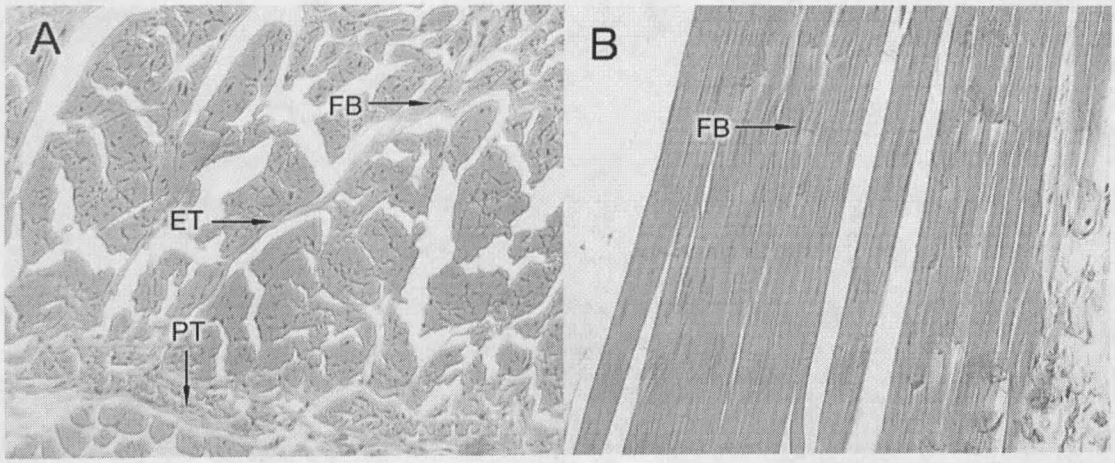

Figure 12. Histological photographs of *Alligator* tendons. A, cross section of Achilles tendon detailing endotenon (ET) divisions, fibroblasts (FB), and a peritenon (PT) sheath (100x). B, the same tendon is longitudinal section (40x).

the dorsal, sacral, and caudal regions.

Hadrosauriformes tendons are peripherally composed of fibrolamellar bone with longitudinally oriented primary osteons. Haversian canals are also present, become dense at the center (Fig. 13A), and are identical with similar tissue from long bone compacta. In some larger tendons, Haversian replacement is dense with many generations of osteons (Fig. 13B). Osteocyte lacunae and canaliculi are not always easily identifiable. Some collagen fibers are visible between osteons (Fig. 13F) though the center is nearly cancellous in some tendons. These fibers sometimes become dense toward the periphery, which often contains an external fundamental system (EFS), denoted by tightly packed LAGs (Fig. 13A and E).

Sections taken across the three tendon layers from the *Brachylophosaurus* are histologically identical. Also, there is no observable histological difference in samples taken from the dorsal, sacral, or caudal regions. But, variation occurs along the length of individual tendons. Sections taken through tendon termini

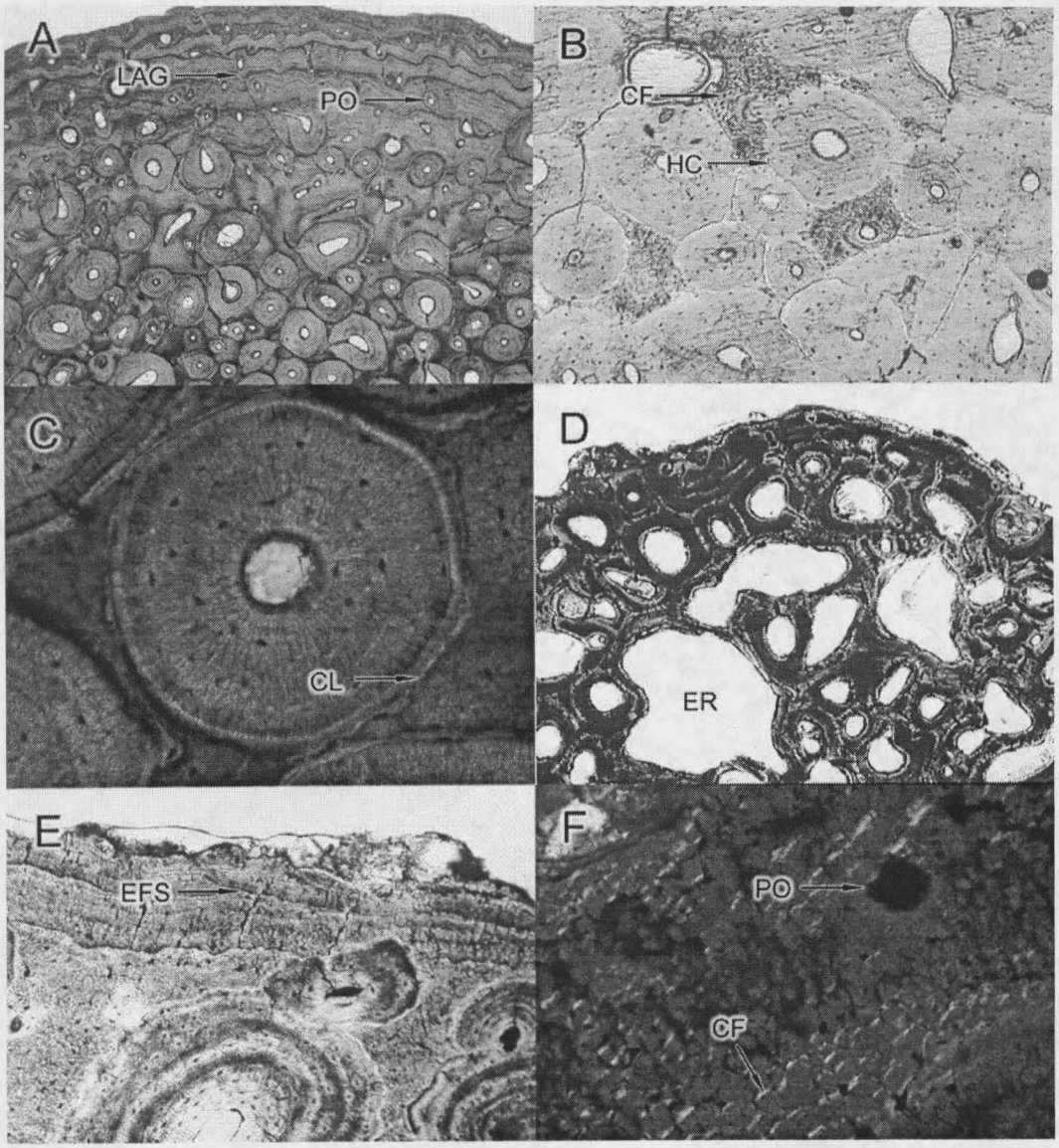

Figure 13. Histological photographs of Hadrosauriformes tendons. A, tendon from *Hypacrosaurus* (cross section, 40x). Notice multiple lines of arrested growth (LAGs), dense Haversian bone and primary osteons (PO). B, tendon from *Edmontosaurus* (cross section, 100x). Note Haversian canals (HC) and collagen fibers (CF) between Haversian bone. C, close up of an Haversian canal from *Hypacrosaurus* denoted by a cement line (CL) (cross section, 400x). D, pathological section of tendon from *Brachylophosaurus* (cross section, 40x). Note high proportion of erosian rooms (ER). E, close up an EFS from a *Brachylophosaurus* tendon (cross section, 100x). F, close up of collagen fibers (CF) and a primary osteon from a *Brachylophosaurus* tendon (cross section, cross nicols, 400x).

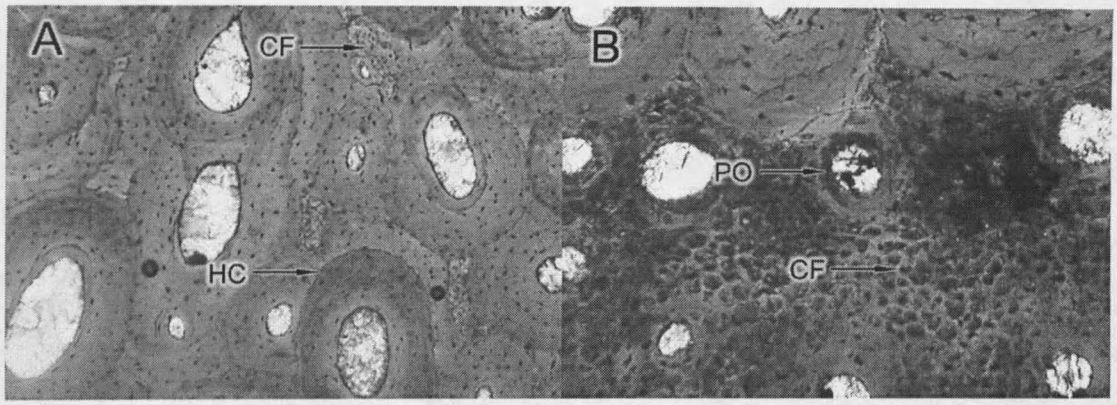

Figure 14. Histological photographs of *Tenontosaurus* tendons. A, central portion of the tendon, dense with Haversian canals (HC) (cross section, 100x). Note collagen fibers (CF) between the canals. B, close up of collagen fibers (CF) and primary osteons (PO) (cross section, 400x).

are filled with collagen fibers and less lamellar tissue. In *Brachylophosaurus*, LAGs vary along tendon length, becoming more abundant at the center.

Several samples were taken from a pathological region in the dorsal aspect of the tail (a common occurrence in hadrosaur tails). Grossly, some tendons in this region continue over the pathological neural spines uninterrupted while others are eroded. Histologically, this tissue is similar to the termini in other *Brachylophosaurus* tendons (Fig. 13D). Both have large erosion rooms. However, the number and size of erosion rooms in the pathological tendon is much greater. While there is no evidence of the pathology's origin (e.g. bacterial infection), the tissue suggests that active growth and repair was occurring at the time of death.

Epaxial tendons from the *Tenontosaurus* caudal region contain longitudinally oriented collagen fibers and primary osteons in the periphery. Several generations of Haversian canals are present at the center, which contains many large resorption cavities that form a reticular cancellous region. Like the Hadrosaur tendons, some fibers are present between osteons even in the central

region with dense Haversian bone (Fig. 14A and B). Some tendons also contain LAGs and an EFS.

Marginocephalia Tendons from the *Pachycephalosaurus* contain a core nearly identical with those seen in ornithopod tendons. That is, tissue is characterized by an abundance of collagen fibers oriented longitudinally. These are interrupted by resorption spaces, primary osteons, and Haversian canals. Vascular orientation parallels the fiber bundles. Surrounding the core is fibrolamellar bone. Vascularity is reduced in this region and has alternating orientation from longitudinal to radial (Fig. 15A). Immediately outside the core, vascularity is longitudinally oriented. More distally is a band of obliquely radially canals followed by a band of radially oriented canals. Radially oriented vascular spaces dominate the perimeter.

Spread through the fibrolamellar section are isolated areas of rough bundled tissue consisting of enlarged collagen fibers (Fig. 15A). These areas look identical to the tendon's center and are globular in shape, though one is band shaped. Osteocyte lacunae in the fibrolamellar regions are smaller than those in regions dominated by rough bundled collagen fibers.

Beyond being epaxial, the anatomical location of the tendon from the *Pachyrhinosaurus* is unknown. A cancellous region occupies the tendon's center (Fig. 15B). The bone forming this cancellous region is lamellar. The periphery consists of fibrolamellar tissue, with longitudinal vascularity (Fig. 15C). Multigenerational Haversian systems are present at the border between the two bone regions, but are obliterated centrally by the lamellar cancellous tissue (Fig. 15D). Lines of arrested growth are absent.

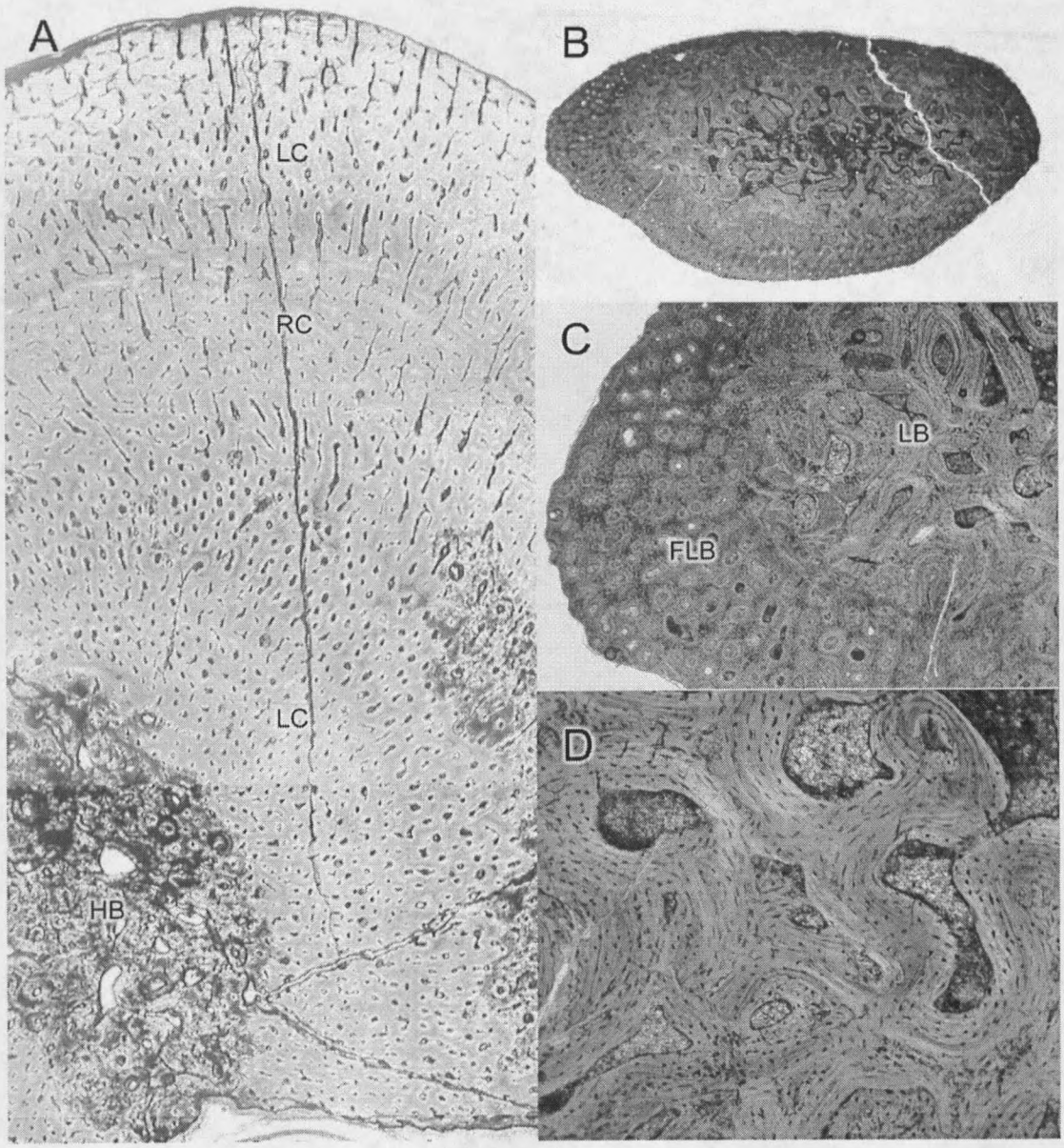

Figure 15. Histological photographs from marginocephalians. A, composite image from *Stygimoloch* (cross section, 40x). Note alternating longitudinal (LC) and radial (RC) canals. Also, note the central core of Haversian bone (HB). B, *Pachyrhinosaurus* tendon (cross section, 10x). C, same tendon at 40x. Note the outer region of fibrolamellar bone (FLB) and interior region of lamellar bone (LB). D, same tendon at 100x in the lamellare region.

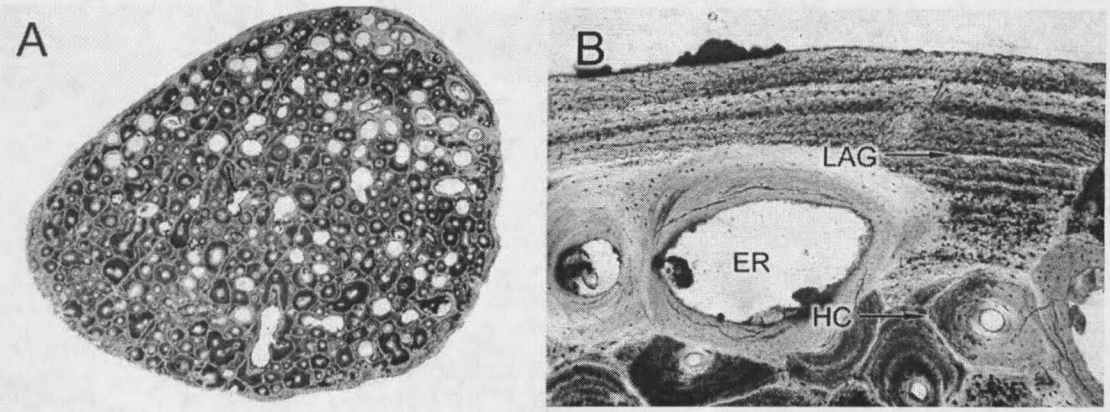

Figure 16. Histological photographs of *Euplocephalus* tendons. A, the whole tendon in cross section (10x). B, detail of periphery in the same tendon (100x). Note how closely multigenerational Haversian canals (HC) extend to the surface. Also, note that the primary tissue contains many lines of arrested growth (LAG). Erosian rooms (ER) are also present.

Thyreophora Samples from an *Euplocephalus* (Ankylosauridae) tail club consist of dense Haversian bone (Fig. 16A). Some erosion rooms are dispersed through the Haversian bone. Vascular orientation is longitudinal. Haversian systems are so developed that no trace of collagen fibers are present except close to the surface (Fig. 16B). LAGs are present in the peripheral region. Osteocyte lacunae are larger in this region and circumferentially oriented.

Saurischian Tendon Histology

Sauropoda The abnormal *Camarosaurus* tendon contains primary collagen fibers and a few primary osteons in the periphery (Fig. 17A). This region is not uniform circumferentially, and in some areas it consists of multiple generations of Haversian canals. Other portions of the periphery are filled with relatively avascular rough bundled tissue. Dense Haversian tissue occurs throughout the center and lacks collagen fibers between canals. The tendon's central part also contains resorption cavities. No LAGs are present in the periphery. Osteocyte

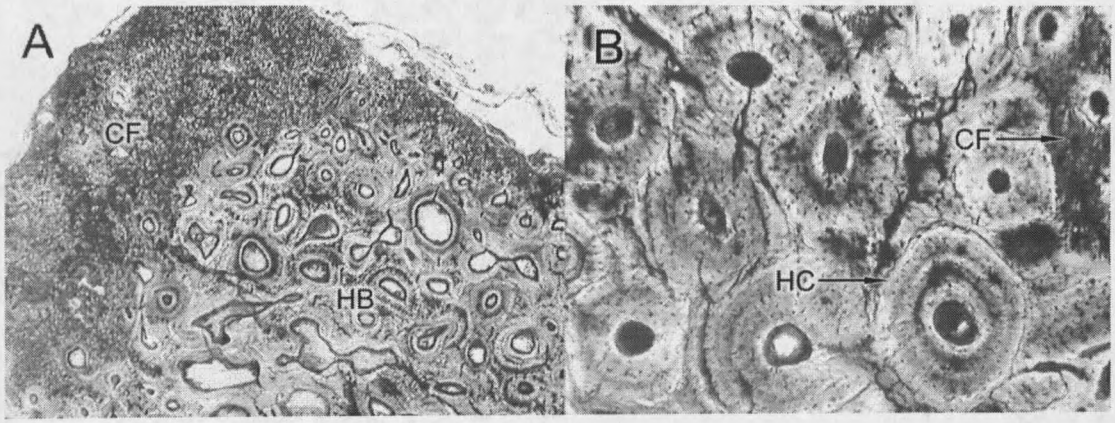

Figure 17. Histological photographs of *Camarosaurus* tendons. A, cross section of tendon (40x). Note the peripheral region of comrpised of collagen fibers (CF) and the central core of Haversian bone (HB). B, close up of central region (cross section, 100x) Note collagen fibers (CF) between some Haversian canals (HC).

lacunae are not specifically shaped and canaliculi are present as thin filaments.

Non-Avian Theropods Several abnormal ossified tendons from the sacral neural spines of an unnamed ceratosaur appear grossly similar to other ossified tendons sampled in this study. These are preserved sections of the muscle-tendon system of the M. transversospinalis (see chapter 1) and thus homologous to the ossified tendons in Hadrosauriformes. Histologically, mineralized collagen fibers oriented longitudinally comprise the tendon (Fig. 18A). The periphery is marked by LAGs (Fig. 18B). Some Haversian canals are present centrally. Fibers are large and rough bundled interior to the first LAG and fine outside of it. This change in fiber structure may indicate the boundary of the original tendon. If so, this would indicate that intratendinous ossification did not develop in terms of onset and offset like ossified tendons in Ornithischians (see chapter 2).

Allosaurus tendons possess a periphery consisting of vascularized fibrolamellar bone tissue (Fig. 18C). Vascular orientation is longitudinal

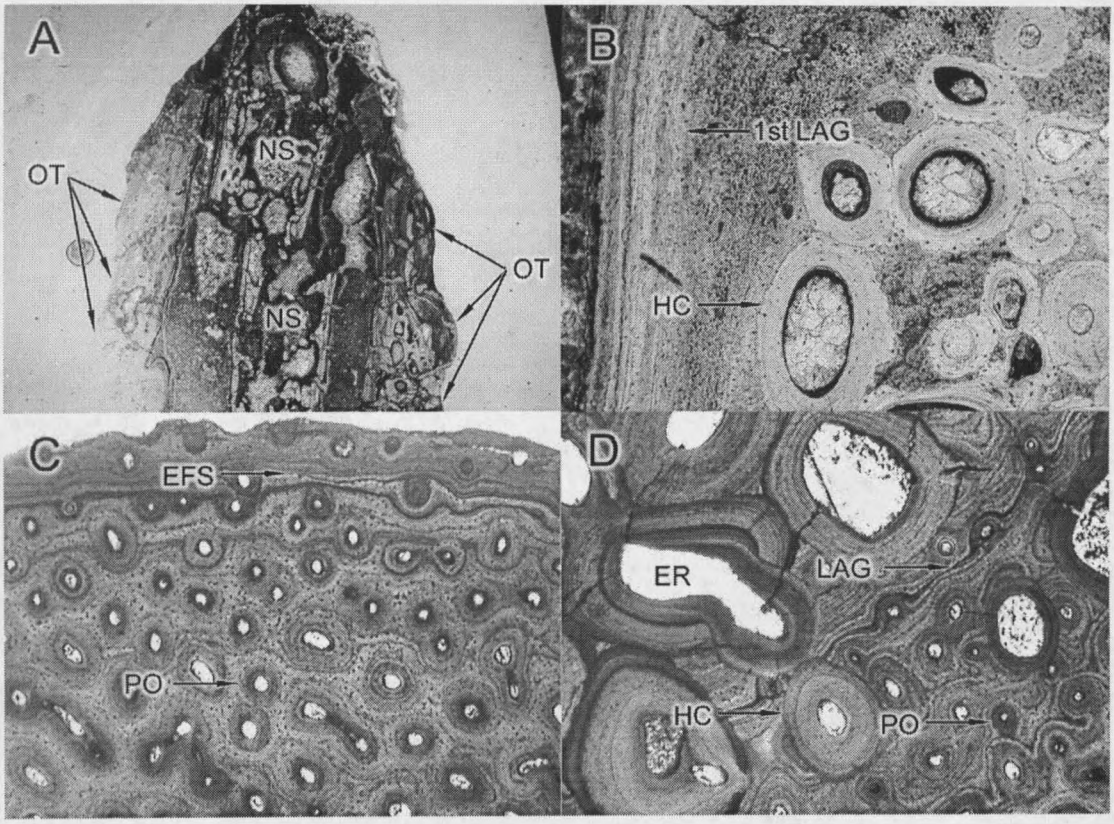

Figure 18. Histological photographs of non-avian theropod tendons. A, cross section across neural spine (NS) and ossified tendons (OT) in a ceratosaur (10x). B, close up of a tendon with Haversian canals (HC) (100x). Note the rough bundled apperance of the fibers interior to the first line of arrested growth (1st LAG). C, an *Allosaurus* tendon (cross section, 40x). Note the fibrolamellar structure with primary osteons (PO) and an EFS. D, central region of the same tendon (100x). Note the erosian room (ER), Haversian canals (HC), primary osteons (PO), and centrally located LAGs.

throughout the tendon. Primary osteons within a longitudinally arranged fiber matrix characterize the periphery. Centrally, it is composed of multiple generations of much larger Haversian canals and resorption rooms (Fig. 18D). The size of the latter forms a central cancellous region. Osteocyte lacunae are generally ovoid in the fibrous tissue and flattened in lamellar tissue. Lines of arrested growth occur throughout the tendon. The interior most line occurs just beyond the central Haversian region. Lines of arrested growth occur sporadically

towards the periphery, becoming tightly packed at the subsurface forming an EFS.

Tail rod bundles from *Saurornitholestes* are poorly preserved. They consist of dense Haversian bone (Fig. 19A). These reach the surface in some places in all tendons. Few resorption cavities are present. The small periphery is filled with longitudinally arranged collagen fibers. Multiple LAGs are visible in all tendons. These lines become tightly packed near the surface indicating an external fundamental system.

The tail rods (elongated prezygapophyses and chevrons) from *Deinonychus* contain tightly spaced rings consisting of ordered avascular fibrous tissue (Fig. 19C). This is fine structured tissue with sparse osteocyte lacunae. A few primary osteons are present in some rods, though two contain concentric rings of primary osteons in the periphery. Several other rods (Fig. 19B) contain central Haversian systems. They are large and adjacent to the vertebral body and have longitudinal orientation. Distal to the vertebrae, the rods become avascular. Centrally, all rods contain a loosely packed fiber core (Fig. 19D).

Neornithes Ossified tendons in *Meleagris* contain a mineralized fiber core in which collagen fiber bundles are still apparent in cross section (Fig. 20A). These bundles are scallop-shaped and separated from the surrounding matrix. These give the mineralized tendon a scaly appearance. In tendons that are heavily ossified (due to increased age or variation within an individual), the spaces among the scalloped fiber bundles is filled in with a new osteoid matrix giving the tissue a more fascicular appearance. Centrally, large irregular erosion rooms are common. A few Haversian systems are present. *Meleagris* tendon histology from this study agrees with published descriptions (Lieberkuhn 1860;

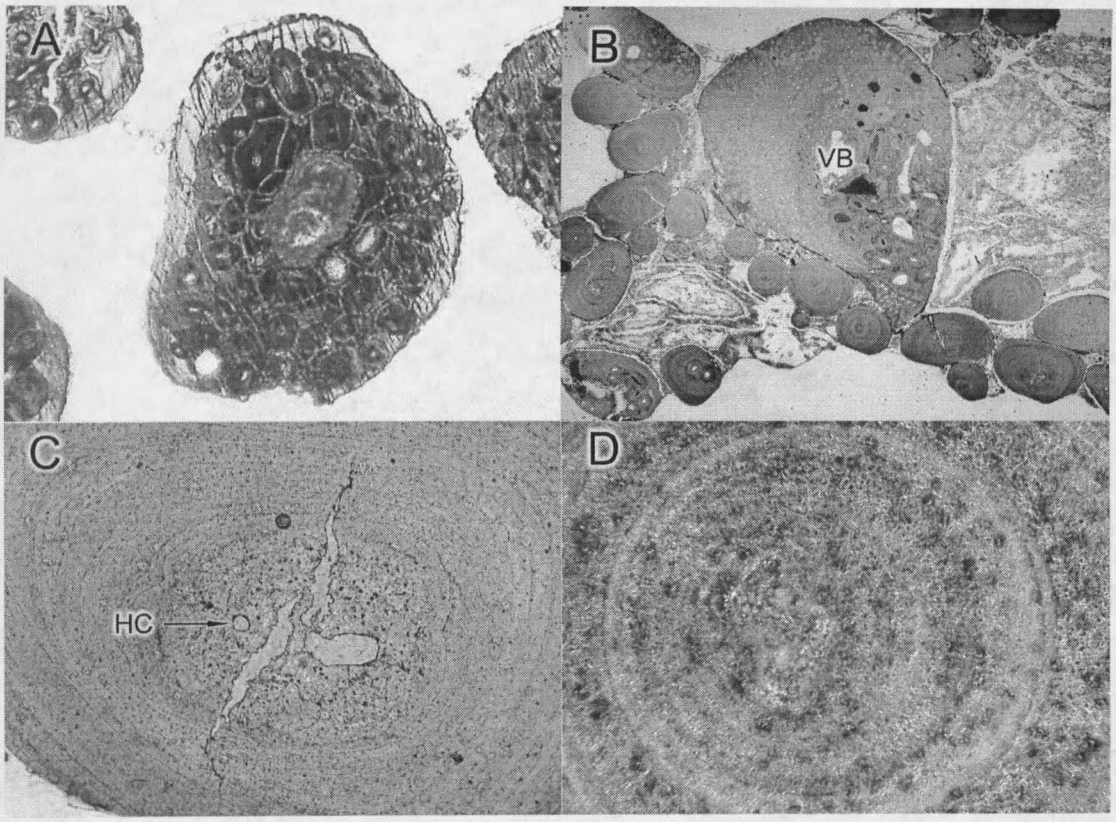

Figure 19. Histological photographs of non-avian theropod tendons "tail rods" or ossified tendons. A, cross section from *Saurornitholestes* (10x). Taphonomic alteration makes detailed interpretation difficult, but note the dense Haversian bone. B, ossified tendons and vertebral body (VB) of *Deinonychus* (cross section, 10x). Note that some exterior tendons are vascular. These are proximal sections close tho their origin. C, close up of a tendon (cross section 100x). Note the fine grained rings and a core of loosely arranged fibers with two Haversian canals (HC). D, close up up central region (cross section, cross polar, 400x). Note the uniform arrangement of longitudinally oriented primary fibers.

Weidenreich 1930; Abdalla 1979).

Longitudinal sections clearly show mineralized areas with fibers that have lost their characteristic waviness (crimp) and become straight (Fig. 20B). Fibroblasts in mineralized regions are hypertrophied and contain large amounts of cytoplasm. These cells appear similar to hypertrophyied chondrocytes.

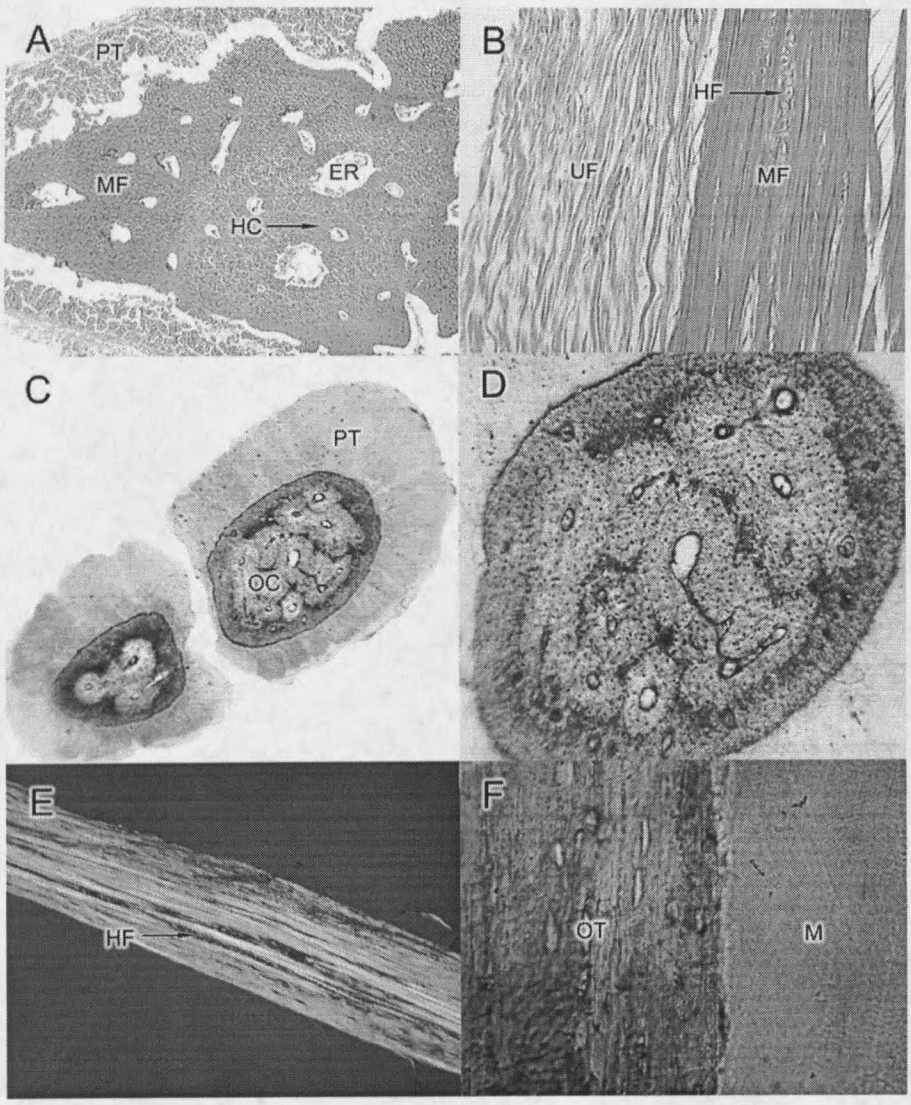

Figure 20. Histological photographs of Neornithes ossified tendons. A, *Meleagris* tendon containing a mineralized core surrounded by a paratenon (PT) (cross section, 40x). Note the matrix of mineralized collagen fibers (MF), Haversian canals (HC), and ersoian rooms (ER). B, longitudinal section of same tendon (100x). Note the exterior unmineralized fibers (UF) and the straightened mineralized fibers (MF) that contains hypertrophied fibroblasts (HF). C, tendon from *Bubo* (cross section, 10x). Note the thick peritenon (PT) surrounding the osseous core (OC). D, close up of the core in the same tendon (100x). E, tendon from *Podilymbus* (longitudinal section, cross polar, 100x). Note the chain of hypertrophied fibroblasts (HF). F, another *Podilymbus* tendon (longitudinal section, 400x). Note obliquely angled muscle tissue (M) attaching directly onto the surface of the ossified tendon (OT).

Long chains of hypertrophied fibroblasts run down the long axis. As with the cross-sections, the central area is mineralized with straight fibers. This core is surrounded by unmineralized tendon tissue with wavy fibers and elongated tenocytes.

Some tendons (i.e. many shank tendons) extend the zone of transformation into the myotendinous part to produce a fan-shaped myotendinous origin. The zone of transformation also extends into the tendon entheses (bone insertions) in many epaxial tendons, which ossify to the neural spine summits. Despite this difference, there is no difference in microanatomy between leg and epaxial tendons.

Thin-sections from *Bubo* appear similar to those of *Meleagris*, but with a very thick peritenon. These thin-sections were taken from 1 cm proximal to the M. extensor carpi radialis insertion point. A clear demarcation occurs between the central osseous core and the unmineralized peritendon (Fig. 20C). The central region consists of primary osteons and first generation Haversian canals (Fig. 20D). Between some Haversian canals mineralized collagen fibers can be seen. Collagen fibers have the same scalloped shape and overall bundled appearance seen in the turkey. LAGs and primary osteons are absent from this tissue.

Lateral tendon sections from the M. longus colli dorsalis thoracica in *Podilymbus* are comparable with those from *Meleagris*. For example, collagen fibers run straight along the longitudinal axis and chains of hypertrophied tenocytes are common (Fig. 20E). Fibroblast shape is fusiform when they are not in chains. But, ossified tendons from *Podilymbus* lack an unmineralized outer tendinous sheath (peritendon). This is evident where the M. longus colli dorsalis thoracica interfaces directly with the ossified tendon without an unmineralized intermediate (Fig. 20F). Therefore, the original myotendinous junction is replaced

by a fleshy attachment along the length of the tendon.

Discussion

The *Alligator* and unmineralized *Meleagris* tendons are indistinguishable. Furthermore, archosaur tendon microanatomy appears identical with normal tendon found in mammals (Kannus 2000). This conforms to the claim that basic tendon structure is conserved within vertebrates (Summers and Koob 2002). It also establishes a basis from which intratendinous ossification in dinosaurs can be evaluated (i.e. normal unmineralized tendon is plesiomorphic for Dinosauria).

Ossified Tendon Diversity and Evolution

Despite the general hyperostosis found in the non-avian dinosaur ossified tendons and the further osseous development seen in the marginocephalians, ossified tendons have many characteristic features. Many workers describe these features in birds and non-avian dinosaurs (Lieberkuhn 1860; Broili 1922; Moodie 1928; Koehnlein 1930; Weidenreich 1930; Johnson 1960; Abdalla 1979). For example, Lieberkuhn (1860) identifies chondrocytes in bird tendons, later correctly termed hypertrophied tenocytes by Retterer and Lelievre (1911). These cells are responsible for the mineralization process. Lieberkuhn (*idem*) also describes the straightened tendon collagen fibers in longitudinal section and the scalloped fascicular appearance of fiber bundles in cross section. Indeed, longitudinally isotropic fibers and vascularity are characteristic of ossified tendons. This orientation is due to the cord-like shape of the tendon precursor tissue.

The other feature that is characteristic of ossified tendons is tenocyte

hypertrophy. This cellular morphology occurs in ossified tendons, cartilage caps, and tendon and ligament entheses. (Haines and Mohuiddin 1968). Haines and Mohuiddin (Idem) identified this phenomenon in tenocytes on the unmineralized side of the blue line (mineralization tide mark) in tendon entheses. There hypertrophied fibroblasts occur in long chains, a structure that appears in ossified tendons as well (Fig. 20B and E). Although these cells are still called chondrocytes due to their cellular morphology (e.g. Suzuki et al. 2002), this in inappropriate (Retterer and Lelievre 1911; Landis and Silver 2002).

Haines and Mohuiddin (Haines and Mohuiddin 1968) also note that osteocyte canaliculi in metaplastic bone are absent, stunted, or looped. This feature was observed in some ossified tendons in this study. But this type of canaliculi is restricted to mineralized tendon tissue. The lamellar bone (osteons) formed in ossified tendons is indistinguishable from normal bone (Lieberkuhn 1860; Weidenreich 1930). Thus, highly remolded ossified tendons lose all traces (hypertrophied tenocytes, collagen fibers, and absent or looped canaliculi) of their ancestral tissue. The only indicative feature left in these cases is isotropic longitudinal vascular orientation, which is a product of the tendon's chord-like gross morphology.

As has been noted (Lieberkuhn 1860; Retterer and Lelievre 1911), the bone laid down during metaplasia is indistinguishable from normal bone tissue. Furthermore, ossified tendon's histological features are uniform across different anatomical regions. There is essentially no difference in microanatomy between leg tendons and those from the back. The wing tendon microstructure of *Bubo* is also similar to *Meleagris* tendon microstructure. However, the peritenon is much thicker, forming a solid border around the osseous core. Given the development of Haversian bone, an indicator of late stage intratendinous ossification, a thick

peritendon maybe a characteristic of wing tendons. Anatomical location of the tendon and associated wing function may account for the thickened peritenon or it may be taxic variation.

Unlike other birds, *Podilymbus* ossified tendons do not possess an unmineralized peritenon. This difference might be caused by age-related differences among specimens. However, it shows that the M. longus colli dorsalis thoracica can directly interface with the ossified tendon by a fleshy attachment. The homologous ossified tendons from *Meleagris* do not interface in a direct bone to muscle attachment. Since ossification begins centrally and spreads outward (Johnson 1960) and all ornithischian ossified tendons have LAGs, they probably ossified the entire tendon, then grew by a periosteum like endochondral bones (see chapter 2), thus interfacing with epaxial muscles like those seen in *Podilymbus*. Because Hadrosauriformes epaxial tendons are homologous with the epaxial ossified tendons in birds (see chapter 1), this is important for epaxial muscle reconstruction. Furthermore, the same type of muscular interface can be used to infer reconstruction from other epaxial ossified tendons found in Ornithischia, such as parallel tendons in *Tenontosaurus*.

The high density of Haversian canals and presence of LAGs, primary osteons, and an EFS indicate that the bone comprising the tendon is as old as the skeletal elements. Histological study of ossified tendons should not rely on individual samples because variance in histology along tendon length could dramatically alter interpretations. For example, a fragment from the center of an ossified tendon would look histologically much older than a sample from near a terminus.

Samples taken from both marginocephalians (*Pachycephalosaurus* and *Pachyrhinosaurus*) are better ossified than tendons from all other dinosaurs.

Pachycephalosaurus tendons possess a loosely packed core consisting of Haversian bone, and longitudinally oriented collagen fibers. Islands of this bone type are found throughout the outer region, which is formed from tightly packed fibrolamellar tissue. The vascular orientation in the outer region alternates between longitudinal and radial. This is the only known ossified tendon (living or extinct) to have such a structure. All other ossified tendons are extremely isotropic, with vascularity and collagen fiber orientation parallel to the long axis. This sample may reveal a developmental constraint. That is, all other ossified tendons are constrained in their collagen and vascular orientation due to the underlying isotropic tendon structure and function. For some unknown reason, vascular orientation alternates in *Pachycephalosaurus*, suggesting a freedom from this constraint. Alternately, radial vascular orientation could indicate a reduction in axial stress during appositional osseous growth.

The other marginocephalian tendon (*Pachyrhinosaurus*) was also more remodeled than other tendons examined in this study. While it does not contain the alternating vascular structure found in the pachycephalosaur, it possesses a cortical region filled with fibrolamellar bone of anisotropic fibers and a medullary region composed of lamellar tissue. Unlike non-marginocephalians, it lacks uniformly oriented collagen fibers. In fact, there are no histological features to suggest that this tissue is an ossified tendon. Ossification development in this sample is unusual, but not unique. Therefore, while the *Pachyrhinosaurus* tendon suggests greater intratendinous ossification maturity in ceratopsians, developmental plasticity and a sample size of one makes interpretations equivocal at the present time.

Tail Rod Tendons

Prezygapophysis elongation is a progressive trend in Tetanurae (Gauthier 1986). Thus, it would seem that the "tail rod tendons" of Maniraptorans are just prezygapophysis extensions. In this scenario, they should be formed in a manner similar to vertebral bone. However, the prezygapophysis and chevron extensions of *Deinonychus* have been described as developing through tendon sheaths taking on periosteal functions (Ostrom 1969; Ostrom 1990; Reid 1997). Considering the intratendinous ossification process in birds (Johnson 1960; Abdalla 1979; Landis and Silver 2002) and hadrosaurs (see chapter 2), this seems unlikely since metaplasia begins centrally in the tendon. The periphery is the last region to mineralize and ossify in normal intratendinous ossification. But this is not the case in the tail rod tendons. Indeed, the opposite is true. They lose vascularity distal to the vertebral body and have an outer region of fine fibrous bone and a central loosely organized fiber core. This unusual histology is most likely the result of small amounts of appositional growth compared with longitudinal growth. Because there are no extant analogues for comparison, the exact developmental nature of these tail rods remains unknown. But, given that prezygapophysis elongation is a trend in Tetanurae (Gauthier 1986), they are probably periosteal bony rods.

Conclusion

In their review paper on ossified tendons in birds, Vanden Berge and Storer (1995) find no physiological or biomechanical function that accounts for their sporadic appearance in Aves. The current study, which includes non-avian dinosaurs and birds, did not bring clarity to the phylogenetic pattern of

intratendinous ossification. The *Bubo* wing tendon contains an peritenon sheath much larger than other ossified tendons. However, because *Bubo* does not have ossified tendons in other areas of the body for comparison, it is unknown if this feature is phylogenetic or functional. Within individual *Meleagris*, there is no variation in terms of metaplastic development or histological structure. These data seem to contradict the common notion that tendons ossify in response to biomechanical stress (Landis and Silver 2002), which would suggest that different tendons throughout the body ossify at different rates as they are subjected to different tensile stresses. Thus, caution should be used when inferring the adaptive significance of intratendinous ossification in birds. Inferring intratendinous ossification function from extinct dinosaurs is even more problematic.

Histological features also seem to be free of body size related constraints. That is, the histology in avian taxa appear virtually identical (save the expanded peritenon in *Bubo*) despite various body sizes. The same is true of non-avian dinosaurs, from the unnamed ceratosaur to *Tenontosaurus*. Thus, size mediated ossification, through progressively greater tensile stress application does not seem to affect intratendinous ossification.

The only discernable phylogenetic difference in tendon histology is the relative degree of osseous development. All extinct dinosaur tendons examined, including the abnormal ossified tendons, are better ossified than those in living birds. Most non-avian dinosaur ossified tendons possess LAGs, primary osteons, and many have an EFS, indicating the presence of a periosteum. Within Ornithischia, marginocephalians appear to experience even greater osseous development in epaxial tendons. This condition is unknown in living animals. Therefore, ossified tendons in extinct non-avian dinosaurs reveal a physiological

process that would remain unknown by studying living animals alone.

No differences where detected in abnormally (i.e. *Allosaurus* or *Camarosaurus* tendon) vs. normally ossifying tendons. And, tendon microstructure was homogenous across the trellis layers in a *Brachylophosaurus*. But, LAGs were found to vary within tendons along their length. It is likely that original tendon fibers are abundantly preserved in a ceratosaur as well as between central Haversian canals in many non-avian dinosaur tendons.

Maniraptoran tail rods do not appear to be a unique form of intratendinous ossification. The fine fibered structure surrounding a loosely organized core was not encountered in any other taxa, living or extinct. A histological survey of Tetanurae zygapophyses could help illuminate the tissue's developmental nature. Tail tendon rod development may also have functional implications because of its impact on caudal muscle structure. Further research is needed to reconstruct the caudal muscles associated with these rods in maniraptorans.

Classically, ossified tendons have been categorized as "grobgebündelte grundsubstanz – faserknochen" or "rough bundled bone tissue" by Weidenreich (1930). This categorization seems appropriate due to the fact that all bone is metaplastic. No data from living or extinct dinosaurs were found to argue with Weidenriech's designation.

CHAPTER 4

OSSIFIED TENDON BIOMECHANICS IN ORNITHOPOD DINOSAURS

Introduction

Hadrosauriformes possess a bony rhomboidal trellis along the dorsal aspect of the spinal column (Fig. 21). It is formed by ossified tendons from the M. transversospinalis (see chapter 1). Although the trellis is present in all archosaurs, an ossified tendon trellis is only known in Hadrosauriformes (Sereno 1986; Sereno 1999) and some birds, such as grebes (see chapter 1). The trellis in Hadrosauriformes has prompted many functional interpretations, which may be divided into aquatic and terrestrial speculations. Various authors (Brown 1916; Colbert 1951) use the trellis to argue that hadrosaurs were semi-aquatic. The ossified tendon trellis is claimed to have functioned by providing additional support and power to lateral movements of the tail while swimming.

Hadrosauriformes are now thought to be terrestrial with horizontal posture (Ostrom 1964; Galton 1970; Norman 1980; Norman 1986). In the first terrestrial interpretation, the trellis (in an *Iguanodon bernissartensis*) is suggested to stiffen the body about the sacrum, counteracting dorsoventral loading from the M. caudofemoralis longus (Dollo 1886). Dollo (*idem*) interprets these animals standing in an erect posture with the tail on the ground. Although iguanodons and hadrosaurs are currently reconstructed with a horizontal posture (Galton 1970), the caudofemoral muscles were still probably important for locomotion as the primary femoral retractor (Gatesy 1995).

Another terrestrial interpretation suggests that the ossified tendons trellis

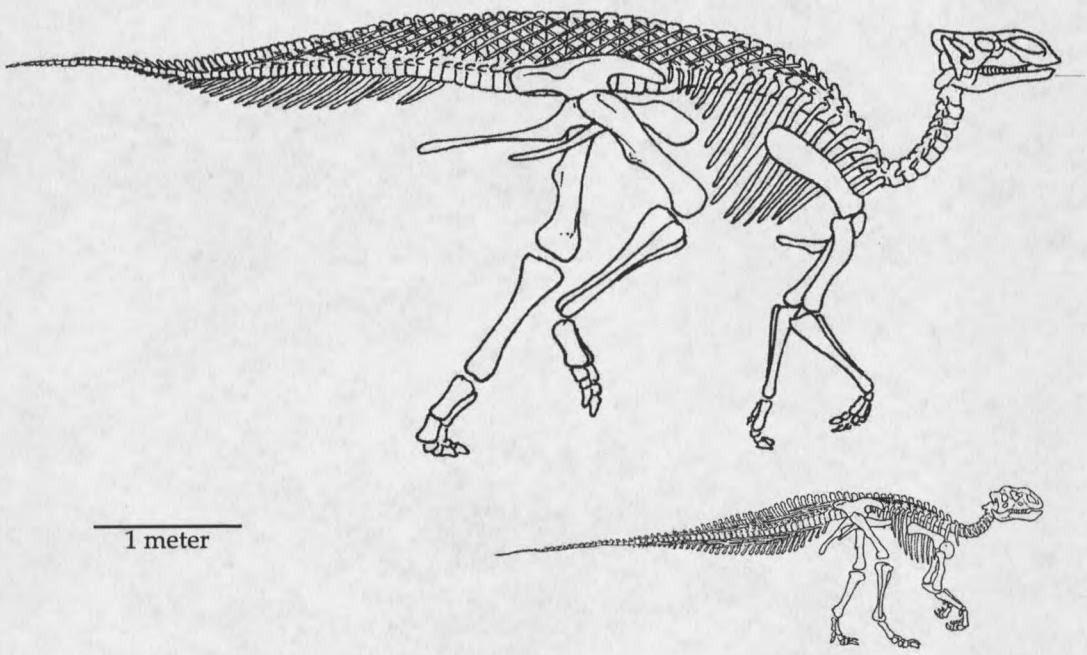

Figure 21. Reconstruction of *Brachylophosaurus* (on top) and *Tenontosaurus* (bottom). The relative sizes depicted are based on MOR 794 and MOR 682, the specimens used in this study.

in Hadrosauriformes resisted sagging of the body about the hips (Ostrom 1964). The trellis arrangement is used as an argument for terrestrial habits because of its similarity to a balanced cantilever bridge, which bears weight through loading cross members. Intratendinous ossification is used as primary supporting data for this argument, because bone has greater tensile strength than tendon. This argument also uses Hadrosauriformes taphonomy (their vertebral column is usually preserved "ram-rod" straight) as supporting evidence (Lull and Wright 1942; Bultynck 1992). Another argument against the semi-aquatic interpretation suggests that the trellis produced mediolateral tail stiffness (Norman 1986).

Other authors claim that ossified tendons did not stiffen the vertebral column at all by noting that long tendons can ossify when transmitting large

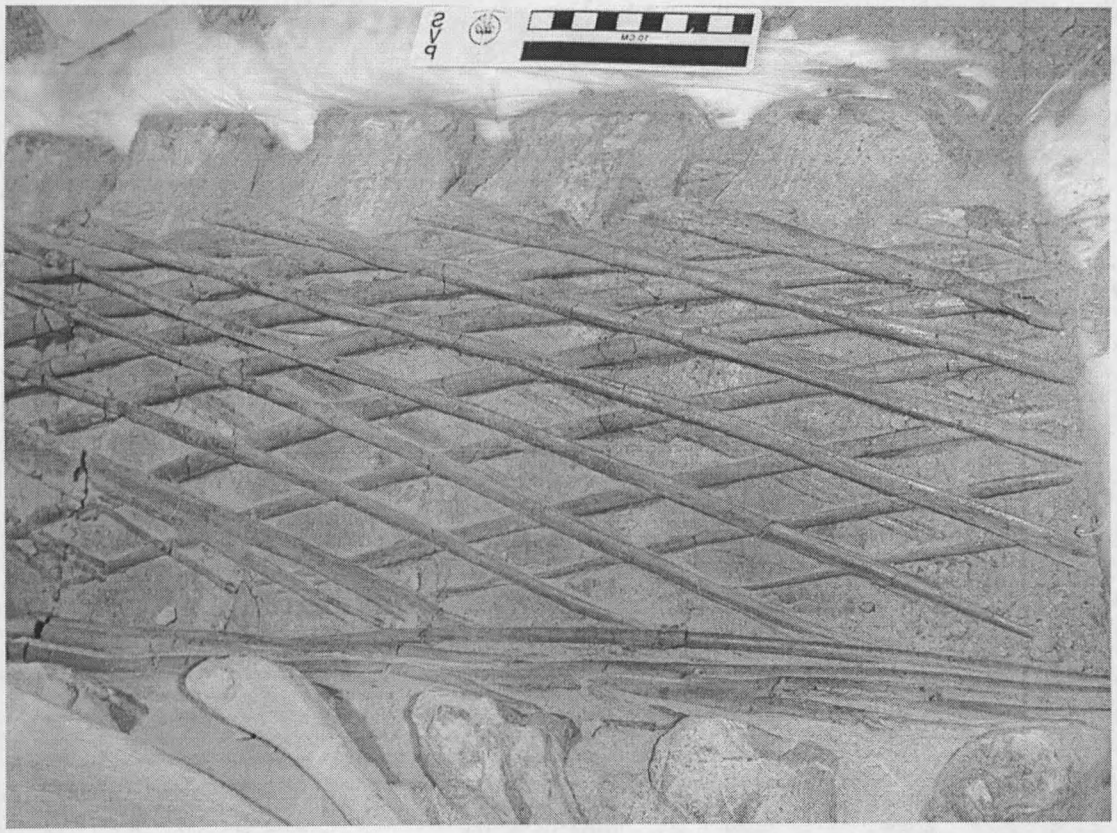

Figure 22. Trellis of ossified tendons from the posterior dorsal region of a *Brachylophosaurus* (MOR 794). Anterior is to the right.

loads (Coombs 1995). This is thought to improve muscle-tendon function by increasing tendon strength and reducing strain. Coombs (*idem*) notes that many birds have ossified tendons and proximally located muscles in their legs. But some birds also have ossified tendons throughout the trunk and neck (Vanden Berge and Storer 1995) where tendon length is not always greater than muscle length. And, there is no functional pattern in birds. For example, owls and cranes possess ossified tendons but their sister groups lack them (Vanden Berge and Storer 1995). In neither case do these birds appear to exhibit different behaviors that would explain intratendinous ossification (Vanden Berge and Storer 1995).

The ossified tendon trellis in Hadrosauriformes has been explained

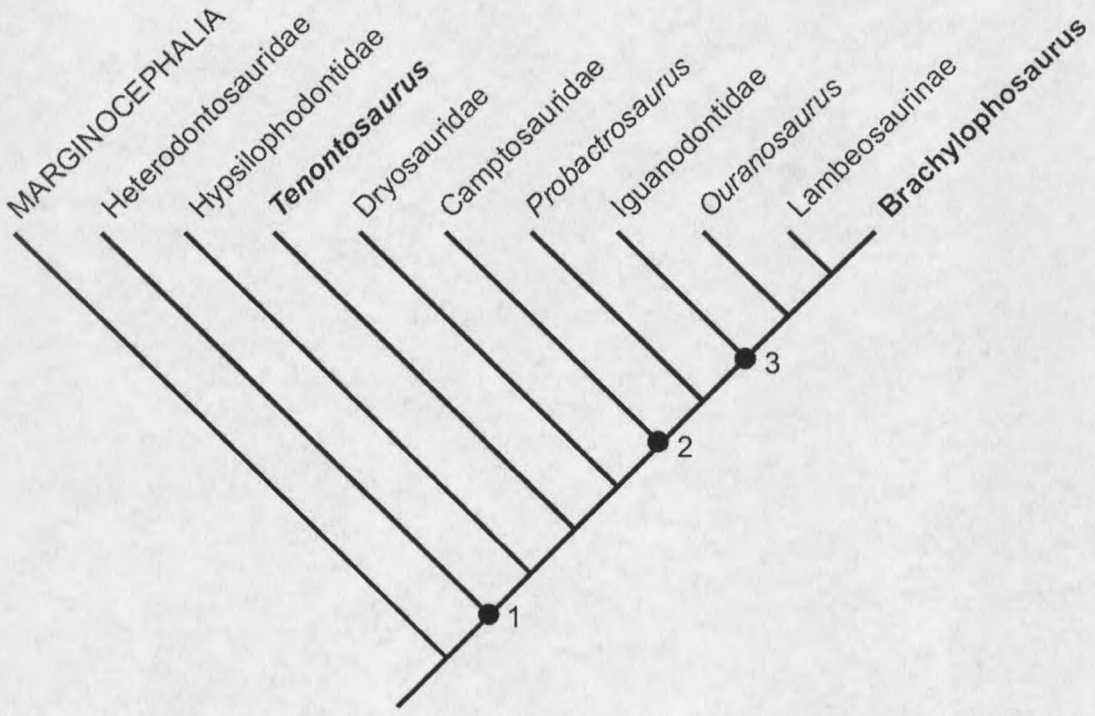

Figure 23. Phylogenetic framework used in this study based on Sereno (1999). Node-based taxa are as follows: 1, Ornithopoda; 2, Ankylopollexia; 3, Hadrosauriformes. Bold taxa are modeled in this study.

using functional morphology as restricting and promoting lateral motion of the tail. Arguments like these, without biomechanical testing, have been used to justify contradictory claims. Specifically, ossified tendons have been used as an argument for and against semi-aquatic hypotheses. Biomechanical analysis of ossified tendons in dinosaurs may provide a more robust method for evaluating their function.

This study has three primary aims. The first is to estimate the biomechanical influence of ossified tendons in basal ornithopods with parallel ossified tendons. The second is to estimate the biomechanical influence of the ossified tendon trellis in Hadrosauriformes. Two hypotheses are evaluated for both taxic models. The first is Dollo's (1886) assertion that the trellis acted like

a brace to resist caudofemoral loading during locomotion (femoral loading hypothesis). The second is Ostrom's (1964) hypothesis that the ossified tendon trellis passively reduced sagging (hogging) about the hips (hogging hypothesis). Both hypotheses are evaluated using static finite element computer modeling to determine the biomechanics of the plesiomorphic parallel network and the apomorphic ossified tendon trellis.

The third aim is to determine functional differences between the models in a phylogenetic framework. This comparison is used to elucidate possible functional ossified tendon evolution in Ornithopoda. Recent paleo-biomechanical studies evaluate their models using phylogenetically extant relatives for which empirical data can be collected (Gatesy 1995; Carrano and Biewener 1999; Rayfield et al. 2001; Hutchinson and Garcia 2002). Such a phylogenetic approach is more robust for testing functional hypotheses about extinct organisms (Weishampel 1995; Witmer 1995). This study includes experimental data from an *Alligator mississippiensis* for model development.

Materials and Methods

Two articulated specimens from the collections at the Museums of the Rockies (MOR) were used to create the dinosaur models in this study: a primitive (*Tenontosaurus tilletti,* MOR 682) and derived (*Brachylophosaurus canadensis,* MOR 794) ornithopod. MOR 682 possesses a complete tail and MOR 794 a roughly 90% complete tail. Only preserved elements were used. A third model was created from a mounted juvenile *Alligator* (MOR OST 130) skeleton.

Skeletal elements were measured directly from specimens with measuring tape, calipers, and a protractor. Individual centra were measured for length

(anteroposterior), height (dorsoventral), and width (mediolateral). The neural spines and chevrons were measured for length (anteroposterior), height (dorsoventral), width (mediolateral), and inclination (from the vertical axis). In some cases (i.e. the *Brachylophosaurus* sacrum), width had to be estimated as an average of the surrounding vertebrae because sections were imbedded in matrix. These morphologic data were used to create three dimensional finite element models in Visual Analysis 3.0 (IES 2000), a structural engineering program. Dorsoventral corresponds to the Y-axis, mediolateral to the Z-axis, and anteroposterior to the X-axis. Centra were modeled as short cylinders whose circular cross-sectional diameter was determined by the average of width and height measurements.

Pin joints and fixed joints were used in Visual Analysis. Joints are fully constrained by default, allowing full force and moment transfer between members (IES 2000). The neural spines were attached to the centra by fixed connections that do not allow translation or rotation. This was done to model the fused neural spine and centrum. Individual vertebrae, chevrons, tendons, and ligaments were joined to one another by pin connections that allow rotation between members. Such non-fused joints were partially constrained, meaning that less than 100% transfer of moments and forces occur (IES 2000). Visual Analysis approximates a partially constrained joint through endzones. Endzones are short regions at member ends that have altered stiffness (E) values. Determining endzone properties for the dinosaur models was estimated from experimental data of the *Alligator* (see below).

Neural spine apical ends were connected with members that had the cross-sectional area of tendons. The models were supported at every sacral centrum by fixed supports that do not allow translation or rotation. All elements

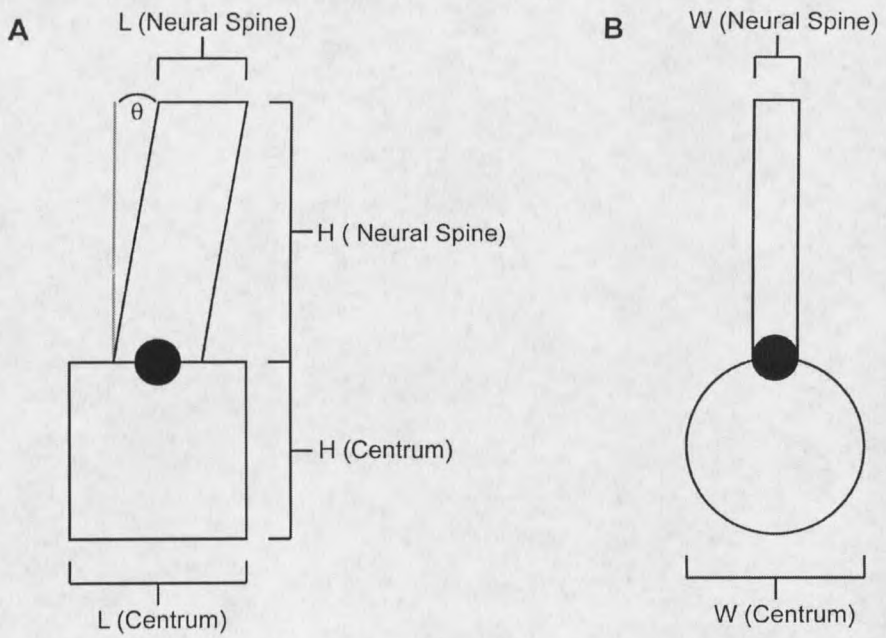

Figure 24. Diagram of modeled vertebra with indicated dimensions in lateral view (A) and frontal view (B). Closed circle indicates a fixed connection.

were given bone material properties (see below), except the ligamentum apicum dorsalis, which was given the material properties of tendon.

Two load cases were then applied to each model. Each load case consisted of two point loads: one applied to the dorsal region and one to the tail region on the centra. All loads had a -y (ventral) direction and 2.0 kN magnitudes in the first case and 10.0 kN in the second case. Only two load magnitudes were used because the models were linear (uniform geometries, material property distributions, and load applications). Skeletal weight was automatically calculated by Visual Analysis and included in all load cases. The results from these two load cases were used to generate data at 1 kN intervals by linear extrapolation.

In each case, loads were placed at the center of mass (COM) for each region. A cylinder was assumed for the dorsal region and a cone for the tail

region. In the brachylophosaur model, the dorsal loads were placed on the tenth dorsal vertebra (1.0 m posterior from the first dorsal) and tail loads on the tenth caudal vertebra (3.4 m posterior from the first dorsal). In the tenontosaur model, the dorsal loads were placed on the tenth dorsal vertebra (0.4 m posterior from the first dorsal) and tail loads on the fifteenth caudal vertebra (1.8 m posterior from the first dorsal).

The preceding steps were used to produce three model variants for each dinosaur. Only the vertebral column and ligamentum apicum dorsalis comprised the first model variant. Tendons were added to the vertebral column in the second model variant. Based on the conservative structure of epaxial muscle tendons in non-avian dinosaurs (see chapter 1), parallel tendons from the M. longissimus dorsi and a trellis from the slips of the M. transversospinalis were included in both dinosaur models. The tenontosaur model also included parallel tendons in the ventral aspect of the tail. In the third model variant, the tendons were ossified by giving them bone material properties. In the tenontosaur model only the parallel tendons were ossified in contrast to the brachylophosaur model where only the trellis was ossified. Comparison among the three model variants for each animal allowed phylogenetic, sensitivity, and functional analyses.

Ultimate stress values were then used to determine when individual members would fail (see below). Member failure was used to indicate the maximum load that the model could withstand before structural failure. Because muscles were not included the actual bearable loads were undoubtedly greater than in these models. Therefore, the results are interpreted in terms of relative spinal column deflection, increased ability to resist failure, and sensitivity to material properties, not absolute values.

The alligator model consisted of only the tail because experimental

deflection data could not be obtained from the dorsal region due to struggling. The load (tail weight) was placed on the fifteenth caudal vertebra (0.1 m posterior from the first caudal) in the alligator model. Only one load case was used, which corresponded to the live alligator's tail weight. This was determined by using the circumference at the base of the tail (13.5 cm) and the tail length (37.0 cm) to calculate volume (assuming a cone). Assuming the density of water (1 g/cm3), and gravitational acceleration (9.8 m/s2), tail mass was calculated to be 179.0 g and its weight 1.8 N. This value is appropriate given the animal's weight of 730.0 g the day the deflection data were taken. Tail deflection data were taken from the alligator by allowing its tail to hang over the table's edge. The skeleton's tail length used to construct the model was 35.0 cm and the live alligator's tail length was 37.0 cm.

Material Properties

Three factors were used in choosing material properties from the literature. The first was to choose bones from similar anatomical regions. The second was to choose bones with potentially similar functions. The third was to select bone properties from phylogenetically related taxa over those of distantly related taxa. Material properties for bone and tendon are common in the literature, though few studies investigate non-mammals (Alexander 1988; Currey 1999a; Currey 1999b; Cubo and Casinos 2000). Tendon modulus of elasticity (E) values for various mammals range from 1 GPa (Rigby et al. 1959) to 1.7 GPa, with a mean of 1.5 GPa (Bennett et al. 1986). An average E value of 1.6 GPa has also been suggested (Alexander 1988). Uncalcified avian tendons possess material properties similar to those in mammals (Bennett and Stafford 1988). The relatively stiff value of 1.6 GPa for E was used because it is less likely to inflate

differences between bone and tendon material properties.

No material properties on vertebrae from living archosaurs have been reported in the literature, so data from human vertebrae were used. The modulus of elasticity for human vertebral bone is highly variable (Roy et al. 1999). The lower end of E for human vertebrae ranges from 2.5 GPa, while the upper end has been reported as high as 25.8 GPa (Guo 2001). An E value of 6.6 GPa for human vertebrae (Ladd et al. 1998) was chosen for its intermediate value. This range seems reasonable, given that the elastic modulus in bending was determined to be 12.0 GPa for *Alligator* femurs and 5.6 GPa for *Crocodylus* frontals (Currey 1988). Various bones from 29 avian species range from 7.5-24.0 GPa (Cubo and Casinos 2000). Like the elastic modulus used for tendons, this relatively flexible value for bone (6.6 GPa) is less likely to overestimate the differences between bone and tendon.

The elastic modulus for ossified tendons has been determined to be 17.7 GPa in *Grus antigone* (Currey 1999a). However, the value used for bone in this study will also be used for ossified tendons for consistency of properties across elements.

Other material properties were required in Visual Analysis, such as density and Poisson's ratio. A value of 0.25 (Ladd et al. 1998) was used for Poisson's ratio and 7.8 kN/m^3 (Nigg and Herzog 1999) for density. However, when changed to double and half of these values, neither was found to affect the model's final results.

Ultimate Stresses

Bone's ultimate bending stress (138.6 MPa) was calculated by multiplying the modulus of elasticity for bone used in this study (6.6 GPa) by the ultimate

strain (0.02) for *Alligator* femur in tension (Currey 1990). Another, nonlinear, method to calculate the ultimate bending stress derived from empirical data (Currey 1999a) produced a value of 75.1 MPa using the equation BS = 15.1E0.85. This value is low compared with bending values found in avian long bones that range from 148.8 - 201.10 MPa (Cubo and Casinos 2000), human femora (208.6 MPa), and bovine (223.8) tibia (Martin et al. 1998). An ultimate bending stress of 138.6 MPa was used because the initial calculation was more consistent with most published data on bending strengths (Martin et al. 1998; Nigg and Herzog 1999).

Bone is weakest in shearing and ultimate shear stress does not vary as greatly as bending or ultimate tensile stress. Values range from 50.4-73.0 MPa, for human compact bone (Reilly and Burstein 1975; Saha 1977; Martin et al. 1998; Turner et al. 2001) with a mean of 62.0 MPa, the value used in this study. Like ultimate shear stress, ultimate compressive stress does not seem to vary greatly. Ultimate compressive stress ranges around 200.0 MPa (Martin et al. 1998; Nigg and Herzog 1999).

The ultimate tensile stress for tendons used in this study was 100.0 MPa, an average determined from mammalian tail and digit tendons (Bennett et al. 1986). Tendinous ultimate tensile stress has been reported to range from 20.6 – 147.0 MPa (Viidik 1966). These data compare well with uncalcified tendons from a heron, which ranges from 77.0-131.0 MPa (Bennett and Stafford 1988). A value of 271.0 MPa was reported for an ossified tendon from *Grus antigone*, (Currey 1999a). The ultimate tensile stress for bone from terrestrial animals ranges from 108.0 MPa for *Alligator* femur to 254.0 MPa for *Grus* tibiotarsus (Currey 1990) with an average of 166.0 MPa, which was used in this study. This average is a close fit to the "typical" value of 150.0 MPa (Martin et al. 1998; Nigg and Herzog

Table 3. Ultimate stress values used for this study. The ultimate stresses for ossified tendons are identical to bone except for tensile stress. See text to see how these values are obtained.

Ultimate Stress (MPa)	Tendon	Ossified Tendon	Bone
Tension σ_u	100	271	166
Compression σ_u	-	200	200
Bending σ_u	-	138	138
Shearing σ_u	-	62	62

1999; Currey 2001).

The material properties above were taken from a variety of sources, each employing slightly different methods, and specimens of different species and ages. Therefore, the values for these properties have all been chosen conservatively. The ultimate tensile strains were calculated ($E = \sigma/\varepsilon$) for each material (tendon, ossified tendon, and bone) and listed in table 4. These values sit comfortably within the ultimate tensile strain range for bone of 0.0045-0.13 (Currey 1990). The ultimate strain for tendon was slightly underestimated, which ranges from 0.08-0.1 (Rigby et al. 1959), and ossified tendon in the *Grus*, which was empirically determined to be 0.062 (Currey 1990). Lower strain values were not surprising considering the conservative values chosen for E. However, the ultimate tensile strain of tendons, ossified tendons, and bone calculated in table 4 agree well with values empirically obtained from turkeys (Bennett and Stafford 1988).

Alligator Results and Partially Restrained Joint Properties

The alligator model produced a dorsoventral tail deflection of -6.4 cm with fully constrained joints. As expected, this is far smaller than the -32.0 cm deflection measured from the live alligator. But, it allowed for partially restrained

Table 4. Calculated ultimate tensile strain values. Ultimate tensile strains are within the range for the respective materials, helping ensure the validity of the modulus of elacticity and ultimate tensile stress used in this study.

	Tendon	Ossified Tendon	Bone
E (GPa)	1.6	6.6	6.6
$\sigma_{u,\ tensile}$ (MPa)	100	271	166
$\varepsilon_{u,\ tensile}$	0.063	0.041	0.025

joint (endzone) properties to be selected. Endzones were placed only in regions where two members joined by pin connections (i.e. tendon-neural spine connections and non-sacral centrum-centrum connections). The alligator model was found to be very sensitive to endzone properties, though partially restrained fixed joints had little impact on the results (increased deflection by 0.1 cm). Endzone properties with 0.2 cm widths and 10% member stiffness produced best fit a deflection of -30.91 cm.

Using endzones (0.2 cm width, 10% stiffness) the alligator model produced a maximum bending stress (about the y-axis) at the first caudal neural spine of -13.0 MPa, well within bone's ultimate bending stress (108 MPa for alligator femur, Currey 1990). The model experienced a maximum shear stress (Vy) of 2.2 MPa, far below (50.4-73.0 MPa) ultimate shear stress common values. The highest axial stress (33.8 MPa) was generated at the apical ligament connecting the last sacral neural spine to the first caudal neural spine. Again, this value was well below the ultimate tensile stress of tendon (around 100.0 MPa, Bennett, Ker et al. 1986). Thus, dorsal epaxial members (just under the skin) were under the greatest tensile stress, conforming to expected results (Alexander and Jayes 1981).

The alligator model results appear valid, insofar that stresses did not

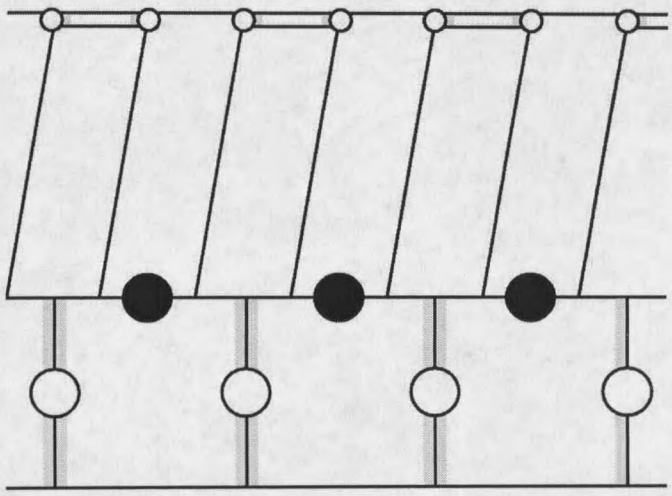

Figure 25. Diagram of the *Alligator* model showing placement of endzones. The shaded areas between the centra and at the apical tendons are the locations of endzones. These short regions (0.2 cm) have altered stiffness values.

exceed material strength. Furthermore, these stresses are within the value range incurred by the limb bones of *Alligator* during locomotion (Blob and Biewener 1999). Therefore, cautious application of modeling the two dinosaurs is justified.

Results

Tenontosaur Model Results

Tenontosaur model results are summarized in table 5. All three tenontosaur model variants experience more tail deflection than dorsal deflection (Fig. 26). Tail deflection is also reduced more by the incorporation of tendons and their subsequent ossification than in the dorsal region. Therefore, the tail is more heavily influenced in terms of deflection than the trunk by inclusion of tendons and their ossification. In both anatomical regions, the vertebral column is stiffened more by tendon inclusion than by ossification. In the tail, however, an increase in stiffness results from intratendinous ossification where the dorsal

Table 5. Summary of tenontosaur model results. These results are used to extrapolate deflection and stress values for loads from 0 to 10 kN at 1 kN intervals. The negative values for the deflection (dy) indicate the ventral direction in the dorsal (D) and caudal (C) regions. The negative values for the bending loads (Fbz) indicate a counter-clockwise direction in left lateral view about the z-axis (about the central transverse axis) in the neural spine of the first sacral vertebra (S1) and last sacral vertebra (S5). Fa denotes axial tensile stress in the apical ligament between the last dorsal and first sacral (T16-S1) and between the last sacral and the first caudal (S5-C1) neural spines.

	Deflection (cm)		Stress (MPa)			
Load (kN)	Dy (D)	Dy (C)	Fbz (S1)	Fbz (S5)	Fa (D16-S1)	Fa (S5-C1)
Model T1: No Tendons						
-2.00	-110.68	-669.40	-238.61	543.48	607.4	1425.47
-10.00	-549.82	-3288.48	-1187.35	2699.01	3022.45	7082.80
Model T2: Tendons						
-2.00	-17.32	-275.46	-94.48	258.84	151.51	373.54
-10.00	-85.97	-1333.84	-470.32	1130.94	753.71	1852.34
Model T3: Ossified Tendons						
-2.00	-14.90	-235.62	-105.73	234.33	138.33	326.33
-10.00	-74.04	-1140.94	-526.27	995.57	688.14	1618.37

region is hardly affected.

The greatest bending stress occurs about the first and last sacral neural spine arches (Fig. 27). This corresponds to peak bending moments about the neural arch, a phenomenon reported to occur in mechanical testing of human vertebrae (Cyron et al. 1976; Cyron and Hutton 1978). As shown in table 5, bending stresses about the last sacral neural spine are greater than bending stresses in the first sacral neural spine at a given load. Furthermore, the bending stress in the neural spines is reduced more by tendon inclusion than by ossification.

Axial stress is greatest in the apical ligament between the posterior (S5-C1) neural spines (Fig. 28). This situation is identical with that seen in the alligator

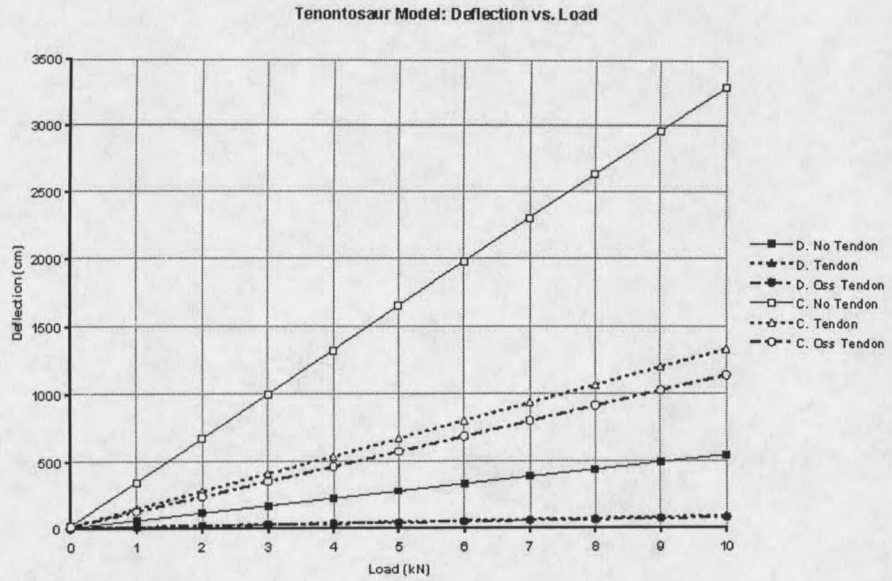

Figure 26. Tenontosaur deflection by load. The caudal region experiences more deflection than the dorsal region. Also, note that the spinal column is stiffened more by the inclusion of tendons than by ossification.

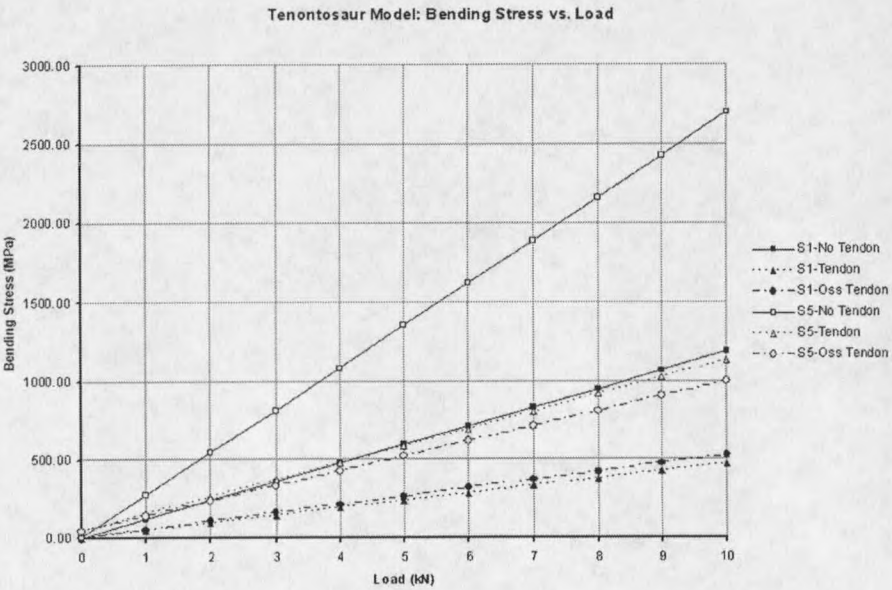

Figure 27. Tenontosaur bending stress by load. The last neural spine of the sacrum (S5) experiences more bending than the first sacral neural spine.

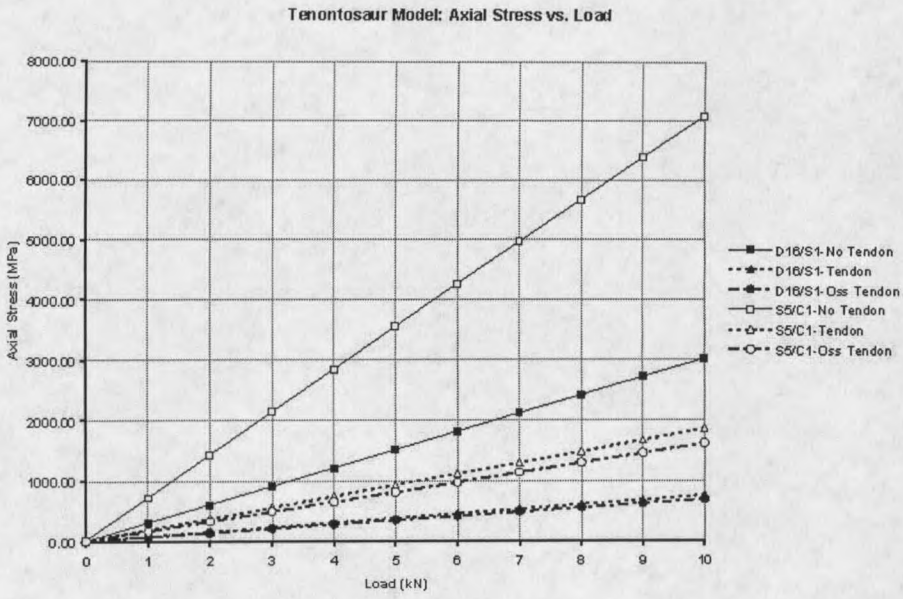

Figure 28. Tenontosaur axial stress by load in the apical ligament connecting the last dorsal (D16) and first sacral (S1), and the last sacral (S5) and first caudal (C1). The S5-C1 ligament experiences more tension than the D16-S1 ligament. Addition of tendons affects axial stress more than ossification.

model and is consistent with lumbar loading in mammals (Alexander and Jayes 1981). Inclusion of tendons significantly reduces axial stress in the D16-S1 and S5-C1 ligaments. In contrast, intratendinous ossification has little impact axial stress reduction. While intratendinous ossification lowers the axial stress in the D16-S1 and S5-C1 ligaments, it also increases the axial stress in the ossified tendons over the posterior sacrum and puts the ossified tendons in the ventral aspect of the tail into compression, though at very small magnitudes.

Shearing is small in the alligator model and in both dinosaur models as well. However, despite a small magnitude, intratendinous ossification increases the shearing stress experienced in the tenontosaur model. When the ossified tendon architecture is considered (parallel to the vertebral axis), such an increase

Table 6. Ultimate loads determined from maximum stresses in model variants with no tendons (NT), tendons (T), and ossified tendons (OT). These loads were calculated using the ultimate stresses (y-value) to calculate the load (x-value) from the linear plots above. In the dorsal region, maximum tension is in the apical ligament between the last dorsal and first sacral and in the caudal region between the last sacral and first caudal. In the dorsal region maximum bending occurs in the first sacral neural spine and in the caudal region in the last sacral neural spine.

	Tenontosaur Model						Brachylophosaur Model					
	Dorsal loads (kN)			Caudal loads (kN)			Dorsal loads (kN)			Caudal loads (kN)		
	NT	T	OT	NT	T	OT	NT	T	OT	NT	T	OT
Tension	0.32	1.3	1.4	0.12	0.52	0.60	1.3	6.1	20.7	1.7	7.1	24.7
Bending	1.2	2.9	2.6	0.50	0.90	1.0	4.4	8.5	16.5	4.1	14.9	44.3

is expected as loads are distributed transversely to the neural spines. Despite this effect, shearing was so far below other stresses that it is not considered further.

The tenontosaur model fails at the S5-C1 apical ligament in tension at 0.12 kN. Addition of the tendons increases failure load to 0.52 kN (a 320% increase). Intratendinous ossification allows the structure to withstand an additional 0.08 kN. Tendon inclusion decreases tail deflection (at failure load) from 55.2 cm with no tendons, to 27.3 cm with tendons (50.6% increase in stiffness), to 23.3 cm with ossified tendons (57.8% increase in stiffness). Dorsal deflection at failure load is reduced from 7.7 cm with no tendons to 1.22 cm with tendons (84.1% increase in stiffness) to 1.0 cm with ossified tendons (86.6% increase in stiffness). Although the dorsal region is stiffened more than the tail on a percent basis, the tail is influenced more in absolute terms. In the tenontosaur model with ossified tendons, the maximum tension shifts from the S5-C1 apical ligament to the apical ossified tendon over the posterior sacrum. However, when this apical ligament fails the tensile stress in the ossified tendon is 210.0 MPa, below the maximum

tensile stress of ossified tendon (271.0 MPa). Therefore, the weakest member remains the S5-C1 apical ligament, despite inclusion of tendons.

Brachylophosaur Model Results

The results for the brachylophosaur models are summarized in table 7. All three brachylophosaur model variants experience more tail deflection than dorsal deflection (Fig. 29). Tail deflection is also reduced more by incorporating tendons and subsequent ossification than in the dorsal region. Therefore, like the tenontosaur model, the tail is more influenced in terms of deflection by tendon inclusion than ossification. The brachylophosaur model is also stiffened more by the adding tendons than through intratendinous ossification, regardless of anatomical region.

The greatest bending stress occurs at the first and last sacral neural spine arches. This result agrees with the tenontosaur and alligator models. As shown in figure 30, bending stresses about the last sacral neural spine are roughly the same (though slightly greater) than the bending stresses at the first neural spine for any given load. Tendon inclusion significantly lowers the bending moments at the neural spines arches. Intratendinous ossification lowers these bending stresses even more, though not as much as the addition of tendons. This effect is caused by the dorsoventral neural spine height.

A maximum bending moment of -5.9 kN*m is produced at the last sacral neural spine at failure load. This is much lower than the -25.0 kN*m bending moment across the hips calculated in Iguanodon using beam theory (Alexander 1985). However, Alexander notes that this value is probably inflated appreciably because his model assumed a point support, where as these models are supported at every sacral centrum. Therefore, this study's results do not

Table 7. Summary of brachylophosaur model results. These results are used to extrapolate deflection and stress values for loads from 0 to 10 kN at 1 kN intervals. The negative values for the deflection (dy) indicate the ventral direction in the dorsal (D) and caudal (C) regions. Negative values for the bending loads (Fbz) indicate a counter-clockwise direction in left lateral view about the z-axis (about the central transverse axis) in the neural spine of the first sacral vertebra (S1) and last sacral vertebra (S9). Fa denotes axial tensile stress in the interspinous ligament between the last dorsal and first sacral (D18-S1) and between the last sacral and the first caudal (S9-C1) neural spines.

	Deflection (cm)		Stress (MPa)			
Load (kN)	Dy (D)	Dy (C)	Fbz (S1)	Fbz (S9)	Fa (D18-S1)	Fa (S9-C1)
Model B1: No Tendons						
-2.00	-35.04	-52.53	-65.93	70.49	143.49	117.04
-10.00	-151.50	-220.74	-302.36	326.10	658.06	541.43
Model B2: Tendons						
-2.00	-8.33	-11.92	-35.62	20.40	35.26	30.38
-10.00	-30.15	-50.56	-162.94	83.80	161.23	139.66
Model B3: Ossified Tendons						
-2.00	-4.20	-3.60	-18.57	6.93	10.73	8.11
-10.00	-11.96	-15.15	-84.93	31.82	49.02	405.0

contradict previous attempts to understand bending stress across the hips in Hadrosauriformes.

Axial stress is greatest in the apical ligament between the anterior (d18-S1) neural spines (Fig. 31). This situation differs from the alligator and tenontosaur models, which experience the greatest degree of tension in the apical ligaments between the last sacral and first caudal neural spines. Inclusion of tendons substantially reduces axial stress in both anterior (d18-S1) and posterior (S9-C1) apical ligaments.

The brachylophosaur model fails first in tension (at 1.3 kN) in the D18-S1 apical ligament (Table 6). Tendon inclusion increases failure load to 6.1 kN (a 361.6% increase). Intratendinous ossification increases failure load to 20.7(a

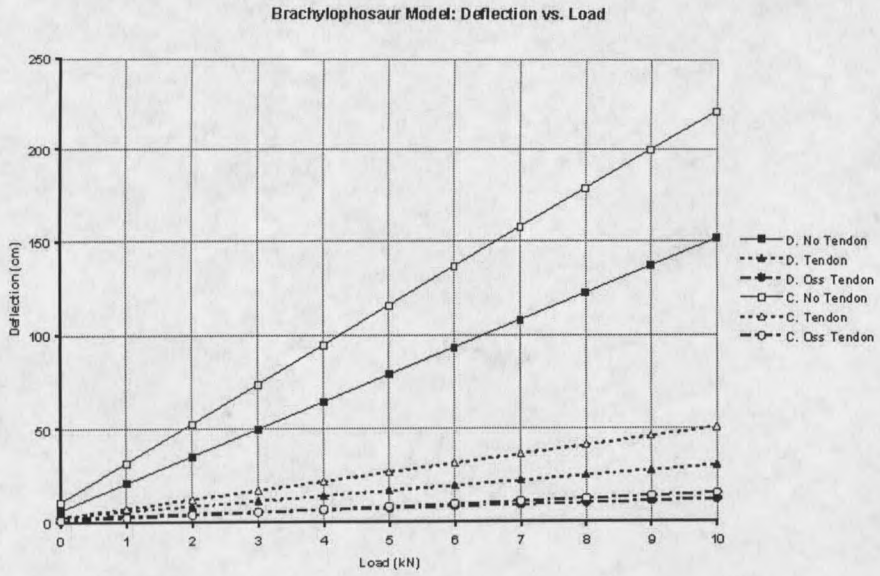

Figure 29. Brachylophosaur deflection by load. The degree of deflection is largely dependant upon inclusion of tendons not by ossification.The caudal region is deflected more than the dorsal region, though overlap exists.

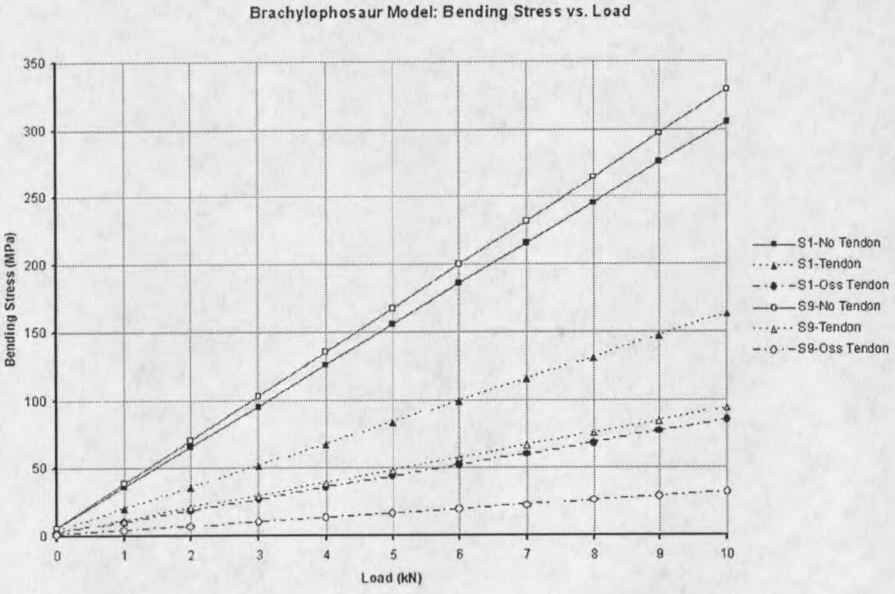

Figure 30. Brachylophosaur bending stress by load. Note that the bending stress, like deflection, is largely dependant on the presence of tendons not ossification. The first and last neural spines of the sacrum (S1 and S9) experience roughly the same degree of bending.

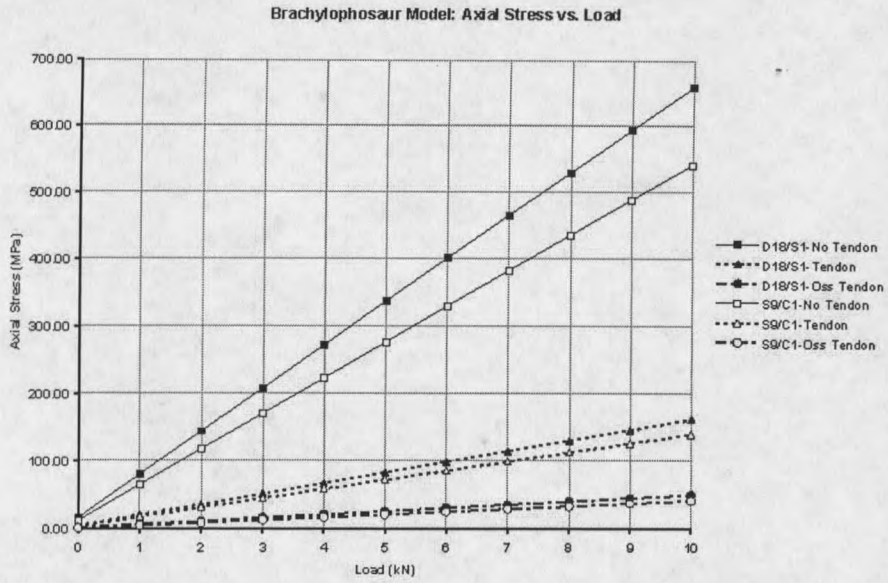

Figure 31. Brachylophosaur axial stress by load in the interspinous ligament connecting the D18-S1 and S9-C1 ligaments. The apical ligament between D18-S1 experiences more tension than the one between S9-C1.

1459.9% increase). The tendons decrease tail deflection (at failure load) from 38.1 cm with no tendons, to 8.6 cm with tendons a (77.4 increase in stiffness), to 2.6 cm with ossified tendons (93.1% increase in stiffness). Dorsal deflection at this load is reduced from 25.1 cm with no tendons to 6.5 cm with tendons (74.2% increase in stiffness), to 3.5 cm with ossified tendons (85.9% increase in stiffness).

Deflection in the models is mainly affected by length of the loaded region and neural spine height. The brachylophosaur model is constructed from a slightly truncated tail, which if complete, would be roughly 50 cm longer. To evaluate this influence, the three brachylophosaur model variants were modified to include the last part of the tail. This increased tail deflection by 29.5% at 2.0 kN and 18.8% at 10.0 kN, inflating the difference between dorsal and tail deflection. At failure (1.3 kN) in the model variant with no tendons, deflection increased

from 38.1 cm to 49.94 cm (a 31.1% increase). In the ossified tendon model variant with a complete tail, deflection increased from 2.6 cm to 6.6 cm at failure load. The model with the complete tail produced a difference of 2.8 cm between dorsal and caudal deflection, while the difference in the tenontosaur model is 47.5 cm at failure load. Therefore, the dorsal and tail regions are roughly equally affected by tendon biomechanics. Furthermore, the model variants with the fully reconstructed tail experience small increases in stress (only a 2.0% increase in bending and less than 0.01% increase in axial stress). Considering these data, the original model with a truncated tail will suffice for structural analysis and hypothesis testing.

Discussion

It has been noted that, despite the promise of using biomechanics to infer function in extinct organisms, many obstacles remain (Lauder 1981; Bryant and Seymour 1990; Lauder 1991a; Lauder 1991b; Lauder et al. 1993; Lauder 1995; Lauder and Reilly 1996). For example factors such as posture, mass, muscular force production, neurological factors (i.e. timing in muscle activation), and so on must be inferred. Each of these factors is an inferential step in which errors can accrue. There is evidence that organisms can evolve novel function directly from morphology while neurological activation patterns remain conserved across the group of interest (Lauder 1991a). Computer models that infer muscle mass and force production have produced interesting results (Hutchinson and Garcia 2002), though the methods used here more closely resemble attempts to understand the skeleton mechanically (Rayfield et al. 2001).

Stress values produced in the models of this study would most likely

be lower in living animals as various connective tissues and muscular loads would help absorb them. Therefore, the results probably overestimate stresses experienced by the members for any given load. Despite this limitation, the computer models can be used to answer specific structural questions. For example, incorporation of ossified tendons into the models were expected to place members (skeletal elements) into compression that were initially in tension, because bone is generally stronger in compression rather than tension (Nigg and Herzog 1999). Compression impacts the brachylophosaur model by affecting bending of the neural spines. The angle of inclination in the M. transversospinalis trellis reduces bending on the neural spine by compressive (-y) load application. This effect is inherent in the trellis architecture, but more pronounced in the brachylophosaur model because of the taller neural spines.

The tenontosaur model contains hypaxial, in addition to epaxial tendons, that experience compression (a maximum of -59.38 MPa in the 2.0 kN load case) far below tensile magnitudes. The structure's stresses are mostly distributed in the epaxial ossified tendons. Indeed, when hypaxial tendons are removed, deflection, tensile and bending stress increase less than one percent. Therefore, hypaxial ossified tendons in primitive ornithopods likely had little structural function in terms of dorsoventral loading.

Some have suggested that the trellis of ossified tendons stiffened the tail laterally (Norman 1986). This conjecture was tested by lateral load cases where loads were applied at the tail's center of mass in the mediolateral direction. There was no difference between model variants in either animal. However, the modeled tendons are applied immediately to the neural spines in these models. Lateral location from the neutral axis of the vertebral column would increase the tendon's ability to stiffen the vertebral column. But proximal application seems

appropriate given archosaur epaxial anatomy (see chapter 1).

It is also possible that epaxial anatomy in hadrosaurs predisposes the tail to structural failure. Indeed pathologies on the neural spines in the tail of hadrosaurs is not uncommon (Rothschild and Tanke 1992). These pathologies consist of broken, fused, and eroded neural spines and ossified tendons. Nothing in the brachylophosaur models suggest that these pathologies were caused by tail biomechanics due to dorsoventral loading. That is, the region in the tail in which these pathologies occur is not a mechanical weak point. Therefore, it is likely that some stress other than loading from body mass caused failure, such as mating, agonistic behavior, or predation.

Evaluating the Femoral and Hogging Hypotheses

The dinosaur model results may also be used to evaluate the femoral loading and hogging hypotheses. Both hypotheses were made for Hadrosauriformes, but can also be used against the *Tenontosaurus* data. The femoral loading hypothesis is supported if the models reduce tail deflection and stress more than dorsal deflection and stress. This is true for the tenontosaur model, where the tail experiences a greater percentage increase in stiffness (7.2% compared to 2.5% in the dorsal region), and deflects more in absolute terms (23.3 cm compared to 1.0 cm in the ossified tendon variant at failure load) due to its longer length. Therefore, the femoral loading hypothesis is supported by the tenontosaur model. The brachylophosaur model experiences reduced deflection nearly equally in the dorsal and tail regions on a percentage basis with the inclusion of the tendons and their ossification (Table 8). In absolute terms, the tail deflects 2.6 cm compared with 3.5 cm in the ossified tendon variant at failure load. Although a complete tail would increase caudal deflection past

Table 8. Percentage changes in the models when tendons are ossified. The deflection row percentages indicate to how much less the model deflected compared to the model with tendons. Bending stress percentages indicate how much less the first sacral neural spine (dorsal column) and last sacral neural spine (caudal column) were loaded in bending compared to the model with a network of tendons. Axial stress percentages indicate how much less the interspinous ligaments between the last dorsal and first sacral neural spines (dorsal column) and the last sacral and first caudal neural spines (caudal column) were loaded in tension, compared to the model with a network of tendons.

	Tenontosaur Model		Brachylophosaur Model	
% Changes	Dorsal	Caudal	Dorsal	Caudal
Deflection	-2.5	-7.2	-11.7	-15.7
Bending σ	4.7	-5.0	-25.6	-18.8
Axial σ	-2.1	-3.4	-17.1	-18.3

dorsal deflection, they would still be subequal. Although the data do not favor the femoral loading hypothesis, it can not be rejected because the tail is still being stiffened by intratendinous ossification.

Equal stiffness in the dorsal and tail regions supports the hogging hypothesis. This is not the case for the tenontosaur model, which experiences a difference between dorsal and tail deflection of 47.5 cm (in the ossified tendon model at failure load). Thus, the hogging hypothesis can be rejected for the primitive ornithopod. Differences between dorsal and tail deflection in the brachylophosaur model (ossified tendon variant) are only 9.2 cm and only 3.1 cm in the model with a complete tail. Ostrom (1964) noted that trellis ossification would provide additional structural support to resist dorsal tension and ventral compression of the vertebral column due to hogging about the hips. According to the models, this is the case as the trellis is loaded in tension, not compression. Furthermore, the hogging hypothesis is a structural claim that posits a reduction in bending stress about the hips. The ossified trellis functions this way by

reducing bending stress approximately 25.6% in the dorsal region and 18.8% in the caudal region. It also reduces axial stress by over 17% in both anatomical regions. In contrast, there is a 2.1% (dorsally) and 3.4% (caudally) difference in the tenontosaur model's ability to reduce axial stress. Since the models fail in tension, the equal degree of axial stress reduction in the brachylophosaur model supports the hogging hypothesis. The ossified trellis' ability to lower internal stresses is largely due to the architecture of the structure enhanced by tall neural spines. Moreover, the brachylophosaur model fails first in tension in the anterior apical ligament (D18-S1), which suggests that dorsal loading is an important factor in this animal. The degree to which tensile stress is reduced is the degree to which epaxial muscles are relieved of load bearing functions, which is substantial in the brachylophosaur model. Thus, results favor the hogging hypotheses for the brachylophosaur model.

A comparison can be made between the two taxa modeled in terms of ossifying different epaxial muscles. The tenontosaur model can be taken as the primitive condition for Ornithopoda. Based on the model's results, the plesiomorphic ossification pattern may have been an adaptation resulting in tail stiffness. As Dollo noted in 1886, this would have locomotor implications because of the caudofemoral muscles couple the hind limb and tail into a functional unit (Gatesy 1995). If tail stiffness increased the moment arm for femoral retraction, tendon ossification could be selectively advantageous. Ossified tendons would reduce required loads from the epaxial musculature to counteract femoral muscles and passively stiffen the tail and increase safety factors. Therefore, intratendinous ossification may have selected for because of locomotor function.

Ossification of the M. transversospinalis tendons (the trellis) in Hadrosauriformes increases tail stiffness by 15.7% (where the tenontosaur

model reduced deflection by only 7.2%). Like *Tenontosaurus*, this likely impacted caudofemoral loading of the tail during femoral retraction. However, the dorsal region is also impacted by the ossified trellis to roughly the same degree. This effect of the ossified trellis may have been important in Hadrosauriformes, which were large animals, in terms of passively supporting the body from hogging about the hips. Moreover, the ossified trellis greatly enhances the vertebral column's ability to bear large loads (237.9% greater than unossified tendons compared to 15.1% in the tenontosaur model). Or, stated another way, the trellis greatly reduces bending and axial stresses suffered by the vertebral column. It is interesting to note that both the tenontosaur and brachylophosaur models fail from tensile loading and that ossified tendons reduce tensile stress on the vertebral column more than bending stress. In addition, they also have higher ultimate tensile stress values than tendon or bone and are thus capable of withstanding larger tensile stresses. This increases the vertebral column's ability to withstand loading in two ways: by lowering internal stresses and by increasing the maximum tolerable stress. Furthermore, the brachylophosaur model with ossified tendons reduces tensile stress by over twice that of the tenontosaur model with ossified tendons. Again, this function may be related to the evolution of large size in these animals.

Conclusions

Ossified tendon biomechanics in ornithopods were examined using computer finite element modeling. While many claims about ossified tendon function have been made, none have been rigorously tested. This study is a first attempt to do so and has produced reasonable results, considering the outcome

of a modeled alligator tail and the location of maximum stresses in the dinosaur models. A model produced from the anatomical data of a *Tenontosaurus tilletti* was used to represent the primitive ornithopod condition that possessed parallel ossified tendons from the M. longissimus dorsi. Another model constructed from a *Brachylophosaurus canadensis* was used to represent the derived condition found in Hadrosauriformes that possessed a trellis of ossified tendons from the M. transversospinalis.

The tenontosaur model with ossified tendons reduced the stresses incurred on vertebral elements, though to a lesser degree than the brachylophosaur model, and actually placed the neural spines under greater shear (though the magnitude was insignificantly small). The apomorphic ossified tendon trellis found in Hadrosauriformes stiffens the vertebral column mostly through tendon architecture and neural spine height. Moreover, the ossified trellis reduced the stresses incurred on the vertebral column more than the ossified tendons in the tenontosaur model, thus allowing far greater loads to be safely born. Since both models were stiffened by the addition of ossified tendons, they probably functioned by passively supporting the tail and trunk, thus reducing the need for epaxial muscular exertion.

Two hypotheses were evaluated concerning the function of ossified tendons. The hogging hypothesis suggests that the vertebral column is stiffened in both the dorsal and tail regions to resist buckling about the hips due to body weight. The femoral loading hypothesis suggests that ossified tendons stiffened the tail to increase the lever arm for femoral retraction. The hogging hypothesis was rejected and the femoral loading hypothesis supported for the tenontosaur model. Neither hypothesis could be rejected for the brachylophosaur model. Also, the effectiveness of ossified tendons to reduce stress and deflection is 2

to 3 times that of the plesiomorphic tendon architecture Ossification of the M. transversospinalis trellis in Hadrosauriformes may have therefore functioned in two ways: in locomotion and in supporting large body size.

APPENDIX

MORPHOLOGIC DATA FOR CHAPTER 4 MODELS

Table 9. Morphologic data from MOR 794 (*Brachylophosaurus canadensis*). Length is in the anterior-posterior direction, height is in the dorsoventral direction, and width is in the mediolateral direction. Height for the neural spine was measured along its longitudinal axis (not vertical). These measurements for the neural spine were taken at their dorsal summits. θ? was measured at the base of the neural arch with a protractor and is the angle between the vertical axis and the neural spine.

Dorsal Section							
Centra				Neural spines			
Vert.	L (cm)	H (cm)	W (cm)	L (cm)	H (cm)	W (cm)	θ
1	10.0	16.0	10.0	1.0	2.0	0.3	60.0
2	10.0	16.0	10.0	1.5	3.0	0.3	60.0
3	10.0	16.0	10.0	1.5	7.0	0.5	50.0
4	10.0	16.0	10.0	2.0	13.0	0.7	40.0
5	10.0	16.0	10.0	3.0	13.0	0.8	30.0
6	10.0	16.0	10.0	7.0	17.0	0.8	20.0
7	10.0	16.0	10.0	7.0	20.0	1.0	15.0
8	10.0	16.0	10.0	7.0	22.0	1.0	10.0
9	10.0	16.0	10.0	8.0	23.0	1.0	5.0
10	10.0	16.0	10.0	8.0	26.0	1.0	0.0
11	10.0	16.0	10.0	8.5	28.0	1.0	0.0
12	10.0	16.0	10.0	9.0	28.0	1.1	0.0
13	10.0	16.0	10.0	9.5	28.0	1.1	0.0
14	10.0	16.0	10.0	9.5	28.0	1.1	0.0
15	10.0	16.0	10.0	9.5	31.0	1.1	0.0
16	10.0	16.0	10.0	9.5	33.0	1.1	0.0
17	10.0	16.0	10.0	9.5	33.0	1.1	0.0
18	10.0	16.0	10.0	9.5	33.0	1.1	0.0

Sacral Section							
Centra				Neural spines			
Vert.	L (cm)	H (cm)	W (cm)	L (cm)	H (cm)	W (cm)	θ
1	9.0	15.0	11.0	9.5	35.0	1.1	0.0
2	9.0	15.0	11.0	9.5	35.0	1.1	0.0
3	9.0	15.0	11.0	9.5	35.0	1.1	0.0
4	9.0	15.0	11.0	9.0	37.0	1.1	0.0
5	9.0	15.0	11.0	9.0	37.0	1.1	0.0
6	9.0	15.0	11.0	9.0	37.0	1.1	0.0
7	9.0	15.0	11.0	8.0	37.0	1.1	0.0
8	9.0	15.0	11.0	8.0	37.0	1.1	10.0

9	9.0	15.0	11.0	8.0	40.0	1.1	20.0

Caudal Section

Centra				Neural spines			
Vert.	L (cm)	H (cm)	W (cm)	L (cm)	H (cm)	W (cm)	θ
1	7.9	13.5	10.7	7.1	43.5	1.0	25.0
2	8.0	13.0	10.5	7.1	43.5	1.0	27.0
3	7.9	13.0	10.3	6.8	41.0	1.0	30.0
4	7.9	13.8	10.2	6.7	40.5	1.0	31.0
5	7.8	13.7	10.0	6.5	38.0	1.0	33.0
6	7.9	13.5	9.8	6.5	37.5	1.0	33.0
7	8.7	13.4	9.6	6.2	35.0	1.0	35.0
8	8.5	13.0	9.5	6	33.0	0.9	38.0
9	8.1	12.5	9.3	5.7	32.0	0.9	40.0
10	8.5	12.5	9.1	5	29.5	0.9	43.0
11	8.2	12.0	8.9	5.7	29.0	0.9	50.0
12	7.9	11.5	8.8	3.8	26.0	0.9	50.0
13	7.7	11.0	8.6	3.2	21.0	0.9	50.0
14	7.8	10.5	8.4	3.1	26.0	0.8	50.0
15	7.7	10.1	8.2	5.1	26.0	0.8	53.0
16	8.0	10.0	8.1	5	28.0	0.8	53.0
17	8.0	9.7	7.9	3.8	27.5	0.8	57.0
18	7.8	9.5	7.7	3.7	26.0	0.8	62.0
19	8.5	9.4	7.5	3.4	26.0	0.7	62.0
20	8.2	9.4	7.4	3.4	25.0	0.7	62.0
21	8.0	8.6	7.2	3.1	25.0	0.7	62.0
22	8.0	8.2	7.0	3.8	23.0	0.7	63.0
23	7.8	8.2	7.0	3.8	23.0	0.7	63.0
24	7.8	8.0	6.9	3.7	23.0	0.7	63.0
25	7.6	7.9	6.8	3.7	23.0	0.7	65.0
26	7.6	7.7	6.6	3.5	22.0	0.6	65.0
27	7.6	7.5	6.5	3.4	21.0	0.6	65.0
28	7.4	7.3	6.4	3.3	21.0	0.6	66.0
29	7.4	7.2	6.2	3.3	20.0	0.6	67.0
30	7.3	7.2	6.1	3.2	20.0	0.5	69.0
31	7.3	7.0	6.0	3.1	19.0	0.5	69.0

Table 10. Morphologic data from MOR 682 (*Tenontosaurus tilletti*). Length is in the anterior-posterior direction, height is in the dorsoventral direction, and width is in the mediolateral direction. Height for the neural spine was measured along its longitudinal axis (not vertical). These measurements for the neural spine were taken at their dorsal summits. Neural spine θ ?was measured at the base of the neural arch with a protractor and is the angle between the vertical axis and the neural spine. Chevron θ ? was measured at the base of the chevron with a protractor and is the angle between the vertical axis and the chevron spine.

Dorsal Section

Centra				Neural spines			
Vert.	L	H	W	L	H	W	θ
1	3.0	3.0	2.7	2.0	3.7	0.5	40.0
2	3.0	3.2	2.9	2.1	3.9	0.5	30.0
3	3.0	3.4	3.0	2.3	5.0	0.6	20.0
4	3.2	3.4	3.4	3.0	5.1	0.6	17.0
5	3.4	3.4	3.8	3.6	5.2	0.6	15.0
6	3.7	3.4	3.9	3.9	5.2	0.6	6.0
7	5.0	3.4	3.9	3.3	5.2	0.6	0.0
8	5.0	3.5	3.1	3.4	6.0	0.7	5.0
9	5.0	3.7	3.3	3.5	6.7	0.8	10.0
10	5.0	3.9	3.4	3.5	6.7	0.9	10.0
11	5.0	5.0	3.5	3.5	6.7	1.1	10.0
12	5.0	5.0	5.0	3.5	6.7	1.3	10.0
13	5.0	5.0	5.5	3.2	7.5	1.2	10.0
14	5.0	5.0	5.2	3.0	8.8	1.2	10.0
15	5.0	5.0	5.2	3.0	8.8	1.2	10.0
16	5.0	5.0	5.2	3.0	8.8	1.2	10.0

Sacral Section

Centra				Neural spines			
Vert.	L	H	W	L	H	W	θ
1	3.7	5.0	5.0	3.5	8.0	0.7	5.0
2	5.0	5.0	5.0	3.5	9.0	0.7	5.0
3	5.0	5.0	5.0	3.5	8.0	0.7	5.0
4	5.0	5.0	5.0	3.5	8.0	0.7	5.0
5	3.5	5.0	5.0	3.5	8.0	0.7	5.0

Caudal Section

Centra				Neural spines				Chevrons			
Vert.	L	H	W	L	H	W	θ	L	H	W	θ
1	3.7	5.2	5.0	3.0	12.0	0.8	0.0	1.5	18.0	0.7	30.0
2	3.6	5.3	3.8	3.0	12.0	1.0	5.0	1.6	17.5	0.8	22.0
3	3.5	5.4	3.7	3.0	12.0	1.2	5.0	1.8	17.0	0.8	15.0
4	3.5	5.5	3.5	3.0	1.5	1.0	5.0	2.1	16.0	0.8	15.0
5	3.5	5.5	3.2	3.0	13.0	0.9	5.0	2.5	15.5	0.8	15.0
6	3.6	3.7	3.2	2.7	12.5	0.8	5.0	2.6	16.0	0.7	22.0
7	3.7	3.5	3.2	2.5	12.0	0.7	5.0	2.8	17.5	0.7	30.0
8	5.0	3.4	3.1	2.2	10.0	0.7	5.0	2.6	17.0	0.7	25.0
9	5.4	3.3	3.0	2.0	9.0	0.7	5.0	2.5	16.0	0.6	40.0
10	5.7	3.2	3.0	2.0	8.0	0.7	5.0	2.2	15.5	0.6	40.0
11	6.0	3.1	3.0	2.0	7.0	0.7	5.0	2.0	15.0	0.5	40.0
12	6.0	3.2	3.0	2.0	7.0	0.7	10.0	1.7	13.5	0.5	40.0
13	6.0	3.2	3.0	2.0	7.0	0.7	15.0	1.5	13.0	0.5	40.0
14	6.2	3.1	3.0	1.8	6.5	0.6	17.0	1.3	13.5	0.5	40.0
15	6.5	3.0	3.0	1.5	6.5	0.6	20.0	1.1	13.0	0.5	40.0
16	6.5	3.0	3.0	1.5	6.0	0.6	22.0	1.0	12.0	0.5	40.0
17	6.5	3.0	3.0	1.5	6.0	0.6	25.0	0.9	11.0	0.4	40.0
18	6.5	3.0	3.0	1.2	5.5	0.6	27.0	0.8	10.0	0.4	40.0
19	6.5	3.0	3.0	1.0	5.0	0.5	30.0	0.7	9.0	0.4	40.0
20	6.2	3.5	3.6	1.0	3.5	0.5	33.0	0.6	8.0	0.4	40.0
21	6.0	3.0	3.2	1.0	3.5	0.5	35.0	0.6	7.0	0.4	40.0
22	5.6	3.0	2.8	0.8	3.2	0.5	35.0	0.5	6.0	0.4	40.0
23	5.3	3.0	2.5	0.8	3.2	0.5	37.0	0.5	5.0	0.4	40.0
24	5.1	2.7	2.5	0.7	3.0	0.5	37.0	0.5	3.0	0.3	40.0
25	5.0	2.5	2.5	0.7	3.5	0.4	40.0	0.5	3.0	0.3	40.0
26	3.9	2.5	2.5	0.6	3.4	0.4	40.0	0.5	3.0	0.3	40.0
27	3.7	2.5	2.5	0.6	3.1	0.4	40.0	0.4	2.0	0.3	40.0
28	3.7	2.4	2.5	0.5	3.0	0.4	40.0	0.4	2.0	0.3	40.0
29	3.7	2.3	2.5	0.5	2.5	0.3	40.0	0.4	2.0	0.3	40.0
30	3.5	2.2	2.5	0.4	2.0	0.3	40.0	0.4	1.7	0.3	40.0
31	3.4	2.1	2.5	0.4	1.0	0.3	40.0	0.3	1.0	0.2	40.0
32	3.3	1.9	2.3	0.3	1.0	0.3	40.0	0.3	1.0	0.2	40.0
33	3.1	1.7	2.2	0.3	1.0	0.2	40.0	0.3	1.0	0.2	40.0
34	3.0	1.6	2.1	0.2	0.7	0.2	40.0	0.2	0.7	0.2	40.0
35	3.0	1.5	2.0	-	-	-	-	-	-	-	-
36	3.0	1.4	1.9	-	-	-	-	-	-	-	-
37	3.0	1.4	1.8	-	-	-	-	-	-	-	-
38	3.5	1.4	1.7	-	-	-	-	-	-	-	-
39	3.0	1.4	1.5	-	-	-	-	-	-	-	-
40	3.0	1.3	1.5	-	-	-	-	-	-	-	-

41	3.0	1.2	1.5	-	-	-	-	-	-	-	-
42	2.9	1.1	1.5	-	-	-	-	-	-	-	-
43	2.8	1.0	1.5	-	-	-	-	-	-	-	-
44	2.6	1.0	1.5	-	-	-	-	-	-	-	-
45	2.5	1.0	1.5	-	-	-	-	-	-	-	-
46	2.5	0.9	1.4	-	-	-	-	-	-	-	-
47	2.5	0.9	1.4	-	-	-	-	-	-	-	-
48	2.5	0.7	1.3	-	-	-	-	-	-	-	-
49	2.3	0.5	1.3	-	-	-	-	-	-	-	-
50	2.4	0.5	1.2	-	-	-	-	-	-	-	-
51	2.4	0.5	1.2	-	-	-	-	-	-	-	-
52	2.4	0.4	1.0	-	-	-	-	-	-	-	-
53	2.4	0.4	0.8	-	-	-	-	-	-	-	-
54	2.3	0.4	0.9	-	-	-	-	-	-	-	-

REFERENCES CITED

Abdalla, O. (1979). "Ossification and mineralization in the tendons of the chicken (*Gallus domesticus*)." Journal of Anatomy 129: 351-359.

Alexander, R. M. (1985). "Mechanics of posture and gait of some large dinosaurs." Zoological Journal of the Linnean Society 83: 1-25.

Alexander, R. M. (1988). Elastic Mechanisms in Animal Movement. New York, Cambridge University Press.

Alexander, R. M. and A. S. Jayes (1981). "Estimates of the bending moments exerted by the lumbar and abdominal muscles of some mammals." Journal of Zoology, London 194: 291-303.

Baumel, J. J., A. S. King, J. E. Breazile, H. E. Evans and J. C. Vanden Berge (1993). Handbook of Avian Anatomy: Nomina Anatomica Avium. Cambridge, Massachusetts, Publications of the Nutall Ornithological Club.

Baumel, J. J., J. A. Wilson and D. R. Bergren (1990). "The ventilatory movements of the avian pelvis and tail: function of the muscles of the tail region of the pigeon (*Columbia livia*)." Journal of Experimental Biology 151: 263-277.

Benjamin, M., T. Kumai, S. Milz, B. M. Boszczyk, A. A. Boszczyk and J. R. Ralphs (2002). "The skeletal attachment of tendons - tendon 'entheses'." Comparative Biochemistry and Physiology, Part A 133: 931-945.

Benjamin, M. and J. R. Ralphs (1998). "Fibrocartilage in tendons and ligaments - an adaptation to compressive load." Journal of Anatomy 193: 481-494.

Bennett, M. B., R. F. Ker, N. J. Dimery and R. M. Alexander (1986). "Mechanical properties of various mammalian tendons." Journal of Zoology, London 209 (A): 537-548.

Bennett, M. B. and J. A. Stafford (1988). "Tensile properties of calcified and uncalcified avian tendons." Journal of Zoology, London 214: 343-351.

Blob, R. W. and A. A. Biewener (1999). "In vivo locomotor strain in the hindlimb

bones of *Alligator mississippiensis* and *Iguana iguana*: implications for the evolution of limb bone safety factor and non-sprawling limb posture." Journal of Experimental Biology 202: 1023-1046.

Boas, J. E. V. (1929). "Biologisch-anatomische Studien uber den Hals der Vogel." D. Kgl. Danske Vidensk. Selk. Skr. Naturvidensk. Mathem. Afd. Series 9(1): 105-222.

Broili, F. (1922). "Uber den feineren Bau der „verknochnerten Sehnen" (verknochteren Muskeln) von Trachodon." Anatomischer Anzeiger 55: 465-475.

Brown, B. (1916). "*Corythosaurus casuarius*: skeleton, musculature and epidermis." Bulletin of the American Museum of Natural History 35: 709-716.

Brown, B. (1933). "A gigantic ceratopsian dinosaur, *Triceratops maximus*, new species." American Museum Novitates 649: 1-9.

Bryant, H. N. and A. P. Russell (1992). "The role of phylogenetic analysis in the inference of unpreserved attributes of extinct taxa." Philosophical Transactions of the Royal Society of London, Series B 337: 405-418.

Bryant, H. N. and K. L. Seymour (1990). "Observations and comments on the reliability of muscle reconstruction in fossil vertebrates." Journal of Morphology 206: 109-117.

Bultynck, P. (1992). "An assessment of posture and gait in *Iguanodon bernissartensis*." Bulletin De L'Institut Royal Des Sciences Naturelles De Belgique 63: 5-11.

Carrano, M. T. and A. A. Biewener (1999). "Experimental alteration of limb posture in the chicken (*Gallus gallus*) and its bearing on the use of birds as analogs for dinosaur locomotion." Journal of Morphology 240(3): 237-249.

Carrano, M. T. and J. R. Hutchinson (2002). "Pelvic and hindlimb musculature of *Tyrannosaurus rex* (Dinosauria: Theropoda)." Journal of Morphology 253: 207-228.

Castanet, J., H. Fancillon-Veillot, F. J. Meunier and A. J. de Ricqlès (1993). Bone and Individual Aging. Bone. B. K. Hall. Boca Raton, Florida, CRC. 7: 329-

339.

Colbert, E. H. (1951). "Environment and adaptations of certain dinosaurs." Biology Review 26: 265-284.

Coombs, W. P. J. (1995). "Ankylosaurian tail clubs of middle Campanian to early Maastrichtian age from western North America, with description of a tiny tail club from Alberta and discussion of tail orientation and tail club function." Canadian Journal of Earth Sciences 32: 902-912.

Cracraft, J. (1988). The major clades of birds. The Phylogeny and Classification of the Tetrapods. M. Benton. Oxford, Clarendon Press. Systematics Association, Special Vol. No. 35A: 333-355.

Cubo, J. and A. Casinos (2000). "Mechanical properties and chemical composition of avian long bones." European Journal of Morphology 38(2): 112-121.

Currey, J. D. (1988). "The effect of porosity and mineral content on the Young's modulus of elasticity of compact bone." Journal of Biomechanics 21(2): 131-139.

Currey, J. D. (1990). "Physical characteristics affecting the tensile failure properties of compact bone." Journal of Biomechanics 23(8): 837-844.

Currey, J. D. (1999a). "The design of mineralized hard tissues for their mechanical functions." The Journal of Experimental Biology 202: 3285-3294.

Currey, J. D. (1999b). "What determines the bending strength of compact bone?" The Journal of Experimental Biology 202: 2495-2503.

Currey, J. D. (2001). Ontogenetic changes in compact bone material properties. Bone Mechanics Handbook. S. C. Cowin. Boca Raton, CRC Press: 19, 1-16.

Currey, J. D. (2002). Bones: Structure and Mechanics. New Jersey, Princeton University Press.

Cyron, B. M. and W. C. Hutton (1978). "The fatigue strength of the lumbar neural arch in spondylolysis." Journal of Bone and Joint Surgery 60B: 234-238.

Cyron, B. M., W. C. Hutton and J. D. G. Troup (1976). "Spondylolytic fractures." Journal of Bone and Joint Surgery 58B: 462-466.

de Pinna, M. C. C. (1991). "Concepts and tests of homology in the cladistic paradigm." Cladistics 7: 367-394.

de Ricqlès, A. J. (1980). Tissue structure of dinosaur bone: functional significance and possible relation to dinosaur physiology. A Cold Look at the Warm-Blooded Dinosaurs. R. D. K. Thomas and C. Olson. Westview, Boulder, CO, American Association for the Advancement of Science, Selected Symposium 28: 103-139.

de Ricqlès, A. J., K. Padian and J. R. Horner (2001). The bone histology of basal birds in phylogenetic and ontogenetic perspectives. New Perspectives on the Origin and Early Evolution of Birds: Proceedings of the International Symposium in Honor of John H. Ostrom. J. Gauthier and L. F. Gall. New Haven, CT, Peabody Museum of Natural History: 411-426.

de Ricqlès, A. J., K. Padian, J. R. Horner and H. Fancillon-Veillot (2000). "Paleohistology of the bones of pterosaurs (Reptilia: Archosauria): anatomy, ontogeny, and biomechanical implications." Zoological Journal of the Linnean Society 129: 349-385.

Dilkes, D. W. (2000). "Appendicular myology of the hadrosaurian dinosaur Maiasaura peeblesorum from the Late Cretaceous (Campanian) of Montana." Transactions of the Royal Society of Edinburgh, Earth Science 90: 87-125.

Dollo, L. (1886). "Note sur les ligaments ossifies des dinosauriens de Bernissart." Archives de Biologie 7: 249-264.

Erickson, G. M., K. Curry-Rogers and S. A. Yerby (2001). "Dinosaurian growth patterns and rapid avian growth rates." Nature 412: 429-433.

Fancillon-Vieillot, H., V. de Buffrénil, J. Castanet, J. Géraudie, F. J. Meunier, J. Y. Sire, L. Zylberberg and A. J. de Ricqlès (1990). Microstructure and mineralization of verebrate skeletal tissues. Skeletal Biomineralization: Patterns, Processes and Evolutionary Trends. J. G. Carter. New York, Van Nostrand Reinhold. 1: 471-530.

Felisbino, S. L. and H. F. Carvalho (1999). "Identification and distribution of type VI collagen in tendon fibrocartilages." Journal of Submicroscopic Cytology and Pathology 31: 187-195.

Forster, C. A. (1990). "The postcranial skeleton of the ornithopod dinosaur Tenontosaurus tilletti." Journal of Vertebrate Paleontology 10(3): 273-294.

Frey, E. (1982). Der Bau des Bewegungsapparates de Krokodile und seine Funktion bei der auatischen Fortbewegung. Fakultät Biologie, Tübingen.

Frey, E. (1985). Biomechanics of terrestrial locomotion in crocodiles. Principles of Construction in Fossil and Recent Reptiles. Sonderforschungsbereich. Stuttgart and Tübingen, University of Stuttgart/University of Tübingen. 4: 145-167.

Frey, E., J. Riess and S. Tarsitano (1989). "The axial tail musculature of recent crocodiles and its phyletic implications." American Zoologist 29: 857-862.

Galton, P. M. (1969). The pelvic musculature of the dinosaur hypsolophodon (reptilia: ornithischia). Newhaven, CT, Peabody Museum of Natural History, No. 131: 64.

Galton, P. M. (1970). "The posture of hadrosaurian dinosaurs." Journal of Paleontology 44(3): 464-473.

Galton, P. M. (1981). "Dryosaurus, a hypsilophodontid dinosaur from the Upper Jurassic of North America and Africa; postcranial skeleton." Palaeontologische Zeitschrift 55(3-4): 271-312.

Gasc, J. P. (1981). Axial Musculature. Biology of the Reptilia. C. Gans and T. S. Parsons. London, Academic Press: 355-435.

Gatesy, S. M. (1994). "Neuromuscular diversity in archosaur deep dorsal thigh muscles." Brain Behavior and Evolution 43: 1-14.

Gatesy, S. M. (1995). Functional evolution of the hindlimb and tail from basal theropods to birds. Functional Morphology in Vertebrate Paleontology. J. J. Thomason. New York, Cambridge University Press: 219-234.

Gauthier, J. (1986). "Saurischian monophyly and the origin of birds." California

Academy of Sciences, Memoir 8: 1-55.

Guo, X. E. (2001). Mechanical properties of cortical and cancellous bone tissue. Bone Mechanics Handbook. S. C. Cowin. Boca Raton, CRC Press: 10, 1-19.

Haines, R. W. and A. Mohuiddin (1968). "Metaplastic bone." Journal of Anatomy 103(3): 527-538.

Harvey, E. B., H. E. Kaiser and L. E. Rosenberg (1968). An atlas of the domestic turkey (*Meleagris gallopavo*). Myology and Osteology. US Atomic Energy Commission. Washington DC.

Hawkins, J. A., C. E. Hughes and R. W. Scotland (1997). "Primary homology assessment, characters and character states." Cladistics 13: 275-283.

Horner, J. R., A. J. de Ricqlès and K. Padian (1999). "Variation in dinosaur skeletochronology: implications for age assessment and physiology." Paleobiology 25(3): 295-304.

Horner, J. R., A. J. de Ricqlès and K. Padian (2000). "Long bone histology of the hadrosaurid dinosaur Maiasaura peeblesorum: growth dynamics and physiology based on an ontogenetic series of skeletal elements." Journal of Vertebrate Paleontology 20(1): 115-129.

Horner, J. R., K. Padian and A. J. de Ricqlès (2001). "Comparative osteology of some embryonic and perinatal archosaurs: developmental and behavioral implications for dinosaurs." Paleobiology 27(1): 39-58.

Hutchinson, J. R. (2001a). "The evolution of femoral osteology and soft tissues on the line to extant birds (Neornithines)." Zoological Journal of the Linnean Society 131(2): 169-197.

Hutchinson, J. R. (2001b). "The evolution of pelvic osteology and soft tissues on the line to extant birds (Neornithines)." Zoological Journal of the Linnean Society 131(2): 123-168.

Hutchinson, J. R. and M. Garcia (2002). "Tyrannosaurus was not a fast runner." Nature 415: 1018-1021.

IES (2000). Visual Analysis 4.0. Bozeman.

Johnson, L. C. (1960). Mineralization of Turkey Leg Tendon. I. Histology and Histochemistry of Mineralization. Calcification in Biological Systems. R. F. Sognnaes. Washington, American Association for the Advancement of Science: 117-128.

Kannus, P. (2000). "Structure of the tendon connective tissue." Scandinavian Journal of Medicine and Science in Sports 10: 312-320.

Kirkendall, D. T. and W. E. Garrett (1997). "Function and biomechanics of tendons." Scandinavian Journal of Medicine and Science in Sports 7: 62-66.

Koehnlein, H. (1930). "Knochenbildung in Sehnen." Arch. LX Klin. Chir. 163: 147-172.

Kusuzaki, K., N. Kageyama, H. Shinjo, H. Takeshita, H. Murata, S. Hashiguchi, T. Ashihara and Y. Hirasawa (2000). "Development of bone canaliculi during bone repair." Bone 27(5): 655-659.

Ladd, A. J., J. H. Kinney, D. L. Haupt and S. A. Goldstein (1998). "Finite-element modeling of trabecular bone: comparison with mechanical testing and determination of tissue modulus." Journal of Orthopedic Research 16(5): 622-628.

Landis, W. J., J. J. Librizzi, M. G. Dunn and F. H. Silver (1995). "A study of the relationship between mineral content and mechanical properties of turkey gastrocnemius tendon." Journal of Bone Mineral Research 10(6): 859-867.

Landis, W. J. and F. H. Silver (2002). "The structure and function of normally mineralizing avian tendons." Comparative Biochemistry and Physiology, Part A 133: 1135-1157.

Lauder, G. V. (1981). "Form and function: structural analysis in evolutionary morphology." Paleobiology 7(4): 430-442.

Lauder, G. V. (1991a). Biomechanics and evolution: integrating physical and historical biology in the study of complex systems. Biomechanics in Evolution. J. M. V. Rayner and R. J. Wootton. Cambridge, New York, Cambridge University Press: 1-19.

Lauder, G. V. (1991b). An evolutionary perspective on the concept of efficiency:

how does it evolve? Efficiency and economy in animal physiology. R. W. Blake. New York, Cambridge University Press: 169-184.

Lauder, G. V. (1995). On the inference of function from structure. Functional Morphology in Vertebrate Paleontology. J. J. Thomason. New York, Cambridge University Press: 1-18.

Lauder, G. V., A. M. Leroi and M. R. Rose (1993). "Adaptations and history." Trends in Ecology and Evolution 8(8): 294-297.

Lauder, G. V. and S. M. Reilly (1996). The mechanistic bases of behavioral evolution: a multivariate analysis of musculoskeletal function. Phylogenies and the comparative method in animal behavior. E. P. Martins. New York, Oxford University Press: 104-137.

Lieberkuhn, N. (1860). "Uber die ossification. Die Ossification des Sehnengewebes." Arch. Anat. Physiol. Wissens. Med. 1860: 824-846.

Likins, R. C., K. A. Piez and M. L. Kunde (1960). Mineralization of Turkey Leg Tendon. III. Chemical Nature of the Protein and Mineral Phases. Calcification in Biological Systems. R. F. Sognnaes. Washington, American Association for the Advancement of Science: 117-128.

Lull, R. S. and N. E. Wright (1942). "Hadrosaurian dinosaurs of North America." Geological Society of America, Special Papers 40: 242.

Martin, R. B., D. B. Burr and N. A. Sharkey (1998). Skeletal tissue mechanics. New York, Springer.

Molnar, R. E. and E. Frey (1987). "The paravertebral elements of the Australian ankylosaur Minmi (Reptilia: Ornithischia, Cretaceous)." Neues Jahrbuch für Geologie und Paläontologie, Abhandlungen 75(1): 19-37.

Moodie, R. L. (1927). „Studies in Paleopathology, XX. Vertebral lesions in the sabre-tooth, Pleistocene of California, resembling the so-called myositis ossificans progressiva compared wth certain ossifications in the dinosaurs." Annals of Medical History 9(1): 91-102.

Moodie, R. L. (1928). "The histological nature of ossified tendons found in dinosaurs." American Museum Novitates 311: 1-15.

Nigg, B. M. and W. Herzog (1999). Biomechanics of the Musculo-Skeletal System. Chichester, New York, Wiley.

Nishi, S. (1938). Muskeln des Rumpfes. Handbuch der vergleichebnden Anatomie der Wirbeltiere, Bd. 5. L. Bolk, E. Göppert, E. Kallius and W. Lubosch. Berlin, Urban und Scwarzenberg: 351-446.

Norman, D. B. (1980). "On the ornithischian dinosaur *Iguanodon bernissartensis* from the lower Cretaceous of Bernissart (Belgium)." L'Institut Royal des Sciences Naturelles de Belgique Memoire 178: 1-103.

Norman, D. B. (1986). "On the anatomy of *Iguanodon atherfieldensis* (Ornithischia: Ornithopoda)." Bulletin de l'Institut Royal des Sciences Naturalles de Belgique, Sciences de la Terre 56: 281-372.

Nylen, M. U., D. B. Scott and V. M. Mosley (1960). Mineralization of Turkey Leg Tendon. II. Collagen-Mineral Relations Revealed by electron and X-Ray Microscopy. Calcification in Biological Systems. R. F. Sognnaes. Washington, American Association for the Advancement of Science: 117-128.

Ostrom, J. H. (1964). "A reconsideration of the paleoecology of hadrosaurian dinosaurs." American Journal of Science 262: 975-997.

Ostrom, J. H. (1969). "Osteology of *Deinonychus antirrhopus*, an unusual theropod from the lower Cretaceous of Montana." Peabody Museum of Natural History, Yale University Bulletin 30: 165.

Ostrom, J. H. (1990). Dromaeosauridae. The Dinosauria. D. B. Weishampel, P. Dodson and H. Osmólska. Berkeley, University of California Press: 269-279.

Parks, W. A. (1924). "Dyoplosaurus acutosqameus, a new genus and species of armoured dinosaur, and notes on a skeleton of *Prosaurolophus maximus*." Geology Series, University of Toronto Studies(18): 50.

Patterson, C. (1982). Morphological characters and homology. Systematics Association Special Volume 21: Problems of Phylogenetic Recosntruction. K. A. Joysey and A. E. Friday. New York, Academic Press: 21-74.

Prieto-Márquez, A. (2001). Osteology and Variation of Brachylophosaurus canadensis (Dinosauria, Hadrosauridae) from the Upper Cretaceous Judith River Formation of Montana. Department of Earth Sciences. Bozeman, Montana State University: 390.

Rayfield, E. J., D. B. Norman, C. C. Horner, J. R. Horner, P. M. Smith, J. J. Thomason and P. Upchurch (2001). "Cranial design and function in a large theropod dinosaur." Nature 409: 1033-1037.

Reid, R. E. H. (1996). "Bone histology of the Cleveland-Llyod dinosaurs and of dinosaurs in general, part I: introduction: introduction to bone tissues." Brigham Young University Geology Studies 41: 25-72.

Reid, R. E. H. (1997). Histology of bones and teeth. Encyclopedia of Dinosaurs. P. J. Currie and K. Padian. San Diego, CA, Academic Press: 329-339.

Reilly, D. T. and A. H. Burstein (1975). "The elastic and ultimate properties of compact bone tissue." Journal of Biomechanics 8: 393-405.

Retterer, E. and A. Lelievre (1911). "Phenonmenes cytologiques des tendons des oiseaux en voie d'ossification." Soc. Biol. C.R. Seanc. Mem. 71: 596-599.

Rigby, B. J., N. Hirai, J. D. Spikes and H. Eyring (1959). "The mechanical properties of rat tail tendon." Journal of General Physiology 43: 265-283.

Romer, A. S. (1923a). "Crocodilian pelvic muscles and their avian and reptilian homologues." Bulletin of the American Museum of Natural History 48: 533-552.

Romer, A. S. (1923b). "The pelvic musculature of saurischian dinosaurs." Bulletin of the American Museum of Natural History 48: 605-617.

Romer, A. S. (1927). "The pelvic musculature of ornithischian dinosaurs." Acta Zoologica 8(3): 225-275.

Rooney, P. (1994). Intratendinous Ossification. Bone Volume 8: Mechanisms of Bone Development and Growth. B. K. Hall. Boca Raton, CRC Press: 47-84.

Roth, V. L. (1994). Within and between organisms: replicators, lineages, and homologues. Homology: the hierarchical basis of comparative biology. B.

K. Hall. London, Academic Press.

Rothschild, B. M. (1987). "Diffuse Idiopathic skeletal hyperostosis as reflected in the paleontologic record: dinosaurs and early mammals." Seminars in Arthritis and Rheumatism 17(2): 119-125.

Rothschild, B. M. and L. D. Martin (1993). Paleopathology Disease in the Fossil Record. Boca Raton, CRC Press.

Rothschild, B. M. and D. Tanke (1992). "Paleopathology of Vertebrates: Insights to Lifestyle and Health in the Geological Record." Geoscience Canada 19(2): 73-82.

Roy, M. E., J.-Y. Rho, T. Y. Tsui, N. D. Evans and G. M. Pharr (1999). "Mechanical and morphological variation of the human lumbar vertebral cortical and trabecular bone." Journal of Biomedical Material Research 44: 191-197.

Rydzewski, W. (1935). «Etudes sur le notarium chez les Oiseaux.» Acta Ornithologica Musei Zoologici Polonici 1: 403-427.

Saha, S. (1977). "Longitudinal shear properties of human bone and its constituents, and the associated failure mechanisms." Journal of Material Science 12: 1798-1806.

Santa Luca, A. P. (1980). "The postcranial skeleton of *Heterodontosaurus tucki* (Reptilia, Ornithischia) from the Stromberg of South Africa." Annals of the South African Museum 79(7): 159-211.

Sereno, P. C. (1986). "Phylogeny of the bird-hipped dinosaurs (order Ornithischia)." National Geographic Research 2(2): 234-256.

Sereno, P. C. (1999). "The evolution of dinosaurs." Science 284: 2137-2147.

Sibley, C. G. (1994). "On the phylogeny and classification of living birds." Journal of Avian Biology 25: 87-92.

Stark, J. M. and A. Chinsamy (2002). "Bone microstructure and developmental plasticity in birds and other dinosaurs." Journal of Morphology 254: 232-246.

Storer, R. W. (1982). "Fused thoracic vertebrae in birds: Their occurence and possible significance." Journal of the Yamshina Institute of Ornithology 14: 86-95.

Sues, H.-D. and P. M. Galton (1987). "Anatomy and classification of the North American Pachycephalosauria (Dinosauria: Ornithischia)." Palaeontographica 198: 1-40.

Summers, A. P. and T. J. Koob (2002). "The evolution of tendon - morphology and material properties." Comparative Biochemistry and Physiology. Part A 133: 1159-1170.

Suzuki, D., G. Murakami and N. Minoura (2002). "Histology of the bone-tendon interfaces of limb muscles in lizards." Annals of Anatomy 184: 363-377.

Traub, W., T. Arad and S. Weiner (1989). "Three-dimensional ordered distribution of crystals in turkey tendon collagen fibers." Proceedings of the National Academy of Sciences 86: 9822-9826.

Turner, C. H., T. Wang and D. B. Burr (2001). "Shear Strength and Fatigue Properties of Human Cortical Bone Determined from Pure Shear Test." Calcified Tissue International 69: 373-378.

Vallois, H. V. (1922). "Les transformations de la musculature de l'épisome chez les vertébrés." Arch. Morph. gen. exper. 13: 1-538.

Vanden Berge, J. C. and R. W. Storer (1995). "Intratendinous ossification in birds: a review." Journal of Morphology 226(1): 47-77.

Viidik, A. (1966). Biomechanics and functional adaptation of tendons and joint ligaments. Studies on the Anatomy and Function of Bone and Joints. F. G. Evans. New York, Springer: 17-38.

Walker, A. D. (1977). Evolution of the pelvis in birds and dinosaurs. Problems of Vertebrate Evolution. S. M. Andrews, R. S. Miles and A. D. Walker. London, Academic Press: 319-357.

Weidenreich, F. (1930). Das Knochengewebe (Grobgebündelte Grundsubstanz - Faserknochen). Handbuch der Mikroskopischen Anatomie de Menschen. Berlin, Springer: 409-416.

Weishampel, D. B. (1995). Fossils, function, and phylogeny. Functional Morphology in Vertebrate Paleontology. J. J. Thomason. New York, Cambridge University Press: 34-54.

Weishampel, D. B. and J. R. Horner (1990). Hadrosauridae. The Dinosauria. D. B. Weishampel, P. Dodson and H. Osmólska. Berkeley, University of California Press: 534-561.

Wilson, J. W. (1994). Histological techniques. Vertebrate paleontological techniques. P. Leiggi and P. May. NY, Cambridge University Press. 205-234: 329-339.

Winkler, D. A., P. A. Murry and L. L. Jacobs (1997). "A new species of Tenontosaurus (Dinosauria; Ornithopoda) from the Early Cretaceous of Texas." Journal of Vertebrate Paleontology 17(2): 330-348.

Witmer, L. M. (1995). The extant phylogenetic bracket and the importance of reconstructing soft tissues in fossils. Functional Morphology in Vertebrate Paleontology. J. J. Thomason. New York, Cambridge University Press: 19-33.

Zusi, R. L. and G. D. Bentz (1984). "Myology of the Purple-throated Carib (Eulampis jugularis) and other hummingbirds (Aves: Trochilidae)." Smithsonian Contributions to Zoology 385: 1-70.